

3. METHODS

3.1 SAMPLE COLLECTION AND ANALYSES

Ground water was collected from various depths in drill holes HBH01, HBH02, KAS02, KAS03, KAS06, KAS07, KAS08, KAS09, KAS12, KAS13 and from side wells SA709B, SA776B, SA813B, SA982B, SA1009B, SA1062B, SA1420A, SA1730A, SA1229A, SA2074A in the HRL tunnel. Calcite fracture fillings were collected from open as well as filled fissures in the drill cores KAS02, KAS03 and KAS06. The granite and additional fracture minerals such as epidote, chlorite, fluorite and pyrite were collected for bulk rock and mineral $\delta^{87}\text{Sr}$.

Stable isotope preparations and measurements were made according to conventional techniques. The isotope data are given in delta-values in (per mil) and the $\delta^{13}\text{C}$ is given with respect to the PDB (Pee Dee Belemnite), $\delta^{18}\text{O}$ to SMOW (Standard Mean Ocean Water) and $\delta^{34}\text{S}$ is related to Canyon Diablo Troilite (CDT). The analyses were performed at the Section of Biogeochemistry at the Department of Geology and Geochemistry at Stockholm University and at Energiteknikk at Kjeller, Oslo, Norway.

Strontium isotope analyses were completed at the U.S. Geological Survey (Yucca Mountain project, Denver, Colorado). Water and carbonate samples were analysed on either a VG Isomass 54E or Finnigan MAT 262 mass spectrometer. $\delta^{87}\text{Sr}$ ratios are relative to a value of 0.70920 for mean sea water as determined by analyses of USGS standard EN-1 which is a *Tridacna* shell collected from Enewetok Lagoon in the western Pacific Ocean.

4. RESULTS

All of the isotopic data are reported as per mil deviations from the aforementioned standards using the following notation:

$$\delta R_{\text{sample}} = [(R_{\text{sample}}/R_{\text{standard}}) - 1] * 1000$$

where R is $^{13}\text{C}/^{12}\text{C}$, $^{18}\text{O}/^{16}\text{O}$, $^{34}\text{S}/^{32}\text{S}$ or $^{87}\text{Sr}/^{86}\text{Sr}$. Uncertainties (2 sigma) in $\delta^{18}\text{O}$, $\delta^{13}\text{C}$, $\delta^{34}\text{S}$, and $\delta^{87}\text{Sr}$ are ± 0.1 ‰ or better. The isotopic data obtained thus far in the investigation are displayed in graphical form in the ensuing discussions.

5. DISCUSSION

5.1 CALCITE FRACTURE FILLINGS

5.1.1 Carbon and Oxygen Isotope Systematics

The $\delta^{13}\text{C}$ variation in the calcite fissure fillings (Fig. 2) display biogenic (-25 to -21 ‰) and typical atmospheric (-13 to -3 ‰) values. In previous work (Wallin, 1990; Tullborg and Wallin, 1991), even lower values around -25 to -40 ‰ are reported. Based on these $\delta^{13}\text{C}$ data, it seems likely that the major part of the calcite precipitates comes from either meteoric or a mixture of meteoric and marine type water.

This conclusion is consistent with the $\delta^{18}\text{O}$ analyses for the same carbonates. Calcite with the lower $\delta^{13}\text{C}$ values reaching -12 to -13 ‰, occurs with fluorite and may possibly be hydrothermal in origin. The slight increase in $\delta^{13}\text{C}$ with depth (Figure 5.1) may be attributed to a larger component of organic carbon input in the shallow waters. This is due to degradation of organic matter and the production of CO_2 which is most likely associated with the sulphate reduction occurring at Äspö (Wallin, 1992).

The extremely low $\delta^{13}\text{C}$ -values which are observed in some carbonates are most likely attributed to a pure organic carbon source (Wallin, 1993; Banwart et al., 1992) with no input of atmospheric signatures, presumably degradation of organic matter (Wallin, 1993; Banwart et al., 1993) or oxidation of deep seated (Arnorsson and Gunnlaugsson, 1985) and/or bacterially produced methane Cheney and Jensen, 1965; Hathaway and Degens, 1969; Shultz and Calder, 1976). In any case there seem to be two major sources for the carbon observed in the calcite fissure fillings; one which is organic and one which is atmospheric.

The large range in the $\delta^{18}\text{O}$ values (+10 to +35 ‰) in the carbonate precipitates indicate a multiple source for these isotopes as well. Most of the $\delta^{18}\text{O}$ values resemble a typical meteoric signature, clustering around +17 to +23 ‰. In Figure 5.2, these intermediate values are designated group B, whereas the higher values which are more characteristic of a marine signature are labelled group A. Two samples have even lower values of about +10 to +11 ‰ (group C, Figure 5.2). These lower $\delta^{18}\text{O}$ values signatures can be explained as precipitates from high latitude or cold climate waters. These lower values have previously been observed at Äspö (Tullborg and Wallin, 1991) and Laxemar (Wallin, 1990).

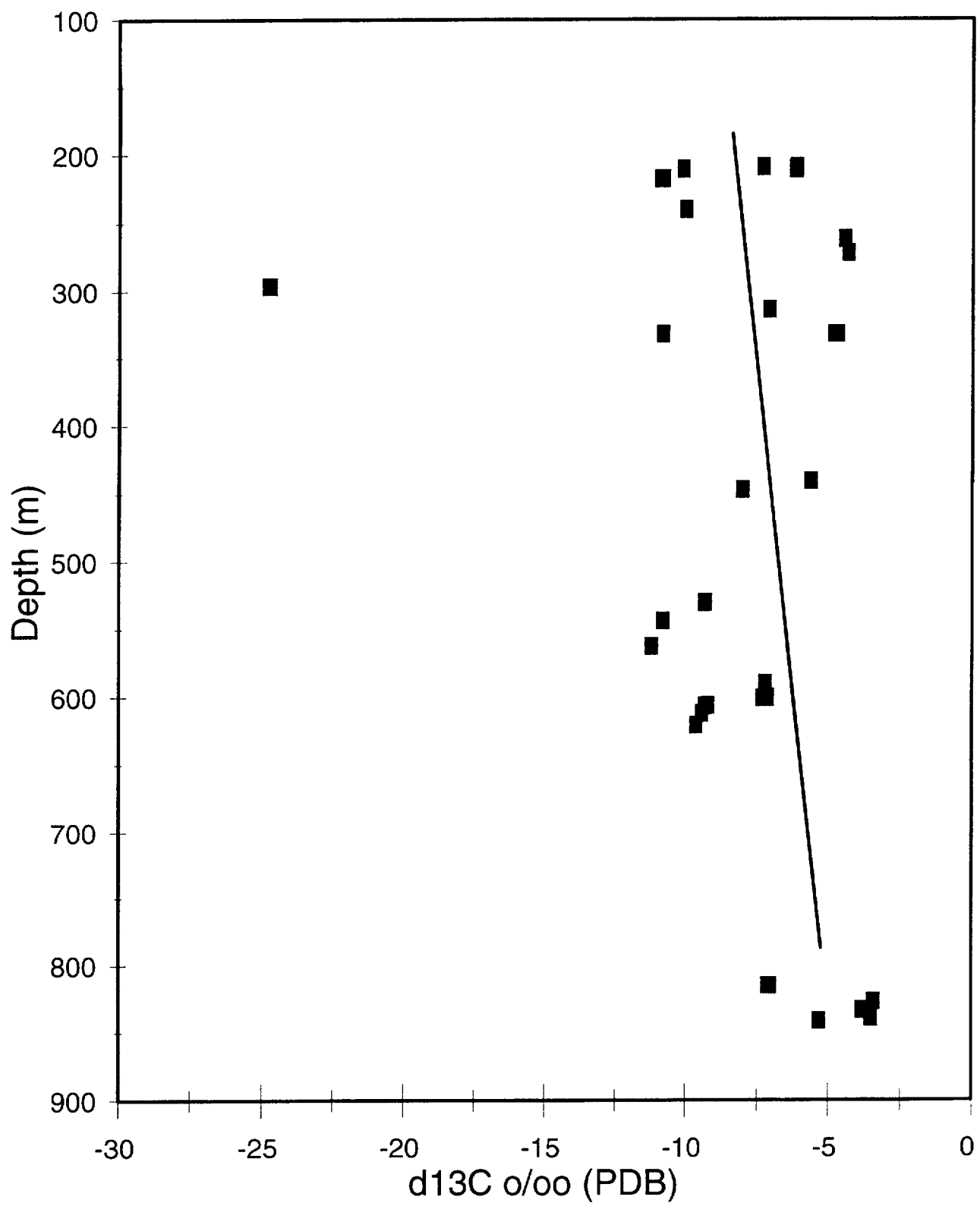


Figure 5.1. $\delta^{13}\text{C}$ values of calcite fracture fillings versus depth.

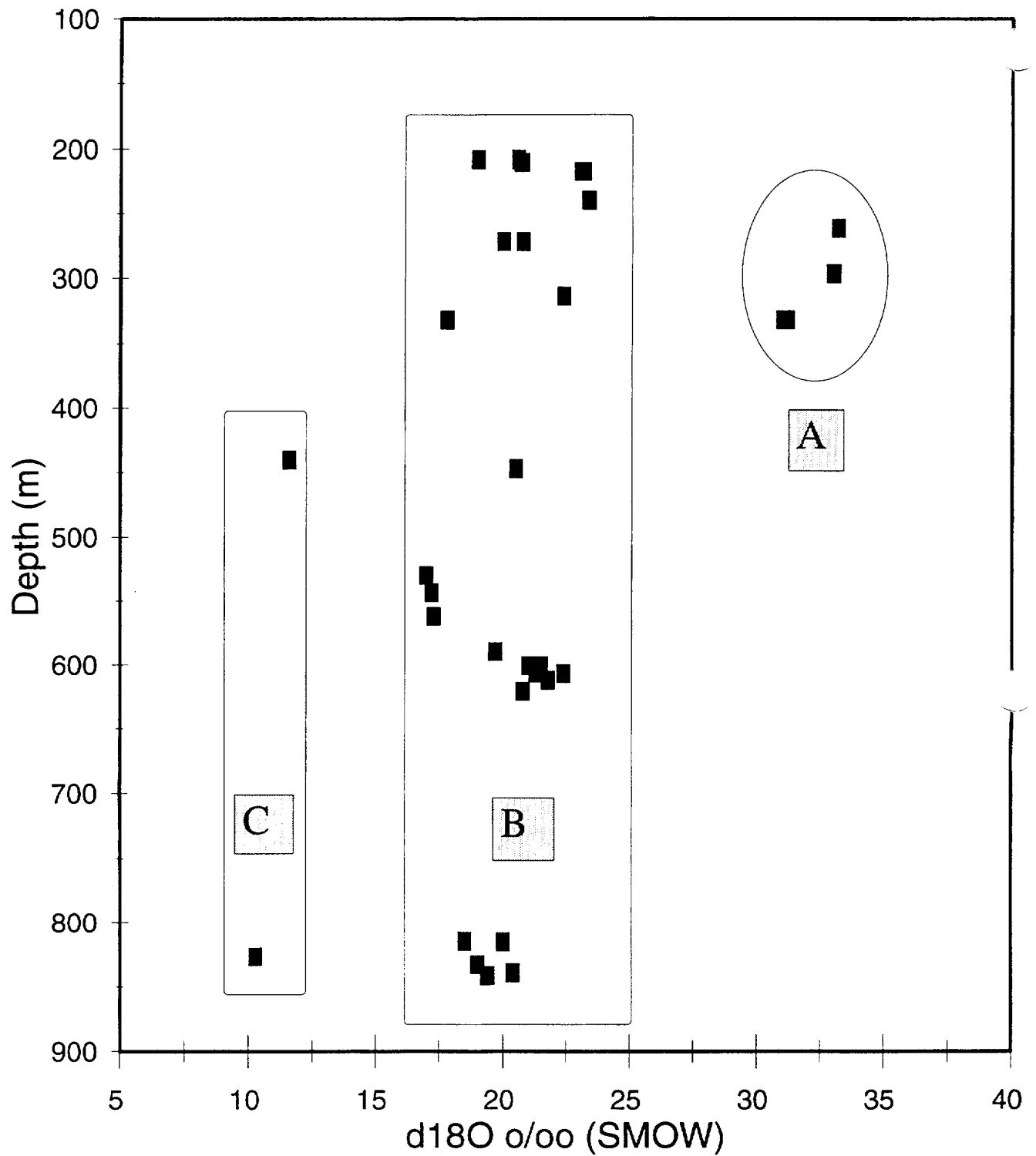


Figure 5.2. $\delta^{18}\text{O}$ values of calcite fracture fillings versus depth. 3 different groups are distinguished; A, B and C. Group A coincide with marine signatures and group B is representative of typical meteoric water precipitates. Group C may represent extremely depleted marine or meteoric water precipitates.

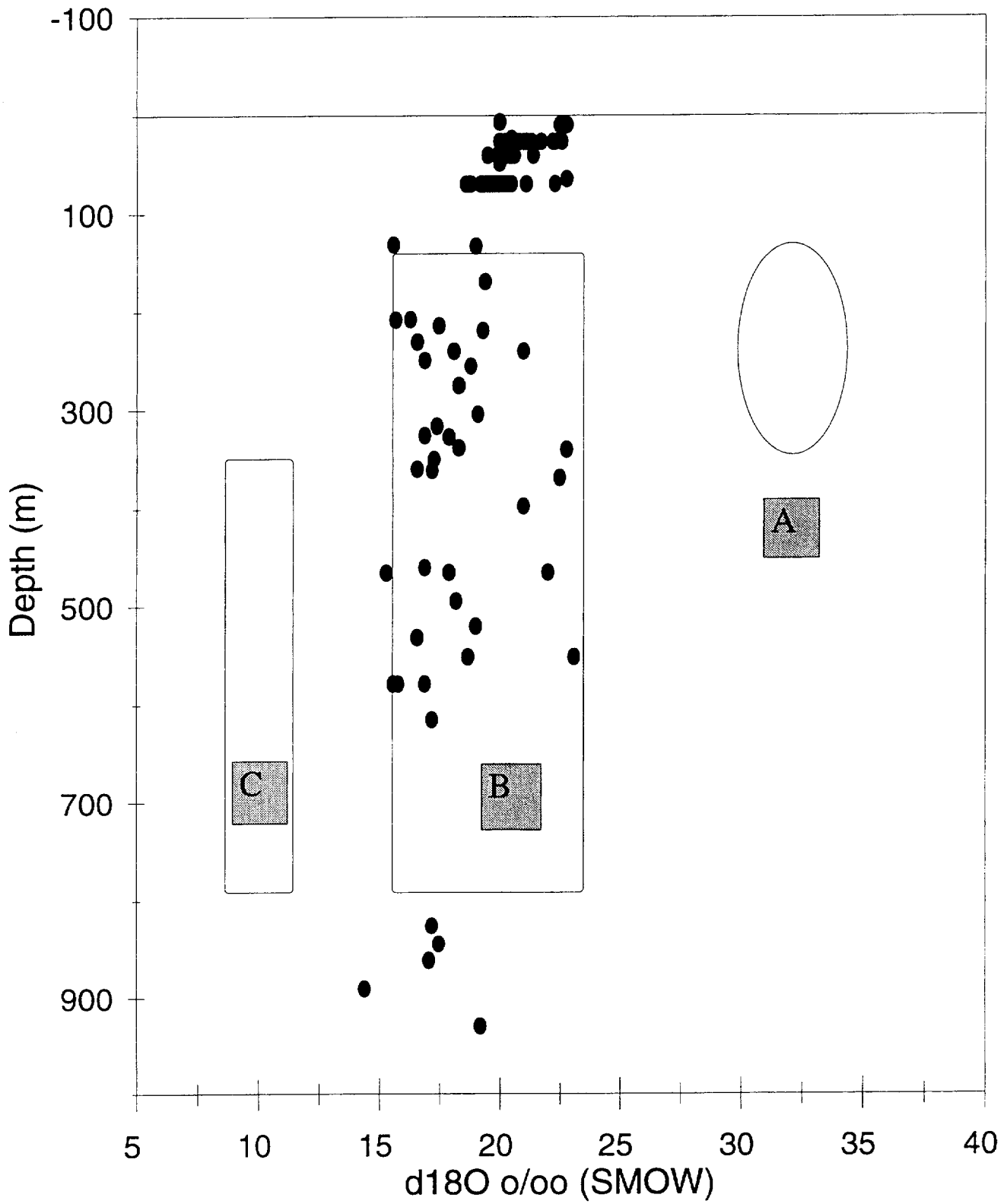


Figure 5.3. Expected $\delta^{18}\text{O}$ values if calcite precipitates were formed from the present day ground water at Äspö. Almost all values fall within the limits of group B calcite precipitates in Figure 5.2.

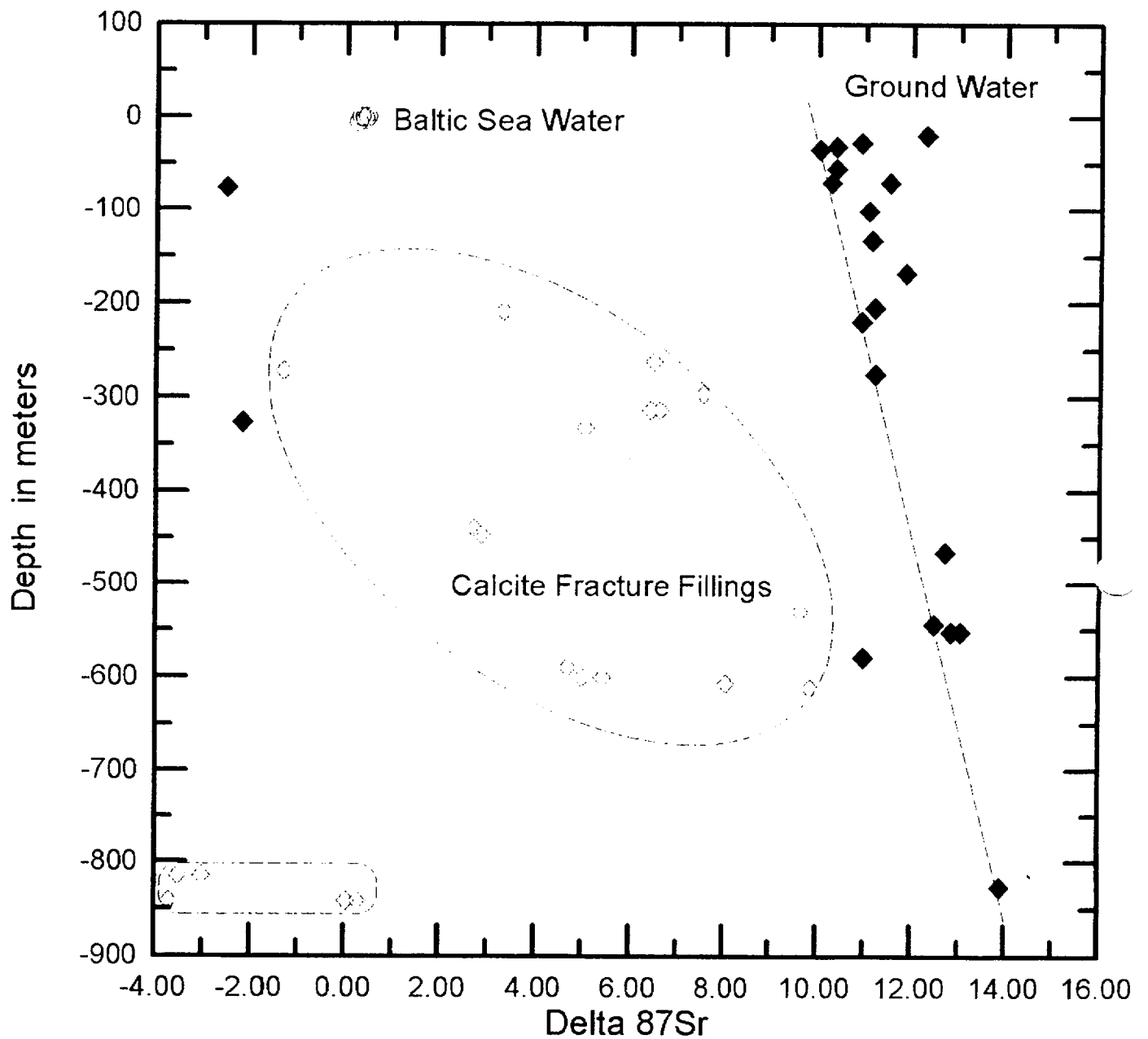


Figure 5.4. $\delta^{87}\text{Sr}$ values in calcite fracture fillings as well as in present day ground water and Baltic Sea water plotted versus depth. As can be seen from this plot the two different calcite precipitates did not form directly from the present day ground water at Äspö.

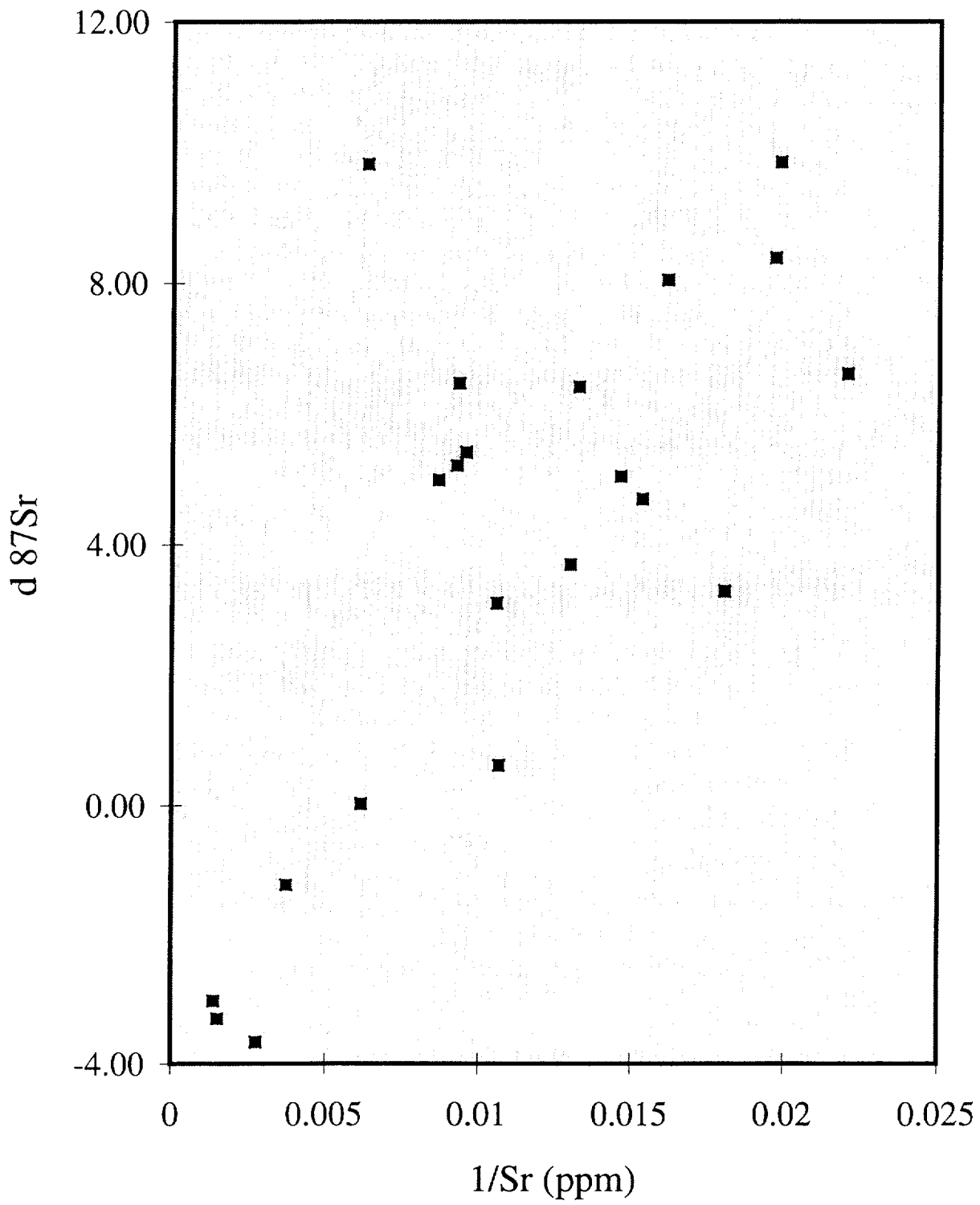


Figure 5.5. $\delta^{87}\text{Sr}$ values of the calcite fracture fillings versus the reciprocal of Sr concentrations.

The group B isotopic signatures resemble values which would be expected for calcites in equilibrium with the waters now observed at Äspö. To demonstrate this, calculated $\delta^{18}\text{O}$ values for calcite in equilibrium with present-day ground water at Äspö are plotted versus depth in Figure 5.3. These calculated values clearly overlap with the field of group B calcites. Moreover, no calcite precipitates would be expected in groups A and C from water like present-day ground water. Hence, we may conclude that the calcites with the larger $\delta^{18}\text{O}$ values around +33 and +35 ‰ must have precipitated from a different water including marine meltwaters. Typical marine calcite precipitates usually fall in a narrow range of +30 to +31 ‰. The $\delta^{18}\text{O}$ values of these calcites are slightly higher but are still consistent with a marine water signature. Obviously, there is evidence of a marine and a meteoric signature for the $\delta^{18}\text{O}$ as reported before (Wallin, 1990; Tullborg and Wallin, 1991). Despite the low $\delta^{18}\text{O}$ values observed a two end-member mixing of the calcites would hence be expected considering the that these two water types must have entered the basement at Äspö during the post-glacial time. Another explanation for the narrow range in the $\delta^{18}\text{O}$ of the ground water at Äspö is that the saline water now observed are marine waters depleted in $\delta^{18}\text{O}$ due to mixing of glacial melt waters or cold climate precipitation. This phenomenon is well known from high latitudes.

5.1.2 Strontium Isotope Systematics

$\delta^{87}\text{Sr}$ values in the calcite fracture fillings vary between -3.6 and +9.9 ‰. Two groups are distinguished in figure 5.4 where $\delta^{87}\text{Sr}$ -values in the carbonates and ground water are plotted versus depth. The deeper calcites have $\delta^{87}\text{Sr}$ from +0.3 to -3.6 ‰ whereas, with one exception at 267 m, the shallower calcites have $\delta^{87}\text{Sr}$ values ranging from +3.1 to +9.9 ‰. Present-day ground water thus far sampled at Äspö has $\delta^{87}\text{Sr}$ values ranging from +9.9 to +13.9 ‰. Thus, there is only slight overlap between the largest $\delta^{87}\text{Sr}$ values for calcite and the smallest values for ground water. Since precipitated calcite would incorporate Sr with the same $\delta^{87}\text{Sr}$ as that of the fluid from which it precipitated, most of the calcites analyzed did not form directly from present-day ground water.

$\delta^{87}\text{Sr}$ values correlate crudely with the reciprocal of Sr concentrations (Figure 5.5) which is consistent with mixing of two end members. This array can be approximated by two end members with $\delta^{87}\text{Sr}$ values between -3 and -4 ‰ and Sr contents of 600 ppm. The other end member would have a $\delta^{87}\text{Sr}$ -value of +8 ‰ or larger and a Sr content of 50 ppm. Rather than mixing, this $\delta^{87}\text{Sr}$ array shown by the calcites could represent the progressive interaction of ground water, similar to that which presently exists in the rock mass, with plagioclase feldspar (small $\delta^{87}\text{Sr}$ and large Sr contents). The precipitated calcites recorded this progressive interaction. Although yet not analyzed, the plagioclase in the granite probably has $\delta^{18}\text{O}$ values between +5 and +10 ‰. The $\delta^{18}\text{O}$ of ground water

interacting with or dissolving the plagioclase would be little affected whereas the $\delta^{87}\text{Sr}$ of the water be easily modified because of the large differences in Sr concentration between the water (typically tens of parts per million) and the plagioclase (plagioclase separated from a sample of granite at the shaft collar near KAS02 has a $\delta^{87}\text{Sr}$ of -6.4 ‰ and a Sr content of 1926 ppm). Although this postulate explains the dichotomy posed by the oxygen and strontium isotopes in the calcites, it does not explain why the source water for the calcites progressively reacted with plagioclase while the present-day ground water does not display such a trend. The ages of the calcite fracture fillings are unknown, and until these ages are constrained, a more comprehensive model cannot be constructed.

5.2

GROUND WATER

A large number of δD - and $\delta^{18}\text{O}$ -isotopes have been analysed in the shallow and deep ground water at Äspö during the past several years. Almost all of the samples plot on the right-hand side of the meteoric water line (Fig. 5.6). This enrichment in $\delta^{18}\text{O}$ in comparison to the δD may be explained by water-rock interactions, including interaction with clay minerals.

The overall average values for the δD and $\delta^{18}\text{O}$ show typical meteoric water signatures. The mean values of the water analyses are converging against the SMOW end-point relative to the meteoric water line (MWL), as the isotopic signature is increasing. This may be a sign of a slight in-mixing of a marine component. This marine signature could very well be a water which is equivalent to present day or "fossil" Baltic sea water.

In a high latitude cold climate a mixing of heavily isotopic depleted melt waters and marine waters from the ancient Baltic sea may easily attain saline waters with low $\delta^{18}\text{O}$ values, similar to what we observe today. This is more or less supported by the fact that a depletion in $\delta^{18}\text{O}$ is accompanied by an increase in chlorinity at Äspö.

The new $\delta^{34}\text{S}$ data, coupled with previous data, confirm a multiple sulphur source for the dissolved sulphate. Shallow and intermediate ground waters have been analysed during the first year of this study and most of the results show marine signatures together with contributions of reduced sulphur. In the plot $\delta^{34}\text{S}$ of versus depth in Figure 5.7, there is large variation in the $\delta^{34}\text{S}$ -values between the shallow water ($+17$ to $+21$ ‰) and deep ground water ($+8$ to $+10$ ‰). The higher values are typical of marine signatures and some of the values coincide with the Baltic sea water signatures of $+19$ ‰. We know from earlier studies (Banwart et al., 1992) that some of these waters may originate from minor proportions of Baltic water injections. Computer modelling of these shallow ground waters suggests that there may be isolated water lenses of "fossil marine waters" which are residing in the near surface fractures (Banwart et al., 1992).

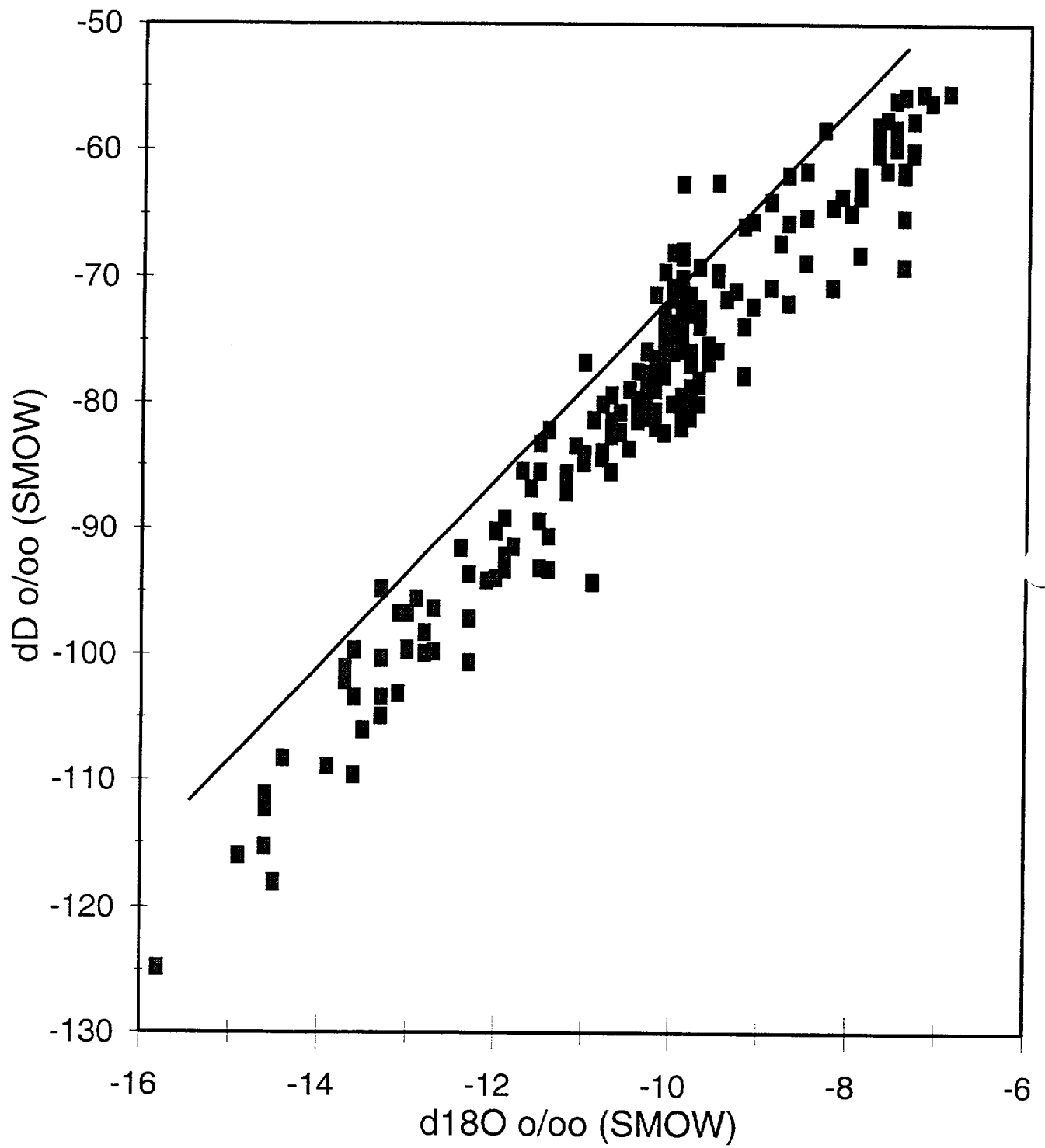


Figure 5.6. δD plotted versus $\delta^{18}\text{O}$ in the ground water from various depth at Äspö.

The variation of $\delta^{34}\text{S}$ in the shallow ground water is most likely caused by a mixing of meteoric water enriched in sulphate and minor proportions of waters with a marine signature.

The intermediate waters plot around +13 to +16 ‰ (Figure 5.7) although three anomalous samples from about 500 m depth are about +19 and +20 ‰. The lowering of $\delta^{34}\text{S}$ in these intermediate waters may be a result of contribution of reduced sulphur from fracture filling sulphides and from the basement rocks. A possible explanation for this might be large scale injections of oxygenated waters which oxidise any sulphides present. Such water inflow can easily have taken place during the isostatic movements during the ice recession of the last glacial period. The $\delta^{18}\text{O}$ -isotope variation in these intermediate waters show signs of water mixing between meteoric and marine waters, which supports this suggestion.

The isolated high $\delta^{34}\text{S}$ -values at about 450 m depth in Figure 5.7 may therefore be conserved "marine signatures" of the dissolved sulphate. Accordingly, an explanation for this must of course be the availability of any sulphides in the fracture fillings which host the injected ground water.

The rapid drop in $\delta^{34}\text{S}$ -values from 500 m depth to about 900 m is most likely due to a Rayleigh distribution of reduced sulphur due to an extensive sulphate reduction (Wallin, 1992). This is a typical pattern in a closed system (Bågander, 1977; Bågander, 1980; Hallberg, 1984) where the deeper values of around +10 ‰ represents the initial sulphate value. All larger values from the deeper part up to the 500 m level are then representing the residual sulphate. Previous studies at Äspö report very low $\delta^{13}\text{C}$ -values of the calcite, exceeding -25 ‰ supporting a closed system for the reduction.

The CO_2 produced due to the degradation of the organic matter results in low $\delta^{13}\text{C}$ signature calcites. This reaction leads to formation of sulfides with relatively low $\delta^{34}\text{S}$ isotopic signatures around -20 ‰. These values are not uncommon at Äspö in the pyrites examined (Wallin, 1992), which hence support a ongoing sulphate reduction in the ground water at Äspö.

Five samples of Baltic Sea water collected in the vicinity of Äspö have $\delta^{87}\text{Sr}$ -values between +0.2 and +0.4 ‰ (mean +0.3) , which can be seen in Figure. 5.4. These are consistent with other measurements of samples throughout the Baltic Sea (Löfvendahl et al., 1990; Andersson, 1992). In marked contrast the samples of ground water have $\delta^{87}\text{Sr}$ values between +9.9 and +13.9 ‰. Clearly, the strontium in the saline ground waters at Äspö is not derived solely from modern Baltic Sea water. Yet the stable isotope data for the calcite fissure fillings (see above) suggest that a component of marine waters has been residing at Äspö.

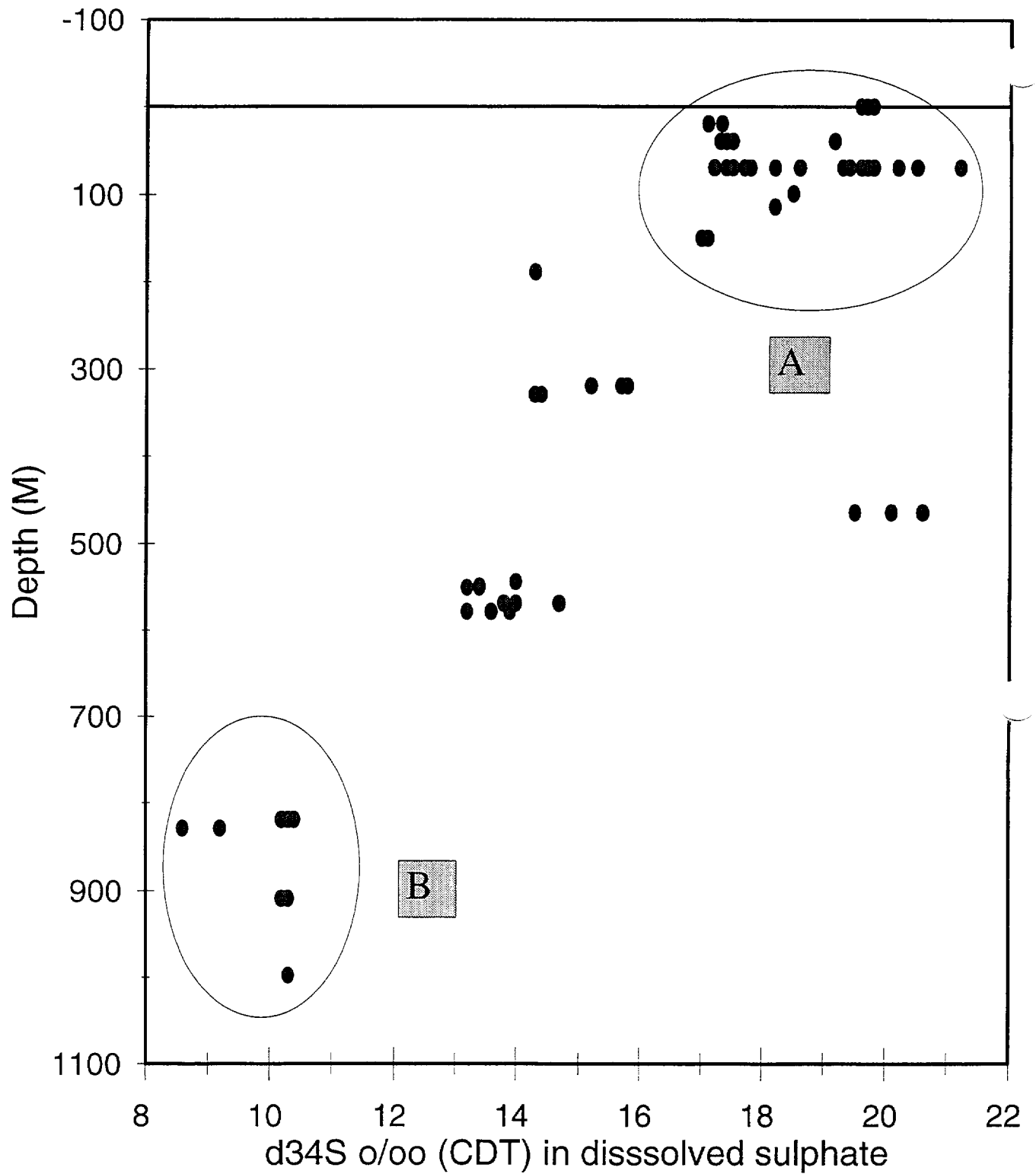


Figure 5.7. $\delta^{34}\text{S}$ values of the dissolved sulphate plotted versus depth. Group A in the shallow waters show typical present day marine signatures around +18 and 20 ‰. Intermediate waters display values around +13 and 15 ‰ and the deep water, resembling group B has values around +10‰.

In ground water at Äspö, $\delta^{18}\text{O}$ generally decreases with increasing chlorinity (Tullborg and Wallin, 1991). The $\delta^{18}\text{O}$ values around -13 ‰ are typical values of meteoric water at higher latitudes, whereas the less negative values around -7 ‰ are more representative of the present-day Baltic Sea water. These values coincide with those reported from the Fennoscandian shield in Finland (Nurmi et al., 1988). The inverse relation between the $\delta^{18}\text{O}$ and chlorinity of Äspö ground water in comparison to the Baltic sea water may be explained in different ways. It is well known that during the in-freezing stage of a large ice sheet from an isolated marine environment the residual marine water will increase in salinity. Moreover, the $\delta^{18}\text{O}$ isotope fractionation factor for ice in equilibrium with water is only 1.002, which means that the $\delta^{18}\text{O}$ -value of the residual water is about -2 ‰ (depleted in $\delta^{18}\text{O}$) relative to the ice which is formed. Therefore, the formation of sea ice leaves the $\delta^{18}\text{O}$ -value of the water essentially unchanged, but causes a significant increase in salinity, similar to the observed ground waters at Äspö. However, the observed water at Äspö is much more negative in $\delta^{18}\text{O}$ than would be expected from a normal sea water freezing. In order to explain such a phenomenon, the initial setting in $\delta^{18}\text{O}$ may have been depleted due to large input of high latitude ocean water or cold diluted water.

A solution to the contradiction between the strontium and stable isotope ($\delta^{13}\text{C}$ and $\delta^{18}\text{O}$) signatures of the ground water and some of the calcite fracture fillings is attained if it is assumed that the strontium in Baltic Sea water has undergone a significant decrease in $\delta^{87}\text{Sr}$ since the last glaciation. The intermediate ground water at Äspö is suggested to be as old as 3500 years on the basis of the development of the sea-level and of radiocarbon analyses. A scenario can be constructed to suggest that the Baltic Sea 3500 years ago contained strontium with much larger $\delta^{87}\text{Sr}$ values. Strontium in the modern Baltic is derived from Precambrian terranes on the north and Phanerozoic sedimentary terranes on the south, and perhaps some influx of sea water strontium from the North Sea. Runoff from the Precambrian terranes has a mean $\delta^{87}\text{Sr}$ of about $+29$ ‰ whereas runoff from the south (Löfvendahl et al., 1990) has a value of about $+1.2$. Because of much higher strontium contents of rivers draining the Phanerozoic terrane, this runoff contributes about 88 percent of the total strontium budget to the Baltic.

As the ice sheet retreated northward during the last glaciation, glacial rock debris, including much fine-grained material such as rock flour, would have been exposed to weathering, erosion, and transport into the Baltic Basin. The fine-grained material would have large $\delta^{87}\text{Sr}$ values like the modern runoff from the Precambrian terrane. Accordingly, we offer the hypothesis that increased influx of Precambrian strontium overwhelmed the runoff from the Phanerozoic terrane to the south to the extent that the $\delta^{87}\text{Sr}$ value for the Baltic was increased to at least the levels of Äspö

ground water. This process may have continued during the isolated stages of the Baltic where no communication took place with the marine water in the west. Using the mean runoff $\delta^{87}\text{Sr}$ -values of Lövendahl et al. (1990) an increase of the contribution in strontium through runoff from the north to 42 percent (compared with a present-day estimate of 12 percent) could have increased the $\delta^{87}\text{Sr}$ value of the Baltic to +13 ‰ .

The discrepancy of the observed $\delta^{18}\text{O}$ -values as well as the $\delta^{87}\text{Sr}$ -values may therefore solely be due to the accumulation of post-glacial runoff waters which are extremely negative in $\delta^{18}\text{O}$ as well. In addition, the sulphate $\delta^{34}\text{S}$ -values (about +14 to +15 ‰) which are observed at intermediate depth at Äspö are significantly lower than those of modern marine water sulphates. This is interpreted as being a contribution of reduced sulphur due to water/rock interaction of the marine or brackish waters in the area. It may, in concert with the model to explain the large $\delta^{87}\text{Sr}$ values by runoff waters from the shield, be due to extensive load of reduced sulphur from the melt water in the recession stage of the ice cover. This hypothesis can be tested by obtaining and analysing $\delta^{18}\text{O}$, $\delta^{13}\text{C}$ and $\delta^{87}\text{Sr}$ of carbonate or phosphate shell or bone material from bottom sediments of the Baltic that extend back to approximately 3500 years.

7. CONCLUSIONS

The results from stable and radiogenic isotope analyses of present-day ground water and calcite fracture fillings indicate an exceedingly complex ground water system. The presence of several generations of calcite and the lack of age control on these fracture fillings limit the extent to which they suggest that several waters have been involved in the precipitation of calcite fissure fillings as well as the nature of the water we observe today at Äspö. We can distinguish several isotopic end-members, and the following provisional conclusions concerning the hydrological picture at Äspö can be made:

- * δD , $\delta^{18}\text{O}$, and $\delta^{87}\text{Sr}$ evidence of meteoric waters and/or glacial melt waters at Äspö.
- * Evidence of fossil marine waters with depleted $\delta^{18}\text{O}$ signatures and high Cl concentrations.
- * Variable $\delta^{87}\text{Sr}$ values of calcite fracture fillings which are crudely correlative with reciprocal Sr concentrations could record progressive and preferential water-rock reaction with plagioclase or other high-Sr phases in the rocks mass. $\delta^{18}\text{O}$ would be little affected by this process because of mass considerations, and $\delta^{13}\text{C}$, of course, would be unaffected because of the lack of C in the silicates.

- * $\delta^{34}\text{S}$ -values of the dissolved sulphate show a multiple source, including marine sulphur, reduced sulphur from the basement and biogenic reduced sulphur due to sulphate reduction.
- * This study demonstrates that the combination of stable and radiogenic isotopes is particularly productive in providing constraints for modelling

ACKNOWLEDGEMENTS

The study was financed by SKB (Swedish Nuclear Fuel and Waste Management Company) and by DOE (U.S. Department of Energy) International Program. Karl-Göran Niderfeldt, Ann-Christin Nilsson and Katinka Klingberg facilitated the ground water sampling and provided additional data from the SKB data base. Shannon Mahan and Kiyoto Futa, respectively, analyzed the water and the calcite samples for Sr isotopes. Peter Wikberg read the manuscript and contributed with valuable comments. We sincerely thank all of these people.

REFERENCES

- Andersson P., Wasserburg G., and Ingri J. (1992). The sources and transport of Sr and Nd isotopes in the Baltic Sea. Earth and Planetary Sciences Letters, 113, 459-472.
- Banwart S., Gustafsson E., Laaksoharju M., Nilsson A.-C., Tullborg E.-L. and Wallin B. (1994). Large-scale intrusion of shallow water into a vertical fracture zone in crystalline bedrock. Initial Hydrochemical Perturbation During Tunnel Construction at the Äspö Hard Rock Laboratory, S.E., Sweden. Water Resources Research, 30:6, 1747-1763.
- Banwart S., Tullborg E.-L., Pedersen K., Gustafsson E., Laaksoharju M., Nilsson A.C., and Wallin B. (1994). Organic carbon oxidation induced by large-scale shallow water intrusion into a vertical fracture zone at the Äspö Hard Rock Laboratory. Conference Proceedings, Migration 93.
- Cheney E. S. and Jensen M. L. (1965). Stable carbon isotopic composition of biogenic carbonates. Geochimica et Cosmochimica Acta, 29, 1331-1346.
- Claypool G. E., Holser W. T. Kaplan I. R. and Sakai H. (1980). The age of sulfur and oxygen isotopes in marine sulfate. Chemical Geology, 28, 199-260.
- Faure G. (1986). Principles of isotope geology, p. 464, John Wiley & Sons, New York.

- Hathaway J. C. and Degens E. T (1969). Methane derived marine carbonates of pleistocene age. Science, 165, 690-692.
- Johansson Å. (1988). The age and geotectonic setting of the Småland-Värmland granite-porphyr belt. Geologiska Föreningens i Stockholm Förhandlingar, 110, 105-110.
- Krouse H. R. (1980). Sulphur isotopes in our environment. In: Fritz, P. and Fontes, J.-Ch., (Eds.), pp. 435-472, Handbook of environmental isotope geochemistry, Elsevier, Amsterdam.
- Löfvendahl R., Åberg G., and Hamilton P. J. (1990). Strontium in rivers of the Baltic Basin: Aquatic Sciences, 52/4, 315-329.
- Nurmi P. A.; Kukkonen I. L. and Lahermo P. W. (1988). Geochemistry and origin of saline groundwaters in the Fennoscandian Shield. Applied Geochemistry, 3, 185-203.
- Shultz D. J. and Calder J. A. (1976). Organic carbon $\delta^{13}\text{C}/^{12}\text{C}$ variations in estuarine sediments. Geochimica et Cosmochimica Acta, 40, 381-385.
- Smellie J. and Laaksoharju M. (1992). The Äspö Hard Rock Laboratory; Final evaluation of the hydrogeochemical pre-investigations in relation to existing geologic and hydraulic conditions. The Swedish Nuclear Fuel and Waste Management Company (SKB), Report 92-31, Stockholm.
- Stanfors R. (1988). SKB hard rock laboratory, Geological borehole description, KAS02, KAS03, KAS04, KLX01. The Swedish Nuclear Fuel and Waste Management Company (SKB), Report 25-88-18, Stockholm.
- Strähle A. (1989). Drillcore investigation in the Simpevarp Area, Boreholes KAS02, KAS03, KAS04 and KLX01. The Swedish Nuclear Fuel and Waste Management Company (SKB), Report 25-88-17, Stockholm.
- Tullborg E.-L. and Wallin B. (1991). Stable isotope studies of calcite fracture fillings ($\delta^{18}\text{O}$, $\delta^{13}\text{C}$ and groundwaters ($\delta^{18}\text{O}$, D). In: Tullborg, E.-L., Wallin, B., and Landström, O., Hydrogeochemical studies of fracture minerals from water conducting fractures and deep groundwaters at Äspö. The Swedish Nuclear Fuel and Waste Management Company (SKB), Report 25-90-01, 1-24, Stockholm.
- Wallin B. (1990). Carbon, oxygen and sulfur isotope signatures for groundwater classification at Laxemar, southeastern Sweden. The Swedish Nuclear Fuel and Waste Management Company (SKB), Report 25-90-12, 1-23, Stockholm.

Wallin B. (1992). Sulphur and oxygen isotope evidence from dissolved sulphates in groundwater and sulphide sulphur in fissure fillings at Äspö, southeastern Sweden, The Swedish Nuclear Fuel and Waste Management Company (SKB), Report 25-92-08, 1-44, Stockholm.

Wallin B. (1993). Organic carbon input in shallow groundwater at Äspö, southeastern Sweden. Proc. ANS Publications Department, Chicago, Illinois, April 26-30, 1993, p. 633, American Nuclear Society, La Grange Park, Illinois.

- C -

**CASE STUDIES OF GROUNDWATER FLOW
MODELLING WITHIN THE ÄSPÖ HARD ROCK
LABORATORY PROJECT**

C.1 The Combined Long Term Pumping and Tracer Test (LPT2) in Borehole KAS06

Ingvar Rhén
VBB VIAK AB
Göteborg, Sweden

ABSTRACT

The long term pumping test and tracer test performed in KAS06, called LPT2, was the first attempt to clarify the transport of solutes on the site scale of Äspö. The test was not intended to be complete regarding the transport parameters needed for nuclide transport modelling. In the operating phase of the Äspö Hard Rock Laboratory more detailed tracer tests and numerical modelling will be conducted. The field experiment had three major parts: a pumping test, a tracer experiment and a tracer dilution experiment. Numerical simulations were carried out both prior to and after the experiments.

The main conclusion from the field experiment is that the present conceptual model of Äspö is sound, but some modifications may be required. These include both the extension and transmissivities of fracture zones. The field experiment has also produced additional information on the properties of the fracture zones like porosity and dispersivity. The cumulative aperture of all hydraulic fractures was estimated to be 10×10^{-3} - 30×10^{-3} m for two different sets of zones. Considering the estimated width of the zones the flow porosities were estimated to 0.02 - 0.1 %. The dispersivities were estimated to be 0.1 - 0.2 of the flow path distance and the Peclet number to be 4-11.

The numerical simulations made prior to the experiment, dealing with the travel time of tracers, were found to be in reasonable agreement with the measurements. The data gathered in the field experiment will however make it possible to pursue the modelling efforts further.

1. BACKGROUND

1.1 ÄSPÖ HARD ROCK LABORATORY

In order to prepare for the siting and licensing of a spent fuel repository SKB has decided to construct a new underground research laboratory.

In the autumn of 1990, SKB began the construction of the Äspö Hard Rock Laboratory (Äspö HRL) near Orskarshamn in the south-eastern part of Sweden

(Figure 1.1). A 3.5 km long tunnel is now excavated in crystalline rock down to a depth of approximately 460 m (Figure 1.1). The laboratory is expected to start operating in 1995, and research concerning the disposal of nuclear waste in crystalline rock can then be carried out.

The pre-investigations for the Äspö HRL started in late 1986. The pre-investigation phase involved extensive field measurements from ground level as well as from boreholes, aimed at characterizing the rock formation with regard to geology, geohydrology, hydrochemistry and rock mechanics. Intermediate reports on the investigations were published in Gustafson et al. (1988), Gustafson et al.(1989), Wikberg et al.(1991), Stanfors et al. (1991) and Almén and Zellman (1991).

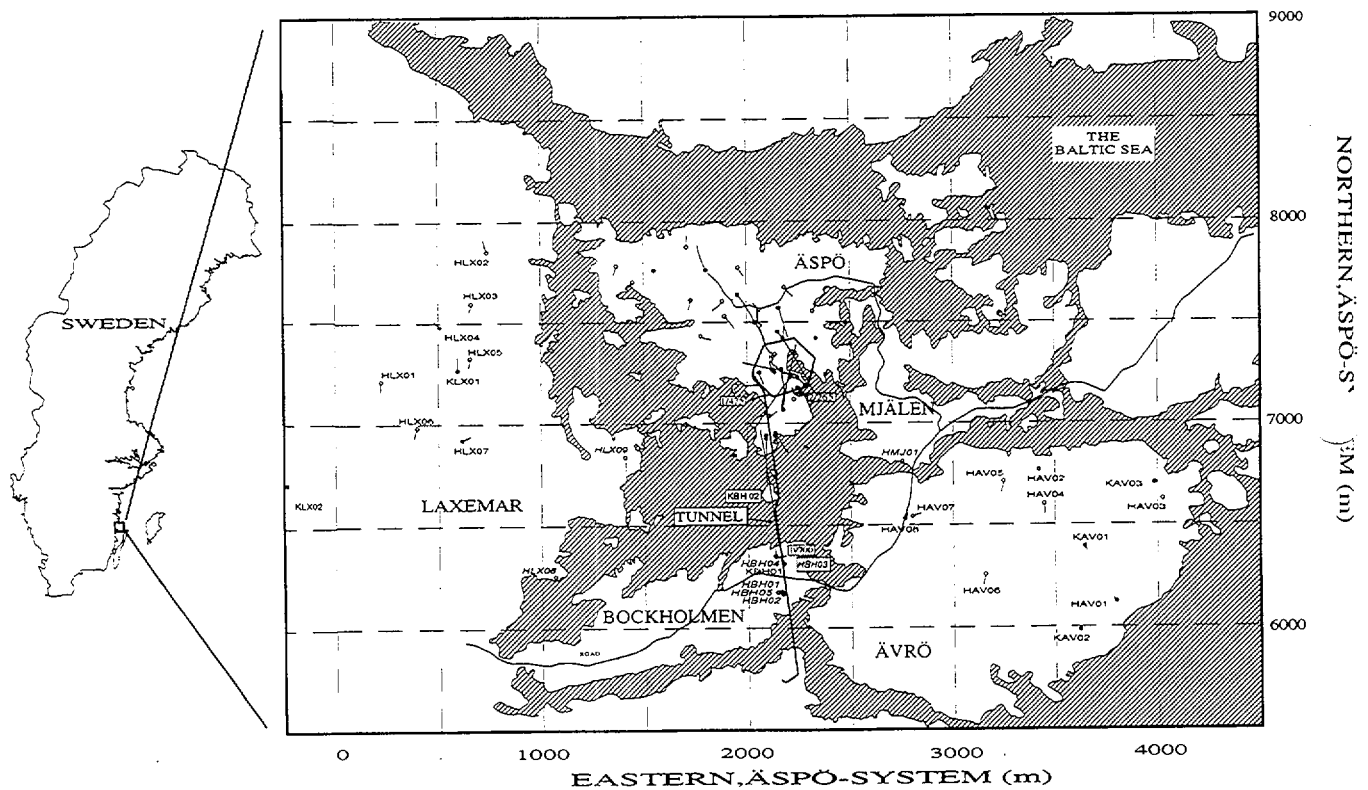


Figure 1.1. Boreholes on Äspö, Ävrö, Hälö, Mjälén and Laxemar. Filled circle = corehole, hollow circle = percussion hole.

1.2

THE LONG TERM PUMPING AND TRACER TEST LPT2

The long term pumping test and tracer test performed in KAS06 (Figure 1.2), called LPT2, was the first attempt to clarify the transport of solutes on the site scale of Äspö. The test was not intended to be complete regarding the transport parameters needed for radionuclide transport modelling. In the operating phase of the Äspö Hard Rock Laboratory more detailed tracer tests and numerical modelling will be conducted.

In the autumn of 1990 the combined long term pumping- and tracer test in borehole KAS06, LPT2, was carried out as one of the last pre-investigations for HRL. The test is reported in Rhén et al. (1992). (A large number of people were involved in the test. Numerical simulations were performed by Urban Svensson (CFE) and most of the field work and evaluation were made by J.-E. Andersson, P. Andersson, C.-O. Eriksson, E. Gustafsson, T. Ittner and R. Nordqvist (Geosigma AB)).

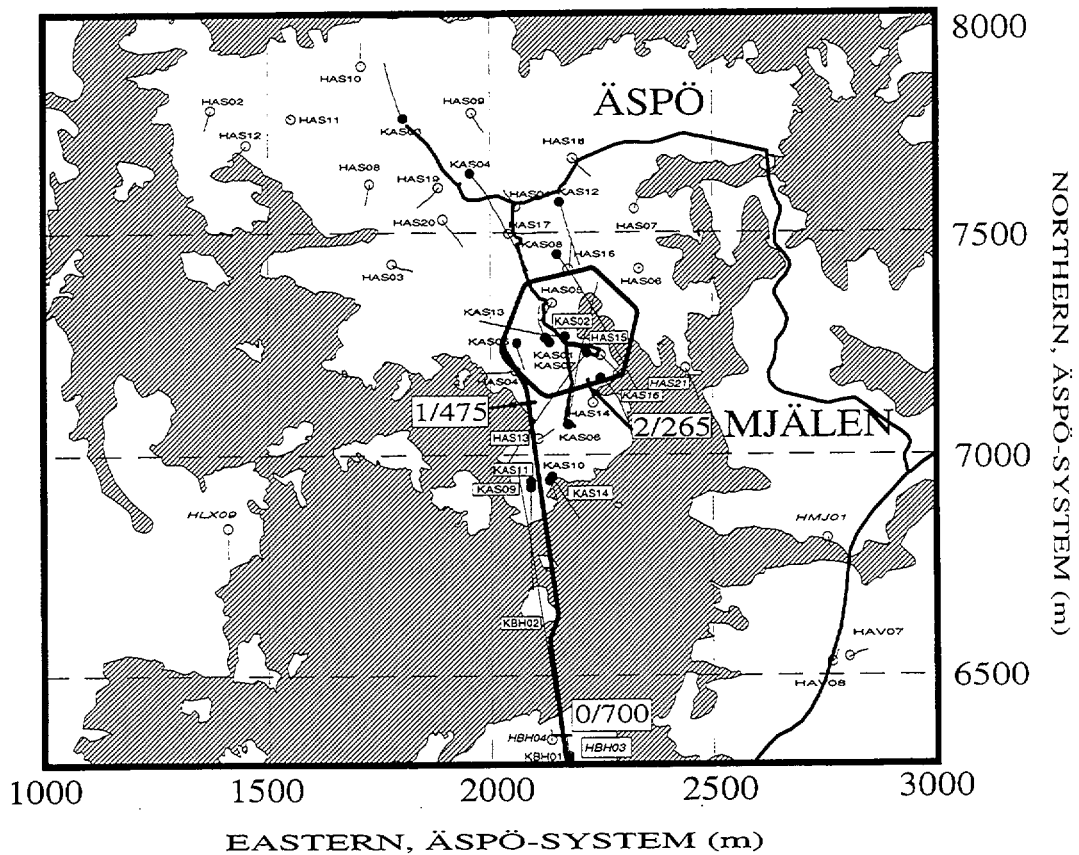


Figure 1.2. Boreholes on Äspö. Filled circle = corehole, hollow circle = percussion hole.

2. GEOHYDROLOGICAL MODEL

2.1 PRE-INVESTIGATIONS

The pre-investigations for Äspö HRL can be divided into three stages: siting stage (1986-1987), site description stage (1987-1988) and prediction stage (1989-1990). Geohydrological investigations during the siting stage comprised first the compilation of available data in data bases (mainly from the national water well records concerning data from Kalmar County, area » 10 000 km²) and reports from the construction of the nuclear power plan O III and CLAB (interim storage of spent fuel) facility and later drilling of shallow percussion boreholes on Äspö, Ävrö and Laxemar (Figure 1.1). In the siting stage three deep coreholes (two about 1 000 m deep and one 500 m), a few more percussion holes on Äspö and one corehole (about 700 m deep) on Laxemar were drilled and investigated. During the prediction stage the investigations were focused on southern Äspö. During two drilling campaigns mainly coreholes were drilled. In all during the pre-investigations 35 percussion boreholes (100 - 200 m deep) and 16 coreholes (200 - 1 000 m deep) were drilled (Figure 1.1). (The diameter (D) of percussion holes was generally 115 mm but up to 162 mm was used. The coreholes were telescope shaped where $D = 155$ to 164 mm in the uppermost 100 m and generally $D = 56$ mm lower down but in a few cases $D = 76$ mm).

During drilling of the percussion boreholes inflow rates and increased fracturing were estimated and drill cuttings were sampled. Groundwater sampling, airlift tests and geophysical logging were also made in the boreholes.

Airlift tests were generally performed for 100 m sections of coreholes. Drawdown and recovery (D + R) were normally approximately 1 h + 1 h. After drilling the coreholes were clean-up pumped for approximately a day and the first estimates of the transmissivity, as seen from the borehole, and the skin factor from the pumping were made. During the clean-up pumping the borehole was also flow-meter logged.

Injection tests were performed in some of the coreholes. Injection tests with a 3 m packer interval were performed with D + R of 10 + 10 minutes. (About 1200 tests were performed during the pre-investigations in 7 coreholes on Äspö and in one corehole on Laxemar). The tests have been evaluated at transient conditions assuming radial flow. The transient evaluation has been considered to give better estimates of the hydraulic conductivity (K) compared to the assumption of stationary conditions as in equation presented by Moye (1967). Transient evaluation has generally given higher values of K (Figure 2.1). The probability distribution of K is more or less lognormal for the injection tests (Figure 2.1).

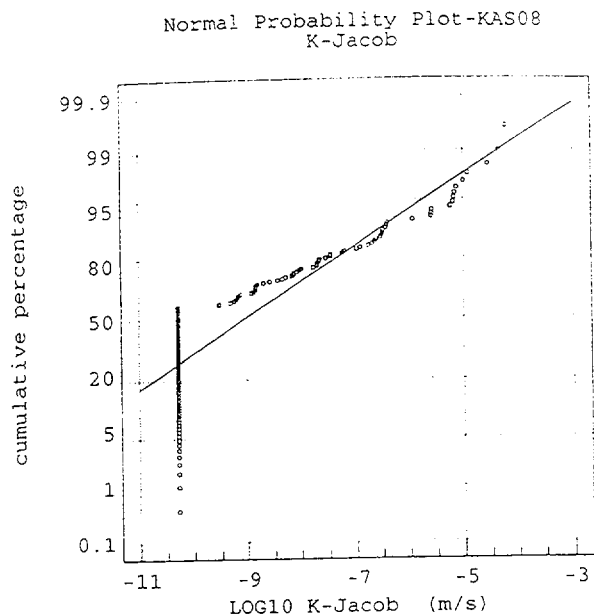
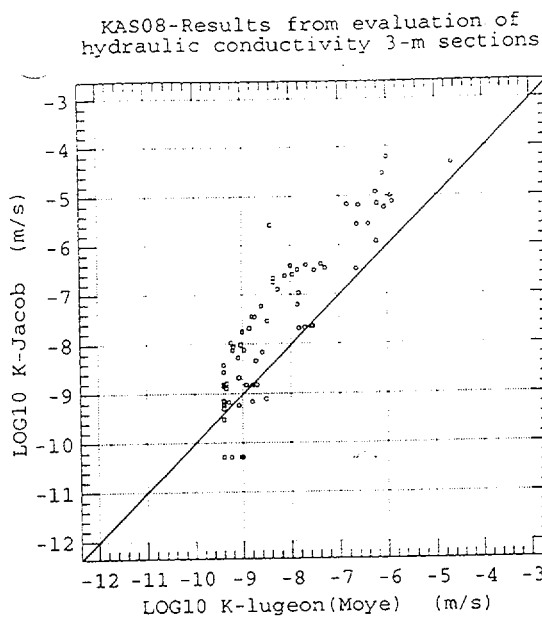


Figure 2.1. Corehole KAS08. Injection tests with test length 3 m. Left: Cross plot between hydraulic conductivity (K) from recovery, transient evaluation (K-Jacob) and the injection period, stationary evaluation (K-Lugeon). Right: Probability distribution of the $\text{Log}_{10}K$ (Measurement limit approximately 5×10^{-11} m/s).

Interference tests have normally had a D + R of 3 + 2 days but two tests had a D + R of 53 + 33 days and 92 + 31 days. In 12 out of 20 interference tests the tested section was surrounded by packers and in the rest the open borehole was pumped. During the first phase of the pre-investigations about 35 observation sections were available and during the last tests over 100 observation section were used for pressure registration. The purpose of the interference tests was to:

- estimate the transmissivity and storativity of an intersected conductive structure.
- identify the direction of and connection between major conductive structures.
- create data sets for future calibrations of numerical groundwater models.

Late during the prediction stage it was decided that the access ramp to Äspö HRL should start at the Simpevarp peninsula (south of Hålö) and not Äspö. One inclined corehole (more or less horizontal), KBH02, was drilled from Hålö towards the south of Äspö. In this corehole it was only possible to

perform three airlift tests. Except for the southernmost part of Äspö there were only a few geohydrological data for the tunnel part up to chainage 1 475 m, southern part of Äspö (Figure 2.2).

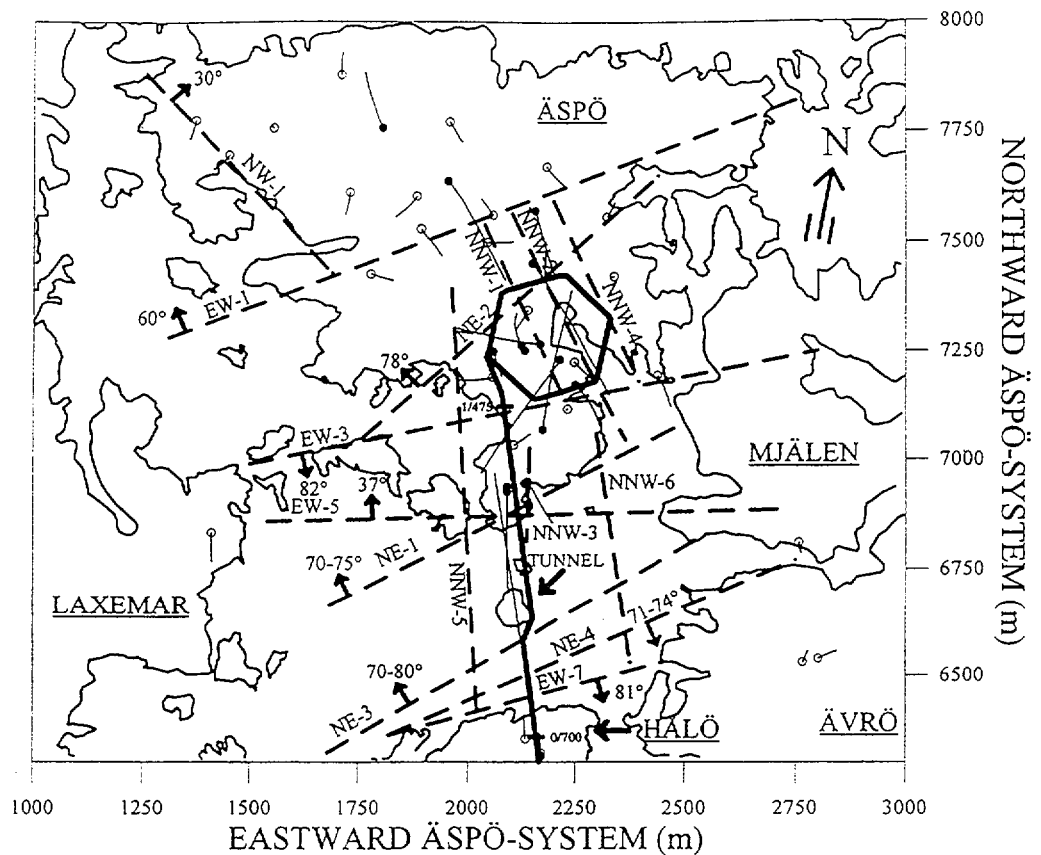


Figure 2.2. Major conductive structures on Äspö.

2.2

MODEL

It was decided early to try to define major conductive structures deterministically. The base for the interpretation of the interference test was the geological structural model. The conductivity of some geological structures was considered low and neglected in the geohydrological model. Some structures were only seen as possible conductive structures, generally just based on geophysics. However, conductive structures striking N-S or NNW, more or less vertical, were estimated to be present from the interference tests. These structures could not be identified from the geological and geophysical investigations. The NNW structures were assumed to consist of more or less extensive single fractures lying in an en-échelon pattern forming conductive structures of rather large extent. (The maximum horizontal stress component are located in the sector $N16^{\circ}W$ to $N65^{\circ}W^3$.)

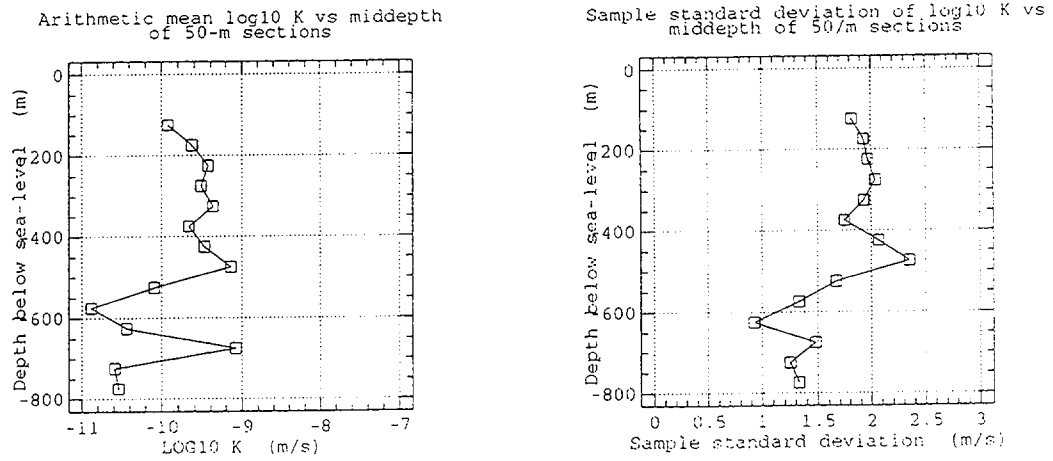


Figure 2.3. Left: Arithmetic mean of $\text{Log}_{10}K$ for 50 m sections (corehole KAS02-08 on Äspö, 3 m-scale injection tests). Right: Standard deviation of $\text{Log}_{10}K$ for 50 m sections (corehole KAS02-08 on Äspö, 3 m-scale injections tests). (Conductive structures, fracture zones, are included in the data in the left and right figures).

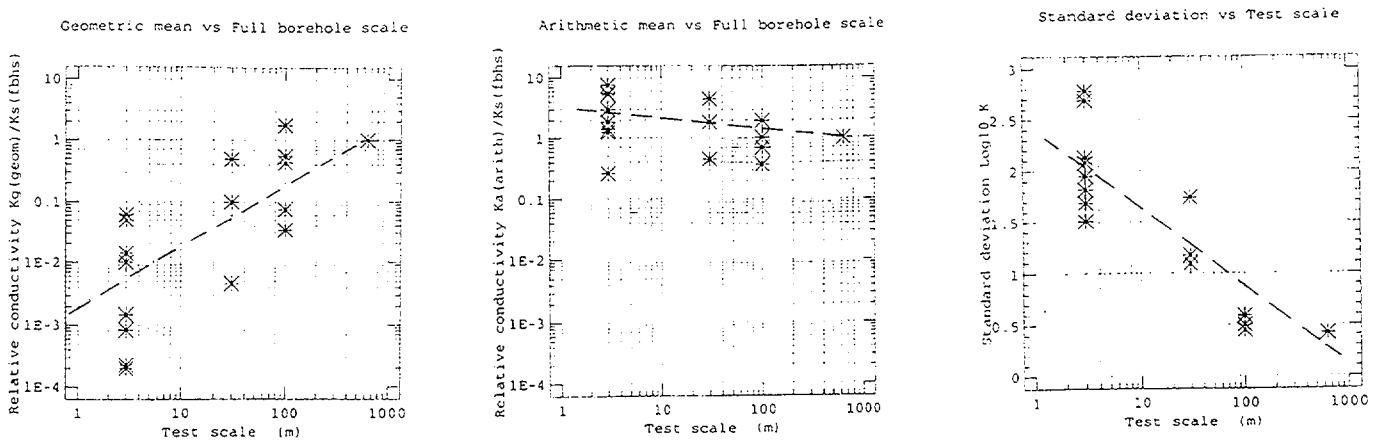


Figure 2.4. Relative hydraulic conductivity and standard deviation for the distribution of $\text{Log}_{10}K$ for different test scales. $K_s = T/L$ where T is the transmissivity evaluated from the test of the entire borehole of length L . (In the figures above L is approximated to 600 m even though L was about 500 to 800 m for the boreholes).

The final model of the conductive structures can be seen in Figure 2.2. The transmissivity (T) range of the structures was $5 \times 10^{-7} - 3 \times 10^{-4} \text{ m}^2/\text{s}$ (structure NE-1 and NE-4 had the largest T and most of the structures $10^{-5} - 10^{-4} \text{ m}^2/\text{s}$).

The hydraulic conductivity between the conductive structures was considered to be stochastic. Äspö was divided into 4 main regions with different geometric mean values of K (K_g) and a decreasing standard deviation of $\text{Log}_{10}K$ (S_{LOG10K}) according to Figure 2.3. The entire Äspö-data set for $\text{Log}_{10}K$ and S_{LOG10K} is shown in Figure 2.3. (It should be noted that below depth 550 m data are from only one corehole.) The regional values of K_g for test scale 3 m were:

- North of EW-1 $K_g = 7.9 \times 10^{-10} \text{ m/s}$
- Between EW-1 and NE-2 $K_g = 3.2 \times 10^{-10} \text{ m/s}$
- Between NE-2 and EW-3 $K_g = 1.0 \times 10^{-10} \text{ m/s}$
- Between EW-3 and NE-1 $K_g = 1.0 \times 10^{-10} \text{ m/s}$

South of NE-1, K_g was assumed to be equal or greater than $1.0 \times 10^{-10} \text{ m/s}$ but was considered uncertain as no injection tests had been performed there.

It was also found that Fine-grained granite was most conductive and that greenstone, diorite and mylonite were least conductive.

It was also shown that the arithmetic mean of $K(K_a)$ was decreasing, the geometric mean of $K(K_g)$ was increasing and the standard deviation of $\text{Log}_{10}K$ was decreasing with increasing test scale (test section length: 3 m, 30 m, 100 m, entire hole. As mentioned above also the hydraulic test duration was longer for larger test section lengths). Empirical relationships were used to scale K_g and S_{Log10K} according to cell size in the numerical groundwater model before the stochastic generation of K for each cell (Figure 2.4). The results in Figure 2.4 are not exactly what could be expected theoretically (Dagan D., 1979) and further evaluations and investigations are needed.

3. LPT2 TEST

3.1 OBJECTIVES

The objective in the pumping test was to evaluate the consistency between the results from LPT2 and the current conceptual model of Äspö (Wikberg et al., 1991) and also to provide a data set for future numerical groundwater flow simulations.

The aim of a large scale three-dimensional tracer test was mainly to give information on how the fracture zones are interconnected but also some estimates on transport parameters such as residence time, dispersivity, flow porosity and

hydraulic fracture conductivity. The experimental results from the tracer tests were also considered to be valuable for future numerical transport simulations.

Tracer dilution measurements were performed both prior to and during LPT2. The purpose of the tracer dilution measurements was to evaluate the consistency with the conceptual model given by Wikberg et al. (1991) and to select borehole sections for tracer injections for the LPT2 test.

Numerical groundwater flow simulations were carried out in advance of the field experiment. This was done for two reasons; the first reason was to get some guidance from the numerical simulations for the planning of the field experiment secondly, the evaluation of the predictive capabilities of the numerical model requires that the results from the model are documented prior to the experiment.

3.2 TEST DESIGN AND PERFORMANCE

3.2.1 General

The tracer test was performed on the southern part of Äspö in the area where the Hard Rock Laboratory is under construction. Groundwater was discharged from the borehole KAS06 creating a converging flow field through hydraulic conductors, i.e. fracture zones, surrounding the borehole. Tracers were injected in 6 packed-off sections in nearby boreholes (KAS02, KAS05, KAS07, KAS08 and KAS12), where these intersect the hydraulic conductors.

The selection of borehole KAS06 and the borehole sections for tracer injection were based on the numerical groundwater flow simulations, the geological and geohydrological model realisations of the Äspö bedrock and the dilution measurements in 12 boreholes (22 borehole sections) made before the LPT test.

3.2.2 Tracer Injections

The first tracers were injected approximately two weeks after the pumping was started, to make sure the tracers were injected in a steady state groundwater flow field.

Three radioactive isotopes and one fluorescent dye tracer were injected in four borehole sections into the fracture system around the pumped borehole. One tracer per injection point was used. Towards the end of the tracer test two additional tracer pulses were injected in a second run in two boreholes not used in the previous run.

The chemical form and half-lives of the used radio tracers are given in Table 3.1.

Table 3.1. Tracer Used.

| Tracer | Half-life | Chemical form | Remarks |
|---------|-----------|-----------------------------------|---------------|
| In-114 | 49.51 d | In(III)-EDTA | metal complex |
| I-131 | 8.04 d | I(I) | negative ion |
| Re-186 | 3.78 d | Re(VI)O ₄ ⁻ | negative ion |
| Uranine | - | Fluorescent dye | |

In the core boreholes, with prefix KAS, usually two sections are available to circulate the groundwater from the isolated section up to the ground surface and back again. This circulation makes it possible to use tracers in one section without contaminating adjacent sections. The circulation pump is located in the upper enlarged part of the borehole in a plastic (PEM) tube (Figure 3.1). The circulation capacity of the section water is measured by a float type flow meter. Pressure gauges are used for monitoring the pressure situation. Injection of the tracers into the circulating section is made with an injection pump which is temporary connected to the trace element unit (Figure 3.2). The injection of the tracer solution is made during one circulation/mixing cycle in order to achieve the best possible initial mixing. Manual sampling of section water for analysis of tracer concentration is also made in the trace element unit.

The tracers were injected with **the intermittent decaying pulse injection technique** (Figure 3.3), that meets the following requirements:

- Possibilities to perform in situ measurements of the tracer inflow levels with gamma spectrometric probe and a multi level sampler when the tracers reach the pumping borehole.
- Well defined in time and space, eg. no dispersion of the tracers in the injection borehole section. No disturbance of the ground water flow field and no tracers forced out to an unknown distance in the adjacent fracture system.
- Minimize the handling and storing of radioactive tracers at the injection borehole.

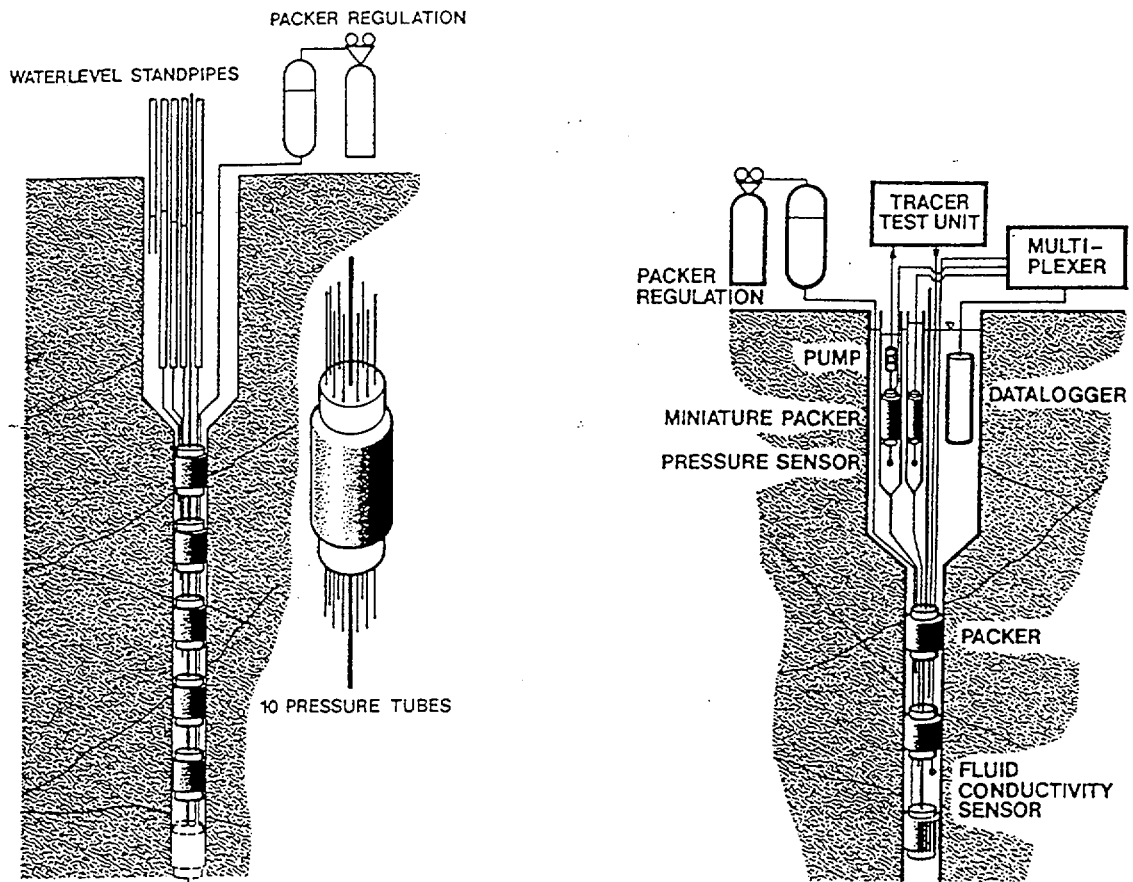


Figure 3.1. Groundwater monitoring. (Almén and Zellman, 1991). Left: Multi-packer system in a telescope shaped borehole. Right: Schematic set-up of monitoring system with the Borre data logger. The figure also shows water circulation equipment for one section, the tracer test unit and the fluid conductivity sensor.

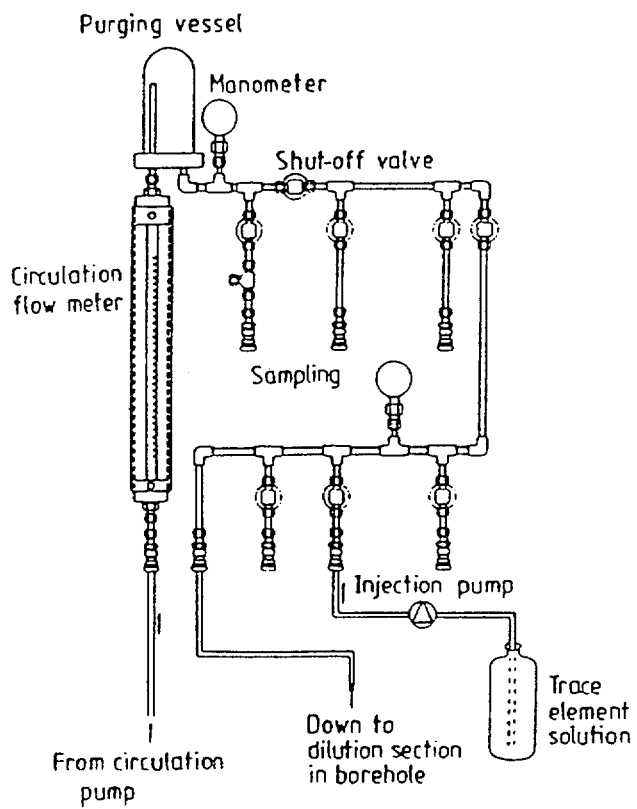


Figure 3.2. Schematic illustration of the tracer unit for tracer injections into the circulation system and water sampling (Almén and Zellman, 1991).

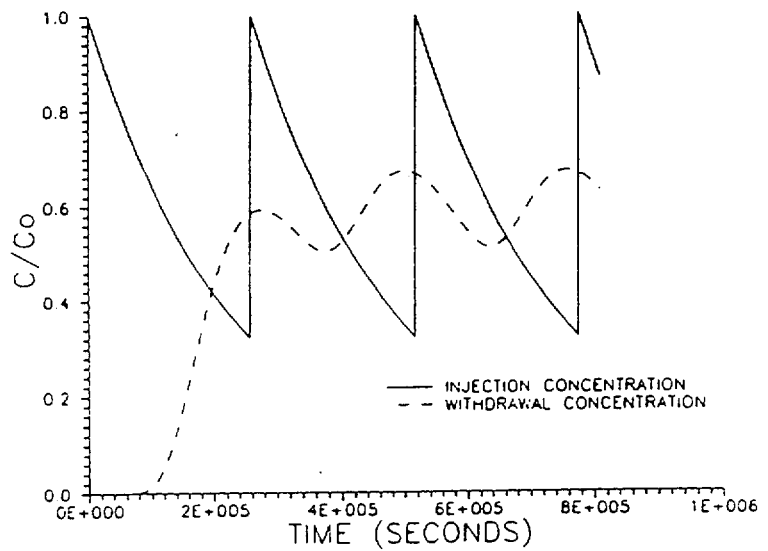


Figure 3.3. Intermittent decaying pulse injection. Example of a theoretical breakthrough curve resulting from an intermittent decaying pulse injection in a stream tube 70 m long and 1 m² cross sectional area (Rhén et al, 1992).

Intermittent decaying pulse injection means that pulses of tracers are injected in a clearly defined borehole section with constant time interval and without excess pressure, e.g. one pulse every third or sixth day. The equipment needed is the same as for measuring groundwater flow with the dilution technique. The injected tracer is diluted by the groundwater flowing through the borehole section. When the concentration has reached a lower limit after a couple of days, a new pulse is injected containing the same mass of tracer that has been released from the borehole section during the dilution process.

The tracers were injected with the following schedule:

- (1) 4 000 ml of concentrated of tracer solution (C_{∞}) was injected with constant flow into the circulation system during one mixing cycle (c f Table 3.3).
- (2) The magnitude of the groundwater flow in the studied section was determined by sampling and analysis of the tracer concentration (C_0). The dilution of the tracer with time is proportional to the groundwater flow.
- (3) From the groundwater flow and mass balance calculations, the amount of tracer that has to be added to reach the initial C_0 concentration in the borehole section during the next injection pulse is determined.
- (4) Repeated injection of 4 000 ml concentrated tracer solution every third (sixth) day according to the procedure (1) - (3) above.
- (5) Continuous monitoring of the groundwater flow by sampling and analysis of the tracer concentration in field every day.

Table 3.2. Tracer Runs.

| Borehole section | Tracer | Run No. ¹ | Injection Type ² |
|------------------|------------------|----------------------|-----------------------------|
| KAS02-4 | Indium (In-114) | 1 | dp |
| KAS05-3 | Uranine | 2 | dp |
| KAS07-4 | Iodine (I-131) | 1 | idp |
| KAS08-1 | Rhenium (Re-186) | 1 | idp |
| KAS08-3 | Rhenium (Re-186) | 2 | dp |
| KAS12-2 | Uranine | 1 | idp |

¹ 1 = initial choice, 2 = additional pulse injection

² idp = intermittent decaying pulse injection, dp = decaying pulse injection

Table 3.3. Tracer Injection Data.

| Borehole section | Injection time (h min) | Injection flow (ml/min) | Injection volume (ml) | Injection no (a) | Injection int (b) |
|------------------|------------------------|-------------------------|-----------------------|------------------|-------------------|
| KAS02-4 | 5.21 | 12.5 | 4 000 | 1 | - |
| KAS05-3 | 14.56 | 27.9 | 25 000 | 1 | - |
| KAS07-4 | 13.31 | 4.9 | 4 000 | 5 | 6 |
| KAS08-1 | 7.2 | 9.5 | 4 000 | 7 | 3 |
| KAS08-3 | 6.53 | 9.7 | 4 000 | 1 | - |
| KAS12-2 | 6.42 | 12.0 | 5 000 | 7 | 3 |

Injection time = one mixing cycle

a) number of injections during the test

b) number of days between each injection

3.2.3 Pumping Borehole KAS06

KAS06 is a 602 metres deep borehole and has an inclination to the horizontal plane of 60° towards the north. The borehole is of telescope type and has a diameter of 164 mm in the uppermost 100 meters and 56 mm below that section. The pumping was done with an open hole configuration with a submersible pump placed 85 metres below the top of the casing (Figure 3.4).

Data for the pumped section is found in Table 3.4.

Table 3.4. Data for the Pumped Borehole KAS06.

| | |
|--------------------------------|--|
| Test section | 0-602 m |
| Open borehole | |
| Dip of borehole | 60° |
| Well radius (wellbore storage) | $91.5 \times 10^{-3} \text{ m}^3/\text{s}$ |
| Flowrate | |
| 0-4320 min | $2.01 \times 10^{-3} \text{ m}^3/\text{s}$ |
| 4320-10439 min | $2.52 \times 10^{-3} \text{ m}^3/\text{s}$ |
| 10439-132595 min | $2.25 \times 10^{-3} \text{ m}^3/\text{s}$ |
| Pumping time | 132 595 min |
| Maximum drawdown | 51.77 m |

Sampling in the borehole was done with a multilevel sampler (Figure 3.4), and the sampling levels were decided from the distribution of the flow into the borehole during pumping (Figures 3.4 and 3.5).

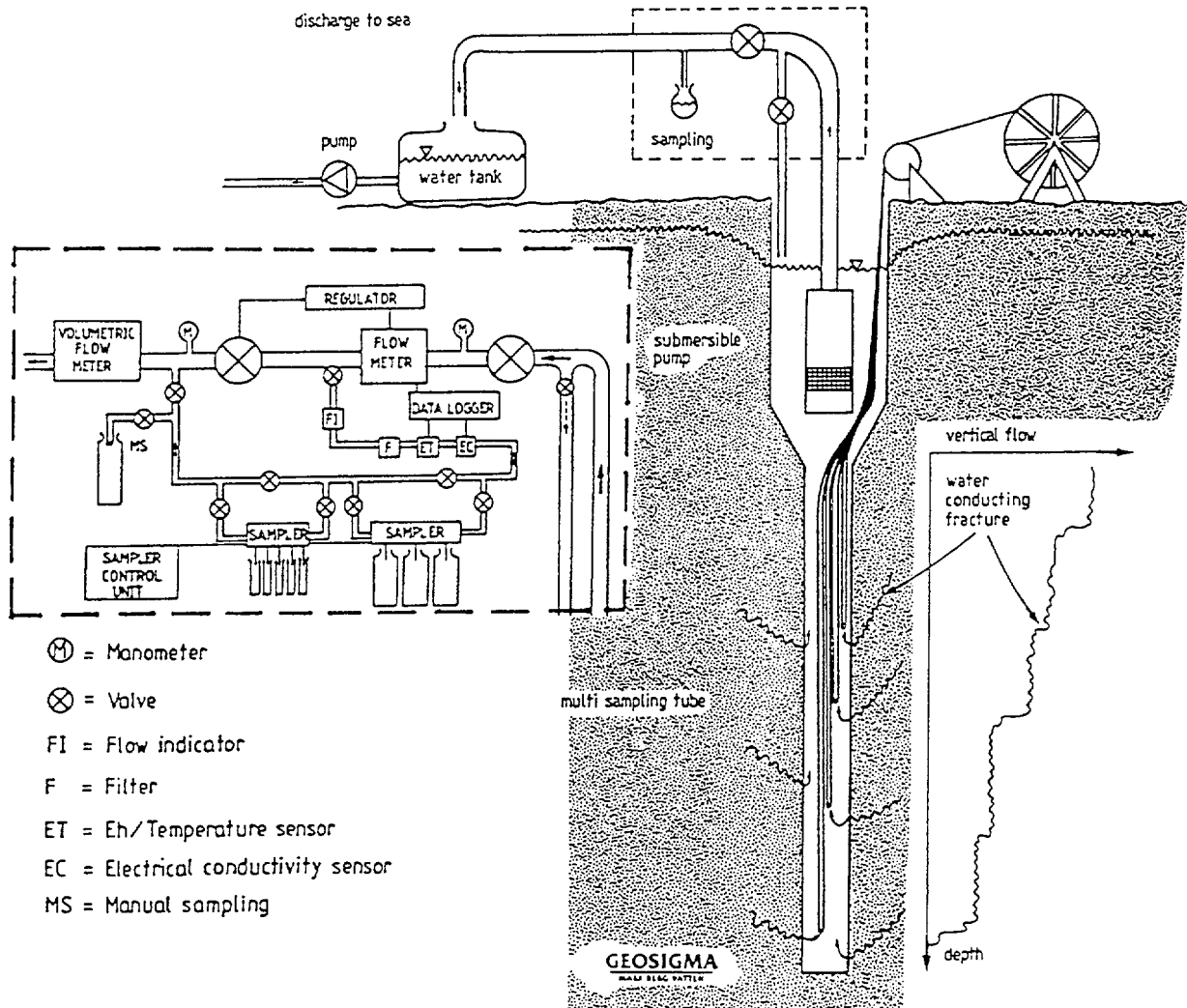


Figure 3.4. Equipment set-up for tracer test carried out during LPT2. On-site recording and analysis of tracers in the pumped water and in-situ sampling of water of inflowing sections of the borehole (identified from flow meter logging) by a multi-level sampling device (Almén and Zellman, 1991).

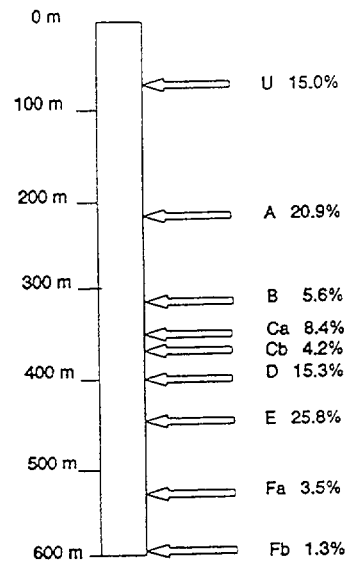


Figure 3.5. Inflow distribution in KAS06 determined from spinner data. Letters A-F refers to the name of the conductor and U to the interval 0-100 meters.

Table 3.5. Sampling Levels.

| Section ¹ No. - m | Hydraulic Label | Conductor ² Section (m) |
|---------------------------------|--------------------|---------------------------------------|
| 8 - 190 | A | 217 |
| 7 - 290 | B | 312 |
| 6 - 340 | C,a | 353 |
| 5 - 360 | C,b | 364 |
| 4 - 390 | D | 399 |
| 3 - 430 | E | 448 |
| 2 - 540 | F,a | 558 |
| 1 - 570 | F,b | 596 |

¹Instrumental section, m along borehole below casing top

²Major hydraulic conductor with its corresponding section

The technical design of the experimental set-up is similar to the one used in the tracer experiment discussed earlier; the set-up is illustrated in Figures 3.1 and 3.2.

The measurement of groundwater flow in a borehole section is based on dilution of an added chemical substance that is mixed in the groundwater in the borehole section and thereafter the concentration in the water is determined at regular intervals. The decrease of tracer concentration as a function of time is proportional to the groundwater flow through the section. This way of measuring groundwater flow is termed dilution technique.

4. RESULTS

4.1 GROUNDWATER FLOW SIMULATIONS

Altogether nine trajectories, assumed to be of interest in the LPT2 experiment, were calculated and illustrated graphically. As an illustration of the simulations only one example is shown, namely injection in KAS02, section B4 (Figure 4.1).

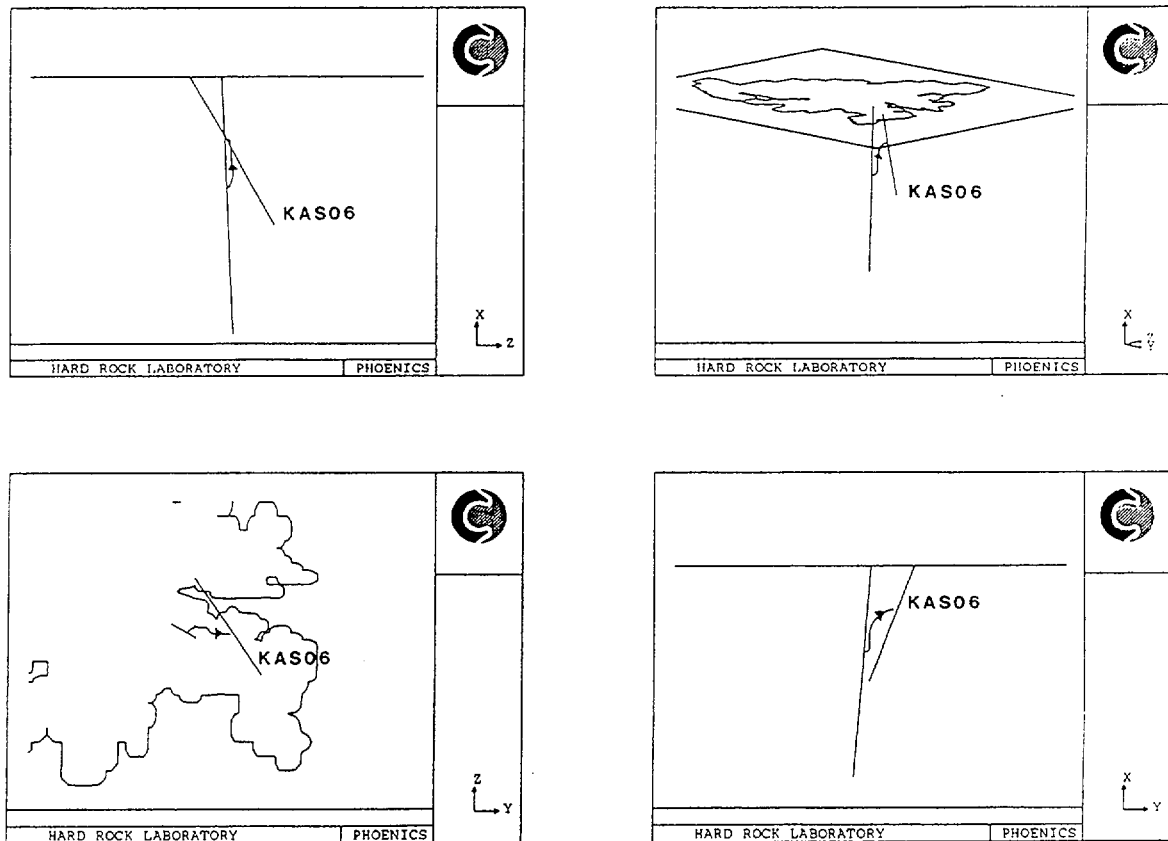


Figure 4.1. Trajectory when injecting in KAS02, section B4.

The inflow to KAS06 during pumping has mainly been estimated from spinner measurements (the flowrate along the borehole can be measured with a spinner during pumping), except for inflow from EW-3 which is estimated from tracer measurements. The total inflow, 2.25 l/s, is estimated to be distributed as follows: EW-3 (15%), NNW-1 (21%), EW-5 (33%), NNW-2 (26%) and EW-X (5%).

A distance-drawdown plot is shown in Figure 4.2. In this plot the total drawdown in each observation section at stop of pumping versus the squared distance to the pumping borehole is shown. For comparison, the Theis type curve is also included in the figure.

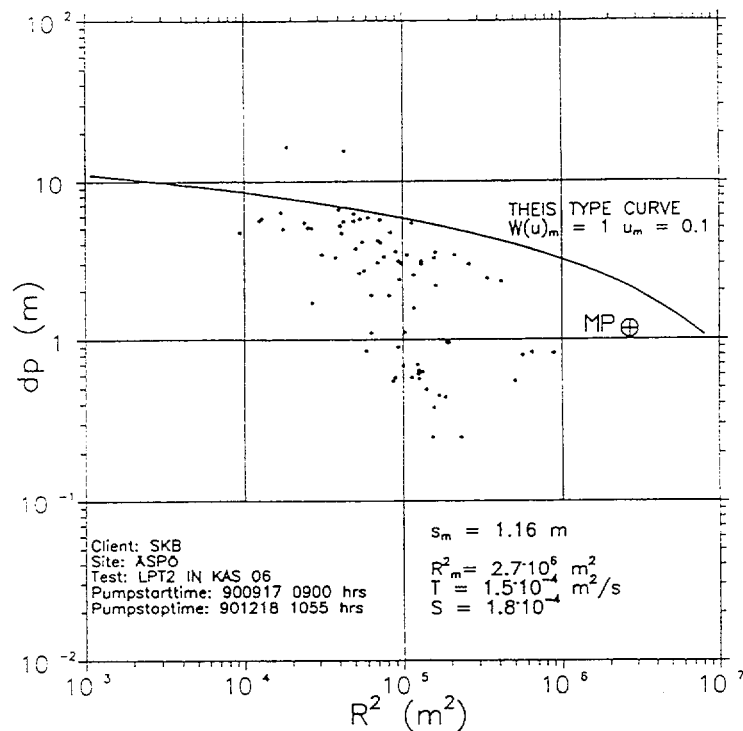


Figure 4.2. Distance-drawdown graph at stop of pumping during LPT-2.

The transmissivities of the fracture zones have been estimated by analyzing the drawdown responses in borehole sections, assumed to be intersected by fracture zones. The general conclusion is that the results from LPT2 support the current conceptual model (Wikberg et al., 1991). LPT2 also indicates that zone EW-3 may be more transmissive than assumed in the conceptual model.

TRACER TEST

The tracer inflows versus time, i.e. breakthrough, were measured along KAS06 by taking samples intermittently at nine identified inflow levels (Figure 3.5). As the same tracer can enter the borehole in several sections the measured value in a certain section has to be corrected for the mass of tracer coming from deeper levels than the studied section.

Indium injected in KAS02, section 4, and Iodine injected in KAS07, section 4, was not found in the withdrawal water. However, both Rhenium and Uranine was found in the analyzed water from KAS06. No tracers were found at levels 1 and 2 (Table 3.4).

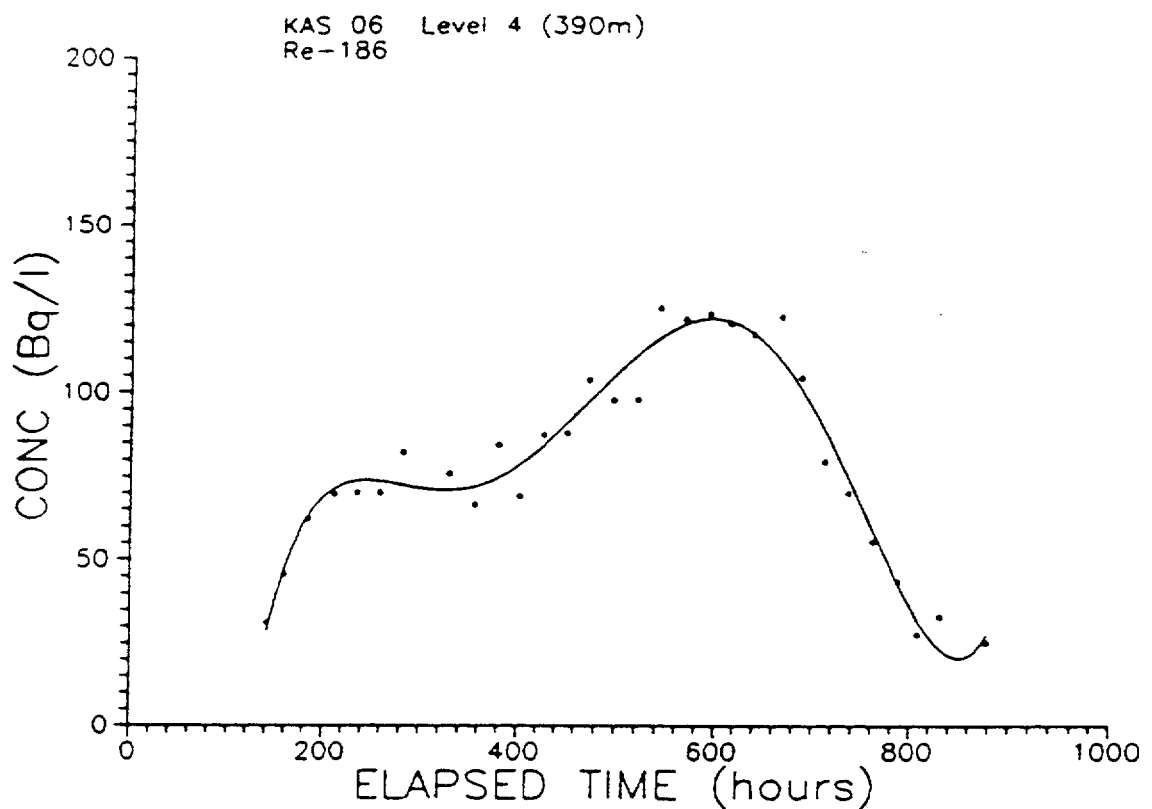


Figure 4.3. Breakthrough of Re-186 at sampling level 390 m in KAS06. Experimental data points and fitted five-degree polynomial (solid line).

As an example the breakthrough at sampling level 4 (390 m) of the tracer injected in KAS08 is shown in Figure 4.3.

The cumulative apertures of the hydraulically active fractures in the fracture zones were estimated to be 5-10 times greater in EW-5 compared to NNW-1 and NNW-2 (10×10^{-3} - 30×10^{-3} m compared to 2×10^{-3} - 5×10^{-3} m). The fracture conductivities are however greater in NNW-1 and NNW-2 compared to EW-5. The conclusion is that EW-5 is built up of many low conductive fractures whereas zones NNW-1 and NNW-2 of a few highly conductive fractures. The calculated flow porosity depends on the estimated width of the zone and if EW-5 is assumed to have a width of 100 m and NNW-1 and NNW-2 5-10 m the flow porosities are in the range of 0.02% for EW-5 and 0.1% for NNW-1 and NNW-2.

The dispersivities were estimated to be one tenth to one fifth of the flow path distance and the Peclet number to be 4-11, where the lower values are representative for EW-5 and the higher for NNW-1 and NNW-2.

4.4 DILUTION MEASUREMENTS

In total 68 dilution measurements have been performed at Äspö HRL (until January 1991). An example of a dilution curve is shown in Figure 4.4.

The flow during natural gradient is generally between 0 and 35 ml/min and the variation seems, according to the scarce data, to decrease with depth, as can be expected, (Figure 4.5).

By applying the equation of continuity for the tracer, and using the dilution curve, it is possible to estimate the groundwater flow through the borehole section. In this process the data were also analyzed individually, looking for consistency and possible measurement errors (like leakage in tube fittings). The final result of the analysis is presented in Table 4.1.

The measured flow rates, both during natural conditions and during LPT2, can be used for an analysis of the consistency of the current conceptual model presented by Wikberg et al. (1991). A large difference between the natural and forced groundwater flow indicates that the analyzed section, and hence the fracture zone, is in good hydraulic contact with the pumped borehole (Figure 4.6). It can, from this analysis, be concluded that the current conceptual model describes the system of fracture zones on Äspö in a realistic way. Improvements are however still possible, as some sections did not respond to the pumping as could be expected (for example KAS02-B4).

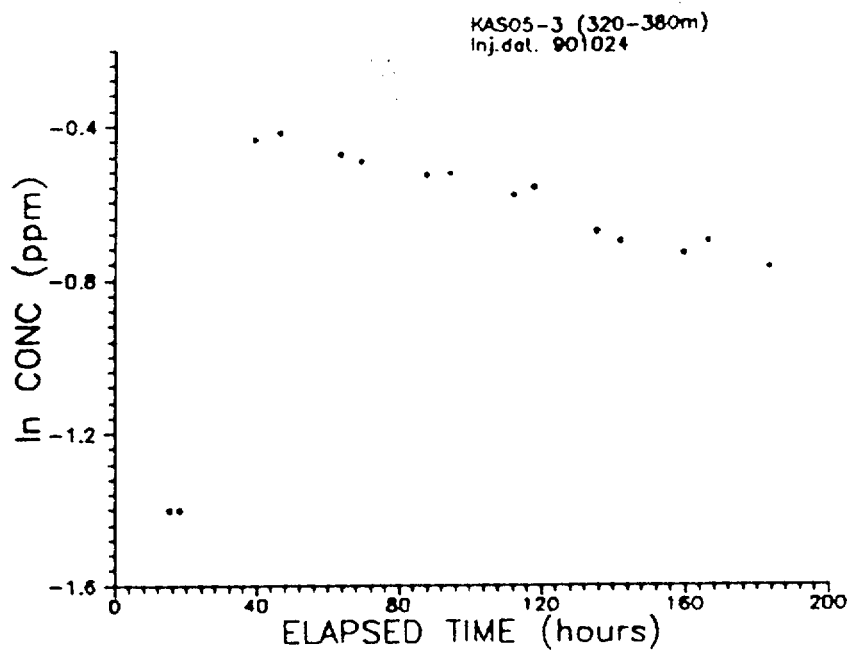


Figure 4.4. Example of a dilution curve.

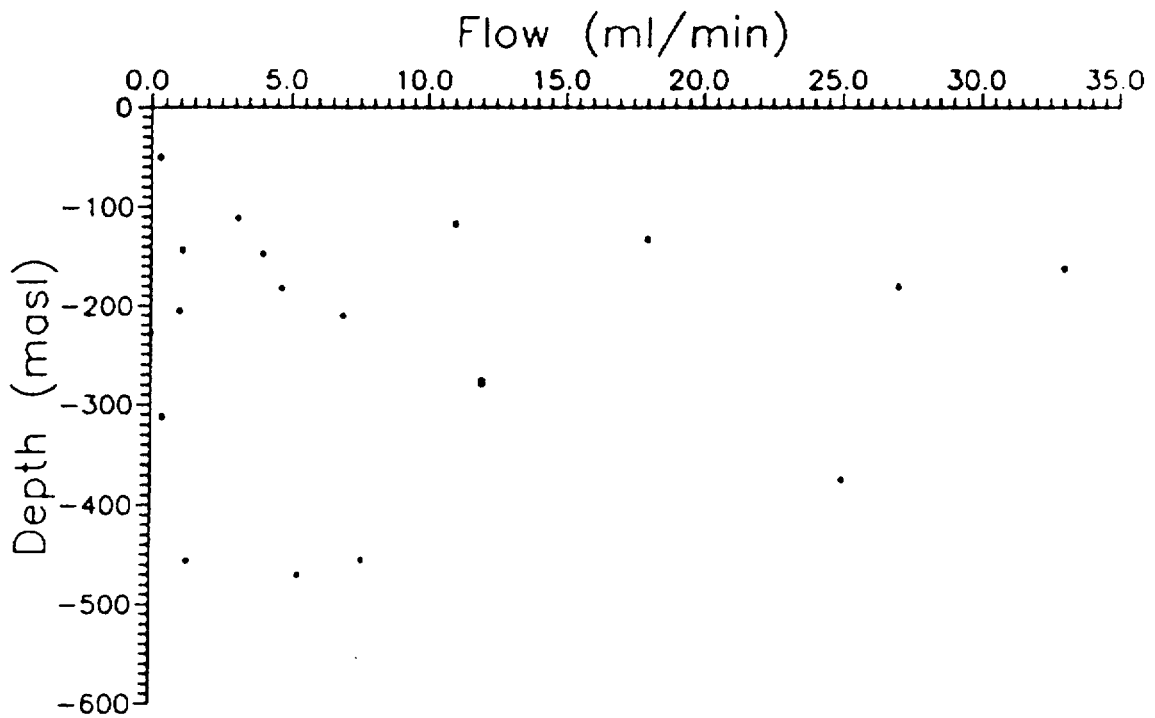


Figure 4.5. Measured flow (through borehole sections) versus depth below ground surface during natural gradient (NG2), (dilution measurements).

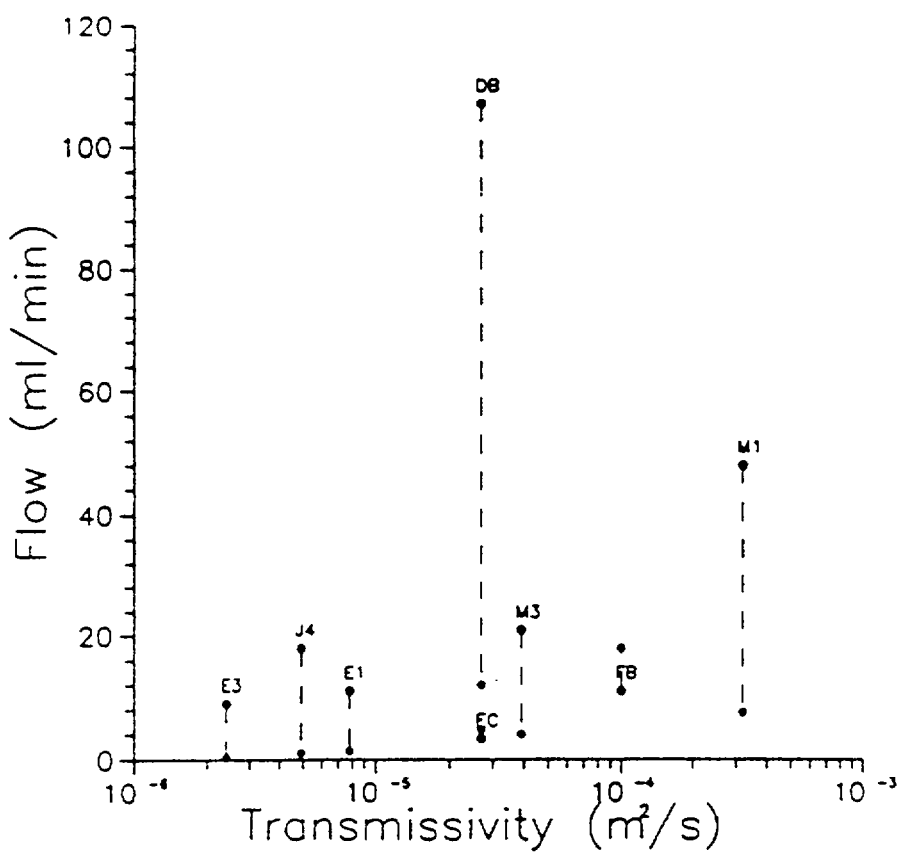
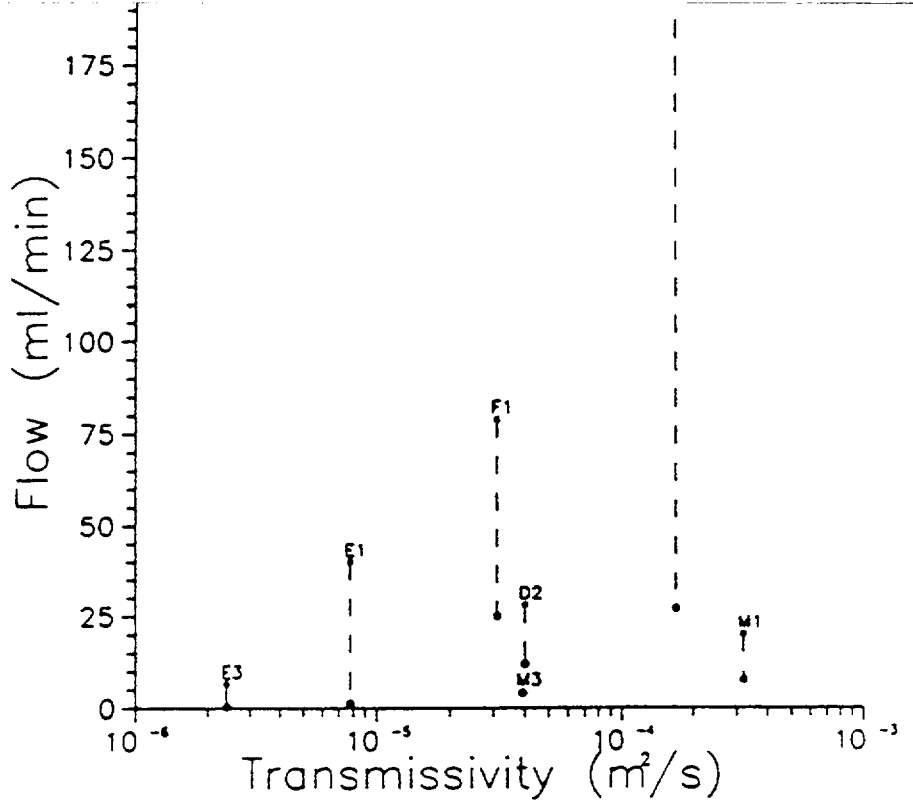


Figure 4.6. Flow (through borehole sections) versus transmissivity (of the zone(s) intersecting the section) during LPT1 (top) and LPT2 (bottom) compared to natural gradient conditions (lower values). The labels on the plot are borehole section codes and these codes can be found in Table 4.1.

Table 4.1. Dilution Rates (Ittner et al, Rhén et al, 1993).

LPT1 and LPT2 are the Long Time Pumping tests 1 and NG1 and NG2 are dilution measurements during Natural Gradient.

| Borehole | Code | Section (m) | Flow (ml/min) | | | |
|----------|------|----------------|---------------|-----|-------|-------|
| | | | LPT-1 | NG1 | NG2 | LPT-2 |
| KAS02-4 | B4 | 309-345 | 1.1 | - | (*) | 2 |
| KAS02-2 | B2 | 800-854 | (*) | - | (*) | 4 |
| KAS03-5 | C5 | 107-252 | - | - | 6.9 | - |
| KAS03-2 | C2 | 533-626 | - | - | (120) | - |
| KAS04-2 | D2 | 332-392 | 28 | - | 12 | - |
| KAS05-3 | E3 | 320-380 | 6.5 | - | 0.4 | 9 |
| KAS05-1 | E1 | 440-549 | 40 | 1.8 | 1.3 | 11 |
| KAS06-5 | F5 | 191-249 | 197 | 25 | 27 | ph |
| KAS06-1 | F1 | 431-500 | 79 | 52 | 25 | ph |
| KAS07-4 | J4 | 191-290 | ph | - | 1.0 | 18 |
| KAS07-1 | J1 | 501-604 | ph | - | 5.3 | - |
| KAS08-3 | M3 | 140-200 | 4.3 | - | 4.0 | 21 |
| KAS08-1 | M1 | 503-601 | 20 | 5.5 | 7.6 | 48 |
| KAS09-4 | AD | 116-150 | | | 11 | - |
| KAS11-5 | CE | 47- 64 | | | 0.3 | - |
| KAS11-2 | CB | 153-183 | | | 33 | - |
| KAS12-3 | DC | 235-278 | | | 0 | - |
| KAS12-2 | DB | 279-330 | | | 12 | 107 |
| KAS13-4 | ED | 151-190 | | | 1.1 | - |
| KAS13-3 | EC | 191-220 | | | 4.7 | 3.3 |
| KAS14-4 | FD | 131-138 | | | 3.1 | - |
| KAS14.2 | FB | 147-175 | | | 18 | 11 |

- = No measurement, ph = pumphole

* = Failed measurement (see text)

5. CONCLUSIONS

5.1 NUMERICAL MODEL

A general agreement between measured and predicted travel times and drawdowns has been found. The travel times can be brought to agreement with a reasonable flow porosity. Drawdown predictions were not carried out prior to the experiment and the comparison is thus not to be considered as a validation. The comparison does anyway indicate that a fairly close agreement can be obtained, which is once again a confirmation that the conceptual model is sound.

5.2 PUMPING TEST

The qualitative and quantitative evaluation of the pumping test LPT-2 is consistent with the overall conceptual model presented in Wikberg et al. (1991). The hydraulic importance of Zone EW-5w and the NNW-fracture system and indirectly also NE-1w is clearly demonstrated. However, the test indicated that some modifications of this model are necessary to satisfactorily explain all drawdown responses observed.

5.3 TRACER TEST

The report concludes that EW-5 is a good but complex hydraulic conductor with many widely spread but interconnected fracture flow paths. NNW-1 and NNW-2 are very good hydraulic conductors with a few narrowly spaced water conducting fractures. EW-3 should be considered as a more important hydraulic conductor than is assumed in the conceptual model.

The measurements were checked for consistency with the current conceptual model. The general conclusion was that the experimental results support the conceptual model presented in Wikberg et al. (1991).

6. FINAL COMMENTS

Several organizations from different countries are now participating in the Äspö HRL project. These organizations have formed a group called "Task force on groundwater flow and transport of solutes". LPT2 has been one of the cases that has been used for numerical groundwater flow and transport simulations, and the results from these modelling will be reported during 1994.

During the excavation of the tunnel the existence of the NNW structures has been confirmed, although their exact character and position still are uncertain.

The structure EW-5 does not appear as a distinct fracture zone intersecting the tunnels. The subhorizontal structures in Wikberg et al. (1991) were considered "possible" and further evaluation is needed in order to see if the mapped subhorizontal features (fractures) in the tunnel may act as conductive "zones".

REFERENCES

Almén K.-E. and Zellman O. (1991). Äspö Hard Rock Laboratory. Field investigation methodology and instruments used in the pre-investigation phase 1986-1990, SKB Technical Report 91-21, Stockholm.

Dagan G. (1979). Models of groundwater flow in statistically homogenous porous formations. Water Resources Research, 15:1.

Gustafson G., Stanfors R., Wikberg P. (1988). Swedish Hard Rock Laboratory. First evaluation of pre-investigations and description of the target area, the island of Äspö. SKB Technical Report 88-16, Stockholm.

Gustafson G., Stanfors R., Wikberg P. (1989). Swedish Hard Rock Laboratory. Evaluation of 1988 year pre-investigations and description of the target area, the island of Äspö. SKB Technical Report 89-16, Stockholm.

Moye D. G. (1967). Diamond drilling for foundation exploration. Civ. Eng. Trans. 7th Inst. Eng. Australia.

Rhén I. (ed), Svensson U. (ed), Andersson J.-E., Andersson P., Eriksson C.-O., Gustafsson E., Ittner T., Nordqvist R. (1992). Äspö Hard Rock Laboratory: Evaluation of the combined long-term pumping and tracer test (LPT2) in borehole KAS06, SKB Technical Report 92-32, Stockholm.

Stanfors R., Erlström M., Markström I. (1991). Äspö Hard Rock Laboratory. Overview of the investigations 1986-1990, SKB Technical Report 91-20, Stockholm.

Wikberg P., Gustafson G., Rhén I., Stanfors R. (1991). Äspö Hard Rock Laboratory. Evaluation and conceptual modelling based on the pre-investigations 1986-1990. SKB Technical Report 91-22, Stockholm.

C.2 The Äspö Redox Experiment in Block Scale

tracer test results obtained 125 days after tracer injections

Erik Gustafsson
GEOSIGMA AB
Uppsala, Sweden

1. INTRODUCTION

The block-scale redox experiment at Äspö HRL includes analysis and interpretation of isotope data and water chemistry, mineralogy and fracture coatings in a vertical fracture zone, breached by the access tunnel at a depth of 70 meters. The chemical composition of sampled groundwaters is evaluated with mixing models. It is concluded that mixing calculations and interpretation of chemical data will be improved if the flow and transport characteristics in the fracture zone studied should be known in more detail. A general picture of the redox zone hydraulics have been possible to obtain from previously performed measurements of hydraulic head in packed-off borehole sections and a pressure build-up test, together with drillcore mapping and fracture mapping of the tunnel perimeter (Banwart et al., 1994). However, some attributes essential for the analysis and understanding of the hydrochemical results could not be revealed by the fracture mapping and hydraulic measurements. These attributes, that may be determined by means of a tracer test, are residence time, dispersion and flow porosity.

2. OBJECTIVES OF THE TRACER TEST

The objectives of the tracer test were primarily to verify hydraulic connections and to determine flow porosity, residence time and magnitude of dispersion. The aim is to provide data useful for the interpretation of the redox zone hydrochemistry.

3. DESIGN AND PERFORMANCE

The Äspö HRL access tunnel intersects the redox zone approximately perpendicular to the shear plane of the fracture zone at a depth of about 70 metres. Figure 3.1a and 3.1b show a section and plan view, respectively, of the fracture zone and the access tunnel. A thorough description of the geological setting of the site is presented in Banwart et al. (1994).

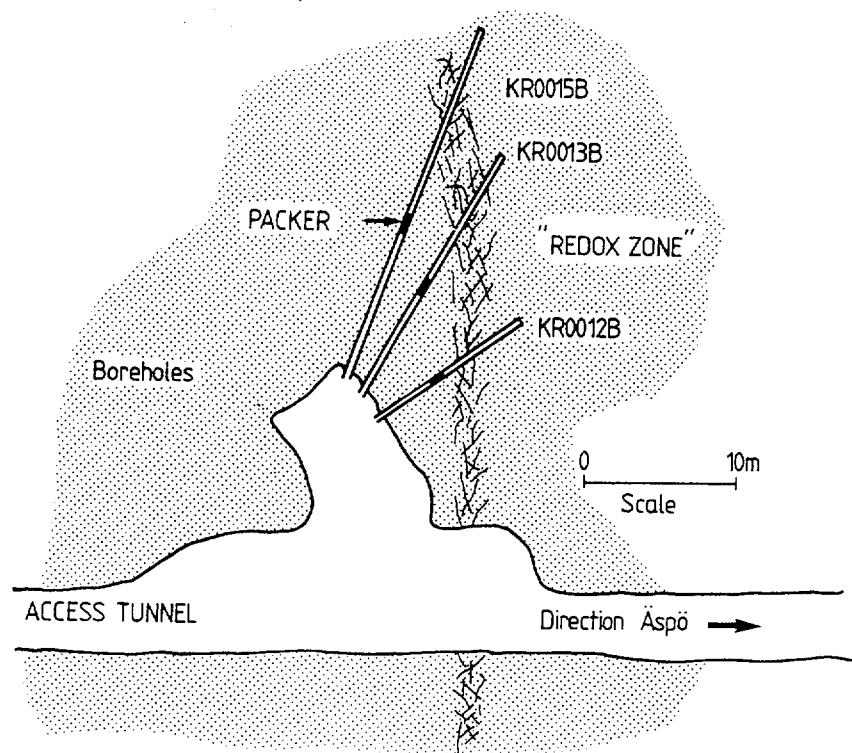
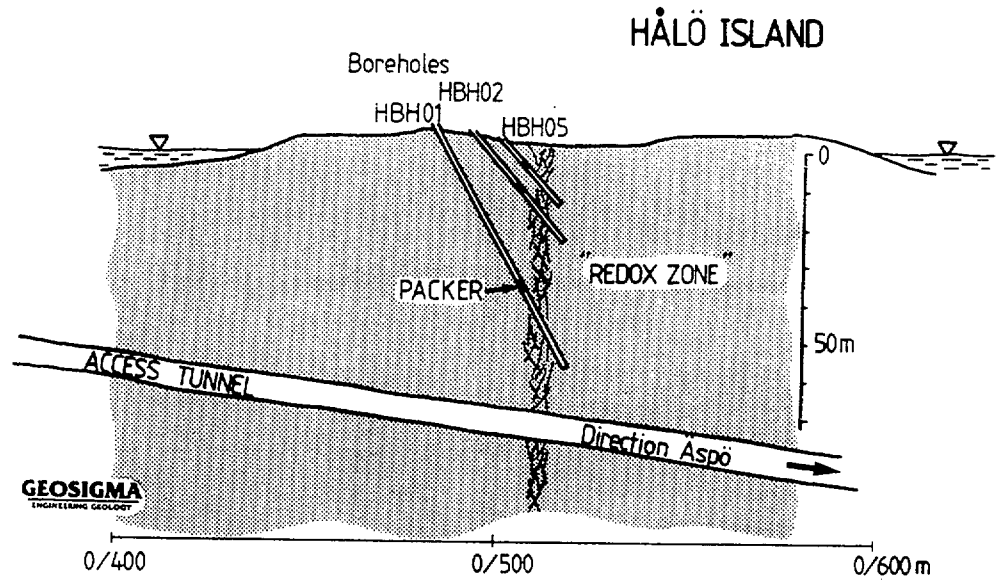


Figure 3.1. (a) Section and (b) plan views of the access tunnel, fracture zone and intersecting boreholes. The plan view shows the side tunnel used for instrumentation, from which three sampling boreholes are core-drilled horizontally into the fracture zone at a depth of 70 m.

The tracer test was performed under hydraulic gradient and flow conditions which since the early part of the block scale redox experiment (August 19 1991) have been dominated by the open borehole KR0013B and drainage by the tunnel. The strongest hydraulic sink was borehole KR0013B, with a continuous discharge flow rate of about 7.6 L min⁻¹. The tunnel drains the fracture zone with about 0.9 L min⁻¹. Tracers were injected in three shallow boreholes; HBH01, HBH02 and HBH05. Three different tracers were used, one in each borehole (Table 3.1).

Table 3.1 Tracers Injected in the Redox Zone

| Borehole | Tracer |
|----------|--------------|
| HBH01 | Amino G Acid |
| HBH02 | Uranine |
| HBH05 | RdWT |

The tracer injections followed the decaying pulse injection technique (Gustafsson and Nordqvist, 1993). The groundwater flowing through the borehole section was labelled with a small amount of tracer solution during continuous mixing. This technique avoids tracer being pushed out to a unknown distance from the injection borehole, or to stagnant parts of the adjacent fracture system. Thus, the injection is well defined in time and space. The tracer was released to the fracture zone following a logarithmic decay, analogous to the principles of dilution measurements (Figure 3.2). A continuous measurement of the tracer concentration in the injection borehole section made it possible to get a measure of the tracer mass release per time unit to the fracture system, which is important to consider when interpreting the resulting breakthrough curves. Groundwater flow rate through the borehole injection section was also calculated, utilizing the concentration versus time data.

Transport of tracer labelled groundwater was measured by analysing water samples taken at the discharge points; the borehole KR0013B and two inflow points in the tunnel roof, TL and TR (Figure 3.3 and 3.4). Complementary sampling was made in the closed observation boreholes KR0012B and KR0015B. Also in boreholes HBH01 and HBH02 samples were taken to measure any tracer transport from more shallow injection points. To check if the hydraulics of the redox zone is mainly two-dimensional, although there may be intersecting fractures, water samples were taken at an additional eight inflow points in the vicinity of the fracture zone intersection in the tunnel. Automatic samplers were used for borehole sampling. Inflow points were sampled manually. The fluorescent dye tracers used in the tracer test were analysed on a spectrofluorometer (JASCO FP-777).

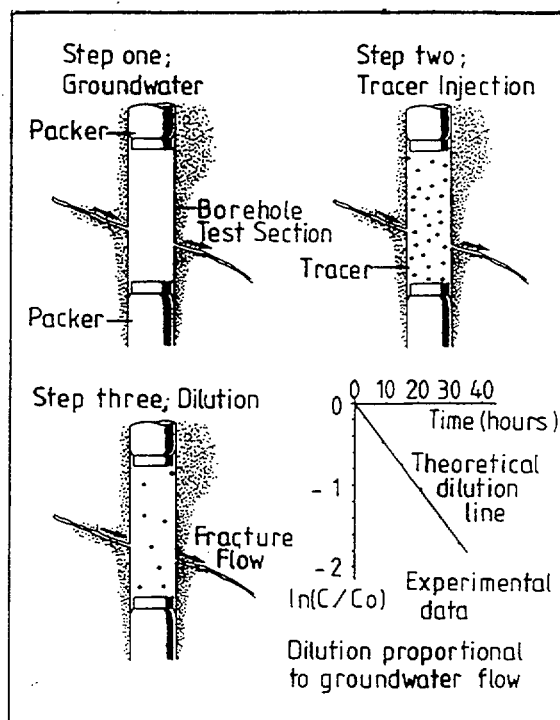


Figure 3.2. Principle of dilution measurement, used for tracer injection and determination of groundwater flow rate in borehole sections.

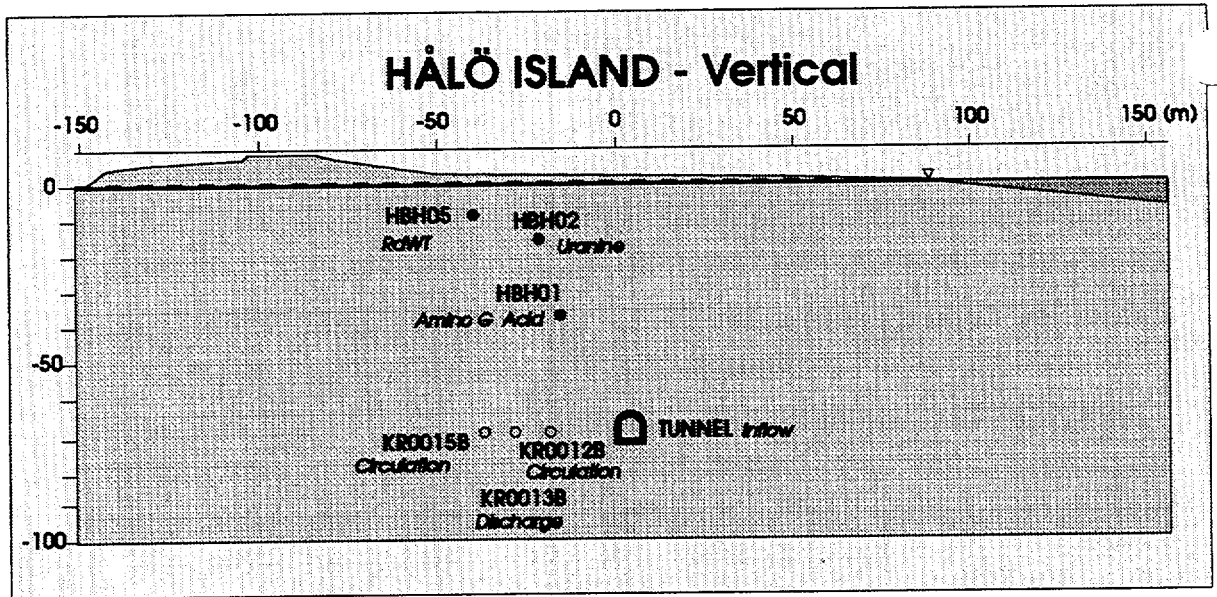


Figure 3.3. Hydraulic sinks and points of tracer injection.

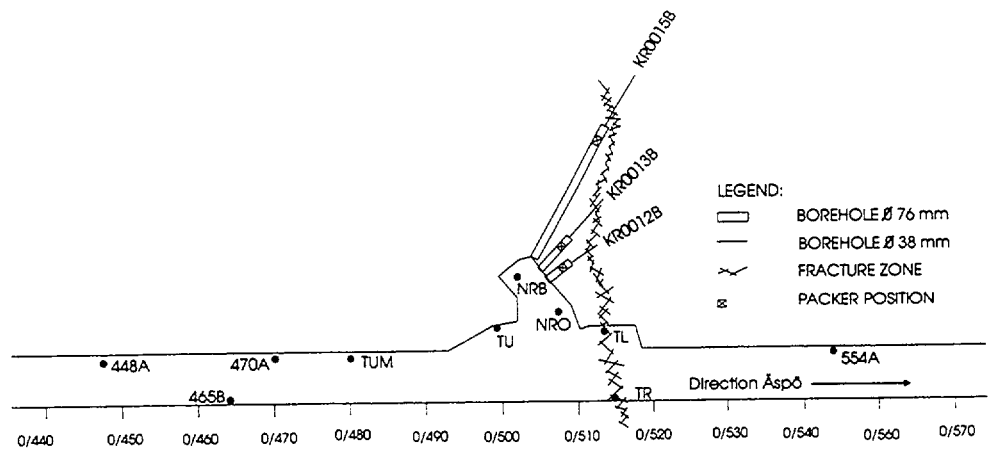


Figure 3.4. Location of inflows (black dots) in tunnel roof and walls. Plan view of access tunnel and redox niche.

4. EXPERIMENTAL RESULTS

4.1 RESIDENCE TIME AND HYDRAULIC SYSTEM

Tracer labelled groundwater from all injection points had reached the tunnel within 3000 hours (125days). The hydraulic connections verified by the tracer test are presented in Figure 4.1. Arrows indicate where groundwater has been labelled with tracer and were that water later has been detected.

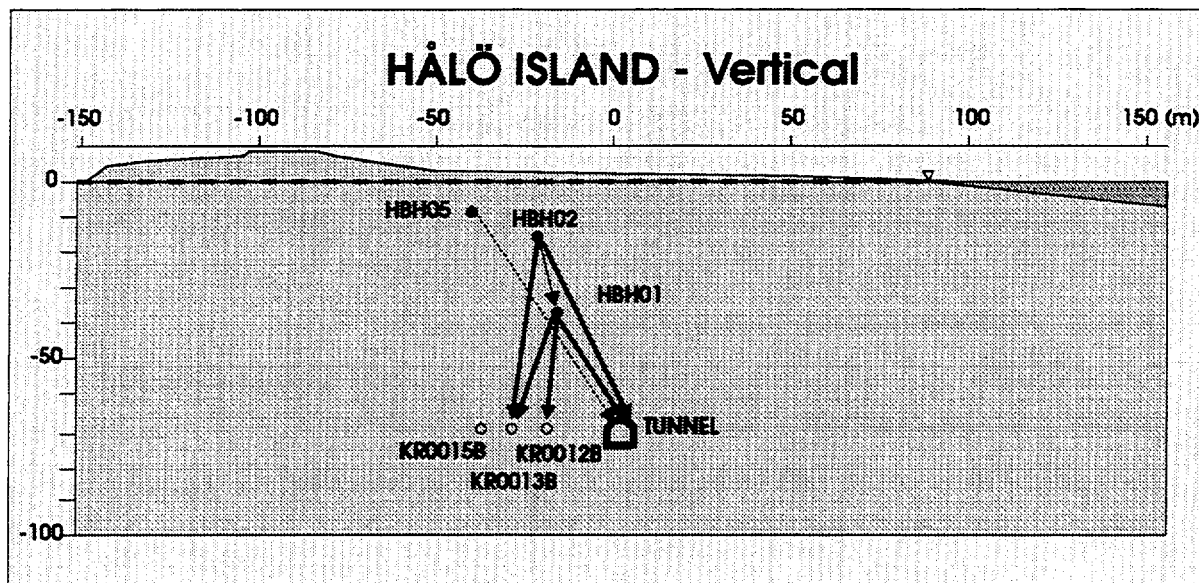


Figure 4.1. Hydraulic connections in the redox fracture zone determined from the tracer test result during 125 days of sampling.

Table 4.1. Groundwater Flow Rate Through the Borehole Sections Intersecting the Redox Fracture Zone.

| Borehole | Rate of through-flow (ml/min) |
|----------|-------------------------------|
| KR0012B | 1.3 |
| HBH01 | 24.0 |
| HBH02 | 0.4 |
| HBH05 | 0.9 |

After 125 days 81 % of the injected Amino G Acid tracer had been recovered at the sampling locations, most of it in KR0013B. The recovery of Uranine (injected in HBH02) was lower, about 17% of which most of it in KR0013B. Only minor amounts of RdWT labelled groundwater from HBH05 reached the sampling locations during 125 days of sampling, although the groundwater flow rate through HBH05 was twice as high as in HBH02, where Uranine was injected.

Residence time and dispersion was determined by parameter estimation. Assuming one-dimensional flow between the points of tracer injection and abstraction the analytical solution by Van Genuchten and Alves (1982) for convective-dispersive solute transport was fitted to the experimental breakthrough curves by non-linear least squares regression (Gustafsson and Nordqvist, 1993). The method considers non-ideal injections and the actual measured tracer mass release per unit time is used as input data for the parameter estimation calculations. Examples of evaluated tracer breakthrough curves are shown in Figures 4.2 and 4.3. A schematic illustration of the residence time in different parts of the redox fracture zone is shown in Figure 4.4.

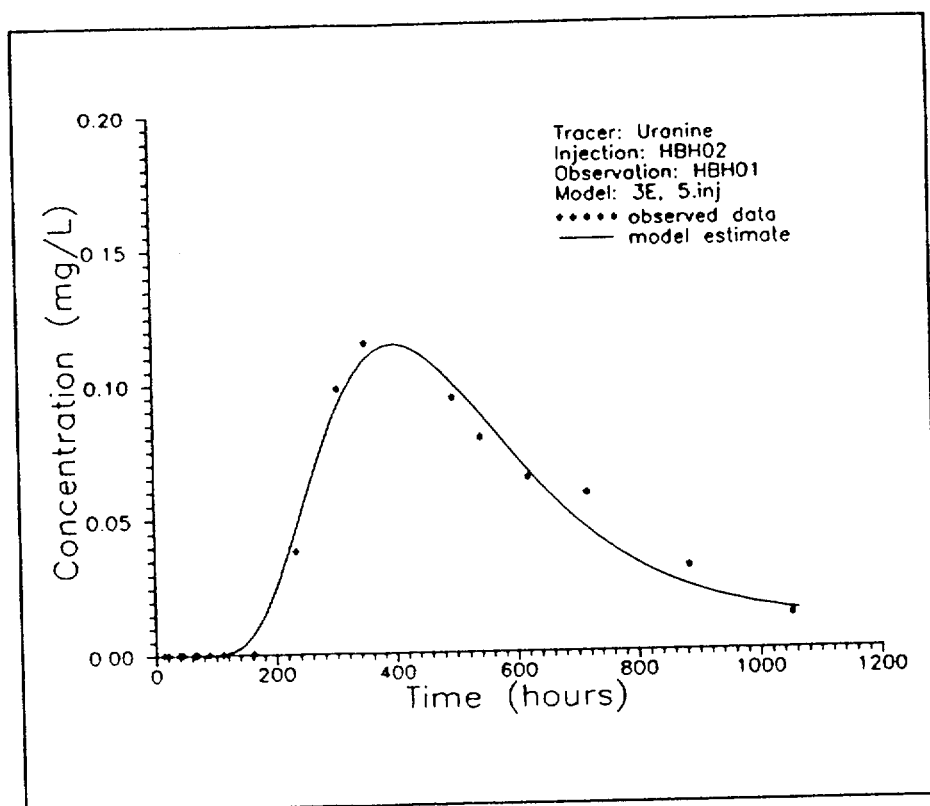


Figure 4.2. Experimental data and model estimate of Amino G Acid tracer breakthrough in KR0013B.

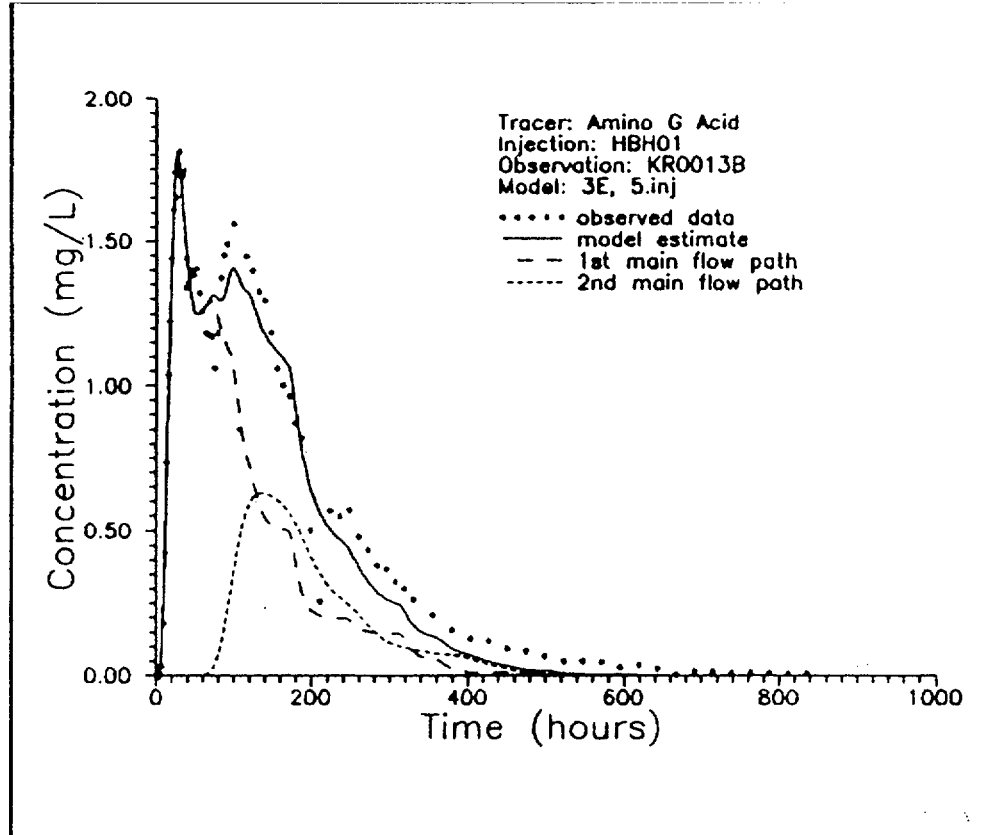


Figure 4.3. Experimental data and model estimate of Uranine tracer breakthrough in HBH01.

The water velocity is apparently much lower in the upper region of the fracture zone than in the lower. From 15 to 70 m the residence time is ranging from 21 to 39 days, but from 40 to 70 m it is only somewhere in between 2 and 9 days. From the shallow borehole HBH05, 7 metres below ground surface, the residence time was estimated to 125 days, or more.

Water flowing through HBH02 passes through HBH01 and further down in the fracture zone, finally entering KR0013B and the tunnel. Thus, water that is sampled in borehole HBH01 originates to some extent from waters having the chemistry of HBH02. No tracer labelled water was detected in the observation borehole KR0015B.

The result of the additional sampling in water inflow points in the tunnel around the redox zone intersection indicated that the zone acts mainly as a two-dimensional flow system. Only in waters from inflow point NRO close to the redox zone, with a relatively low rate of inflow (35 ml/min) tracers were found in small amounts outside the interpreted fracture zone.

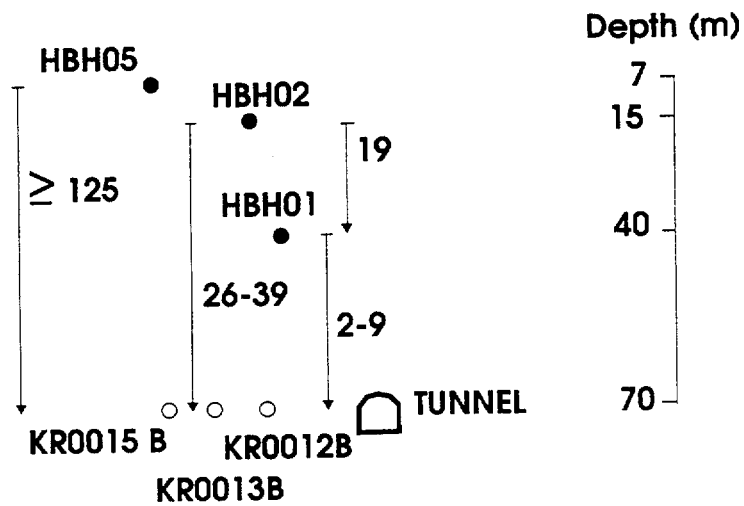


Figure 4.4. Schematic illustration of groundwater residence times (days), based on interpreted tracer breakthrough curves.

4.2 DISPERSION

Interpreted dispersion lengths are generally larger than 1/10 of the transport path length, a number often referred to in the literature for subsurface flow systems. Here about 1/5 of the transport path length was obtained for the tracer flow paths HBH01 to KR0013B and HBH02 to KR0013B. In flow paths ending in the left side of tunnel, with an inflow rate of about one tenth of KR0013B, the interpreted dispersion length was even larger, 1/3 of transport path length.

In the lower region of the redox zone, represented by tracer solute transport from HBH01 to KR0013B, the dispersion length for the first and second main flow path was estimated to 6.4 and 0.7 m respectively (6.0 and 55.1 expressed as Peclet numbers). Solute transport from shallower parts of the zone down to tunnel depth, represented by HBH02 to KR0013B transport, showed a dispersion length of 14.7 m and a Peclet number of 4.1, which demonstrates the solute transport being more disperse in the shallow parts than in the lower region of the zone, represented by transport from HBH01 to KR0013B.

Flow porosity was calculated with the interpreted residence time as the basic variable. Both radial and linear flow fields were considered, although radial flow field is judged to be the best approximation close to the hydraulic sink. Calculations were made following the analytical expressions given by Gustafsson and Nordqvist (1993). Flow porosity determined between points HBH01 and KR0013B, i.e. between intermediate and tunnel depth, is within 0.5 - 1.6 % assuming a radial flow field. The linear flow assumption gives a higher porosity, 6.1 %. Flow porosity between the shallow part of the fracture zone and the depth of the tunnel (HBH02 and KR0013B) is estimated to 2.5 - 3.6 % assuming radial flow, and 14.6 % assuming linear flow.

5. SUMMARY AND DISCUSSION

The tracer test verified that hydraulic connections exist in the fracture zone between the injection boreholes, located at depth ranging from 7 to 40 m, and the deep sampling boreholes and the tunnel at 70 m depth. The zone acts mainly as a two-dimensional flow system and especially from the depth of 15 m and below it is well connected.

Tracer test results show that the waters that during the course of the redox experiment have been sampled at 7, 15 and 40 m depth in the fracture zone finally enters the sampling locations at depth and constitutes a part of the water sampled in borehole KR0013B and of inflow points to the tunnel (TL).

Water residence times are about 5 days from 40 m down to 70 m depth, and from 15 m down to 70 m is about 30 days. Starting at 7 m depth (HBH05) the residence time was determined to be 125 days or more down to the sampling at 70 m depth (KR0013B). The difference in residence times is larger than what can be expected only by geometry, i.e. distance and radial flow to the sampling point. Tortuous, disperse flow and higher flow porosity in shallower part of the fracture zone is probably the explanation to the long residence time from shallower parts.

Dispersion is large, generally dispersion length is larger than 1/10 of transport path length ($Pe \leq 10$). Solute transport is judged to be more disperse in the shallow parts than in lower region of fracture zone. Dispersion lengths were estimated to 15-20 m ($Pe = 4-3$) from the shallow part of the fracture zone (HBH02 15m) down to tunnel depth. In deeper parts of the zone dispersion lengths from 40 m (HBH01) and down to 70 m are of the order of 4-12 m ($Pe=10^{-3}$).

Flow porosities are within 0.5 - 3.6 % assuming radial flow field. Higher values are representative for upper part of the fracture zone.

Chemical reactions and interactions are strongly favoured in the shallow part of the redox fracture zone due to large dispersion, high flow porosity and long residence time. In the deeper part the conditions for downward solute transport are opposite, with short residence time, lower dispersion and lower flow porosity.

REFERENCES

Banwart S, Gustafsson E, Laaksoharju M, Nilsson A-C, Tullborg E-L, Wallin B (1994). Large-scale intrusion of shallow water into a vertical fracture zone in crystalline bedrock: Initial hydrochemical perturbation during tunnel construction at the Äspö Hard Rock Laboratory, southeastern Sweden. Water Resources Research, Vol.30, No.6, pp 1747-1763.

Gustafsson E, Nordqvist R (1993). Radially Converging Tracer Test in a Low-Angle Fracture Zone at the Finnsjön Site, Central Sweden: The Fracture Zone Project - Phase 3. Swedish Nuclear Fuel and Waste Management Co., Report TR 93-25, Stockholm.

Van Genuchten M.Th., Alves W.J. 1982. Analytical solutions of the one-dimensional convective-dispersive solute transport equation. U.S. Dep. of Agric. Tech. Bull. 1661, 149 pp.

Karsten Pedersen
Göteborg University
Göteborg, Sweden

1. IDENTIFICATION OF PRESENT BACTERIA BY ANALYSIS OF 16s-rRNA GENE SEQUENCES - A NEW TECHNIQUE

A basic requirement in the work with bacteria is good methods for the identification of different bacterial species and coherent bacterial groups. The practice of methods such as numerical and chemical taxonomy has greatly influenced our views on how bacteria should be characterized, classified and identified. However, the development and deployment of nucleic acid based techniques is presently changing the current approach. It has been found that the DNA-sequence for the bacterial ribosomal 16S-unit is very suitable for identification. This sequence has conservative regions that are the same for all or large groups of bacteria as well as variable regions that are unique for single species. By the synthesis of short PCR-primers for the conservative regions, 16S-rRNA gene from very small samples can be amplified to amounts suitable for cloning and sequencing (Stackebrandt and Goodfellow 1991). The obtained sequences can subsequently be compared with sequences available in databases (Olsen et al 1991). There are also methods to synthesise species-specific sequences with fluorescent or radioisotopic labels. Such RNA-probes can be used for the in situ identification of single bacteria. The described techniques have now opened doors that earlier have been hermetically closed.

A common problem in the study of bacteria in nature is that only a minor part of all the observed bacteria can usually be successfully enriched and cultured. The 16S-technique now makes it possible to achieve information without culturing! This is because the DNA from all present organisms can be extracted, amplified with PCR, cloned, sequenced and analysed. This technique was applied on samples from Äspö and the results are presently being analysed and will be reported separately. Details about the technique can be obtained from Ekendahl et al. (1994).

2. SAMPLING

Groundwater was sampled from five different borholes through the fracture zone intersected by the Äspö tunnel at 70 m below ground. The sampling was performed in December 1992. Boreholes HBH02 (10 m) and HBH01

(45 m) were drilled from the surface while the three vault boreholes KR0012, 13 and 15 were drilled from a vault 70 m below ground perpendicular through the fracture zone. Present bacteria were filtered on 0.2 µm polycarbonate filters, extracted, cloned and sequenced.

3. ANALYSIS OF 16s-rRNA GENE SEQUENCES - RESULTS

The number of clones sequenced from each borehole sample was 12 (one still missing in KR0015). The average detection limit for a specific species will then be approximately 8%. A summary of the sequencing results in table 1.2 is presented in table 1.1. This table shows that all clones in HBH02 were unique and did not appear in any of the other sampled boreholes. Further, it can be seen that HBH01 shares between 2 to 4 clones with the vault boreholes KR0012 to KR0015. Finally, the vault boreholes share one identical clone each.

Table 1.1 The Numbers of Identical Clones Shared Between the Different Boreholes Sampled in the Redox Zone.

| Borehole | HBH02 | HBH01 | KR0012 | KR0013 | KR0015 |
|----------|-------|-------|--------|--------|--------|
| HBH02 | 12 | 0 | 0 | 0 | 0 |
| HBH01 | | 12 | 2 | 4 | 3 |
| KR0012 | | | 12 | 1 | 1 |
| KR0013 | | | | 12 | 1 |
| KR0015 | | | | | 11 |

4. CAN BACTERIAL DNA SIGNATURES BE USED AS TRACERS FOR GROUNDWATER FLOW, MIXING AND ORIGIN?

The possibility of using DNA analysis as a tracer tool for ground waters is only reliable if bacterial populations in the ground water environments are stable. Earlier results from the Stripa mine indicate this to be the case.

There, we found very stable populations of bacteria that also differed in composition between sampled boreholes (Ekendahl and Pedersen 1994, Ekendahl et al 1994). In the Äspö tunnel, we have returned to one of the boreholes sampled one year earlier (preliminary data, not reported here) and we found approximately the same bacterial DNA representation as when sampled the first time. This indicates the DNA analysis to be a very strong tool for tracing groundwater origins and mixing. Different ground waters must be expected to have different and specific DNA signatures, not only identifying the ground water but also revealing information about its character as different bacteria thrive in species specific water environments. The DNA analysis results in table 1.1 show similarities in DNA composition between the surface borehole HBH01 and the vault boreholes KR0012, KR0013 and KR0015 indicating the vault borehole ground waters to have partly common origins in the HBH01 ground water. It also indicates HBH02 to have an origin and water composition different from the other sampled boreholes because no one of the HBH02 clones appeared elsewhere. This is in agreement with the tracer hydrochemistry data suggesting this shallow borehole to have a poor hydraulic connection to the deeper part of the fracture zone.

The methane content in the ground water has been shown to be of a biogenic origin. The DNA data analysed this far did not indicate any archeobacterial sequences, thereby excluding methanogenic bacteria in the analysed ground waters. They may be present in concentrations below the present detection limit for the DNA analysis (8% here, depends on the number of clones sequenced) and/or are they attached to fracture surfaces. Finally, it is possible that the methane production occurs elsewhere, in the sea bottom, the root zone or in very shallow ground waters and that the methane found is transported with the groundwater from areas with active methanogenesis.

Table 1.2 The Results from Sequencing and Grouping of Sequences Sampled from Boreholes in the Fracture Zone and Summarized in Table 1.1.

| clone | HBH02 (L) | HBH01 (M) | KR0012 (N) | KR0013 (O) | KR0015 (P) |
|--------------|-----------|-----------|------------|------------|------------|
| code | 10 m | 45 m | 70 m | 70 m | 70 m |
| A53n | | | 1 | | |
| A58l | 4 | | | | |
| A59p | | | | | 2 |
| A17o | | | | 1 | |
| A18p | | | | | 1 |
| A19p | | | | | 1 |
| A21n | | | 1 | | |
| A20n | | | 1 | | |
| A36o | | | | 1 | |
| A34o | | | | 1 | |
| A32l | 1 | | | | |
| A52p | | | | | 1 |
| A55n | | | 3 | | |
| A29mnp | | 3 | 1 | | |
| A31p | | | | | 1 |
| A26ou | | | | 3 | |
| A30m | | 1 | | | |
| A24otp mn | | 6 | 1 | 4 | 1 |
| A45l | 2 | | | | |
| A62l | 1 | | | | |
| A4o | | | | 1 | |
| A42l | 1 | | | | |
| A46l | 1 | | | | |
| A43l | 1 | | | | |
| A22l | 1 | | | | |
| A56n | | | 1 | | |
| A14jsn | | | 1 | | |
| A33p | | | | | 1 |
| A35o | | | | 1 | |
| A51p | | | | | 1 |
| A54n | | | 1 | | |
| A57n | | | 1 | | |
| A61upm | | 2 | | | 2 |
| Σ clones | 12 | 12 | 12 | 12 | 11 |

REFERENCES

Ekendahl S., Arlinger J., Ståhl F., Pedersen K. (1994). Characterization of attached bacterial populations in deep granitic groundwater from the Stripa research mine with 16S-rRNA gene sequencing technique and scanning electron microscopy. Microbiology,140, 000-000 (in press).

Ekendahl S., Pedersen K. (1994). Carbon transformations by attached bacterial populations in granitic ground water from deep crystalline bed-rock of the Stripa research mine. Microbiology,140, 000-000. (in press)

Olsen G.J., Larsen N., Woese C.R. (1991). The ribosomal RNA database project. Nucleic Acids Research,19, 2017-2021.

Stackebrandt E., Goodfellow M. (1991). Nucleic acid techniques in bacterial systematics. Nucleic acid techniques in bacterial systematics. pp 329. John Wiley & Sons, Chichester.

Luis Moreno and Ivars Neretnieks
Department of Chemical Engineering and Technology
Royal Institute of Technology
100 44 Stockholm

ABSTRACT

A new program for modelling coupled reactions, equilibrium/kinetic and transport is presented. The program is based on the quasi-stationary state approximation (Lichtner, 1988). It assumes kinetic controlled reactions for the precipitation/dissolution of minerals and equilibrium for aqueous speciation. The program has been tested in different situations and the results of these calculations agree well with observations or results obtained with similar programs.

SUMMARY

When fluid flows through a porous medium, the dissolved constituents can react with the solid material. Solid phases may dissolve, precipitate, or react with some constituents. Rapid reactions produce sharp reaction fronts propagating through the medium. Low fluid velocity in the ground makes diffusion important which may also play a major role in transport from the interior of the solid.

The description of this kind of mechanisms requires the use of models and programs that simulate coupled reaction, equilibrium/kinetics and transport. Neretnieks (1993) recently summarized the properties and capabilities of the most commonly used programs.

We have studied several types of problems by using these models: degradation of concrete by simultaneous intrusion of carbonate, sulphate, protons, magnesium (Zhu, 1988), evolution of hydrolysis and redox fronts in an open pit uranium mine in Poços de Caldas in Brazil (Bäverman, 1993), leaching of copper (Casas et al., 1993), leaching of copper from mine tailings (Strömberg et al., 1994), etc.

There are many computer programs for calculating geochemical evolution, but most of them fail to calculate sharp redox fronts. One promising approach for sharp reaction fronts is to use the kinetic dissolution of minerals and the quasi-stationary state approximation (Lichtner, 1988). The program CHEMFRONTS (Bäverman, 1993) is based on these concepts. Moreover, it uses a changing discretization. The borders of regions containing the same minerals are determined after each time step. The

resolution of the location of the fronts can be made with extremely high accuracy in contrast to what is possible with finite difference/element models.

Calculations made by using this program show a good agreement with observations or with results calculated by other similar programs.

1. INTRODUCTION AND BACKGROUND

When fluid flows through a porous medium, the dissolved constituents can react with the solid material. Solid phases may dissolve, precipitate, or react with some constituents. Rapid reactions produce a sharp reaction front propagating through the medium. Low fluid velocity makes diffusion important which may also play a major role in transport from the interior of the solid. Redox fronts in the subsurface may be formed when, for example, pyrite reacts with water containing oxygen.

Our model concepts are based upon mass balances along a flow path of infiltrating reactants such as acid rain and oxygenated water by flow as well as diffusion, reactions with the minerals and, if present, organic matter. The reactions may be controlled kinetically or by diffusion in the larger rock particles. In addition to kinetics the description of the local chemistry accounts for dissolution and precipitation as well as ion exchange and sorption reactions. These models cover simple analytical solutions of a few dominating reactions such as proton and oxygen reactions with the buffering minerals to only simulate the evolution of hydrolysis and redox fronts in time and space as well as very elaborate fully coupled flow, transport and chemical reaction programs where many tens of dissolved species and minerals can be described.

Different problems have been studied with these models using the simple models where possible, because they give good insight, and more complex models when needed. Problems studied include, long term (>100 years) degradation of concrete by simultaneous intrusion of carbonate, sulphate, protons, magnesium etc. and leaching of calcium, sodium, silica etc. (Zhu, 1988). One study concerned the evolution of hydrolysis and redox fronts and the associated formation of uranium mineralization in an open pit uranium mine in Poços de Caldas in Brazil (Bäverman, 1993). In this study, it was very encouraging to find that our simulations were able to predict the chemical composition of the water as well as the mineral sequencing very well using only the information of original rock composition. Even the simulated evolution in time over millions of years as interpreted from the rate of movement of the different fronts was in accordance with observations. These basic model concepts have also been applied to leaching of copper from blocks of ore in a copper mine in Chile (Casas et al., 1993). Recently a study on the reactions in and leaching of copper from Aitik mine tailings were made using these models (Strömberg et al., 1994). At present we are adapting the models for simulation of the

chemical evolution and leaching of incinerated household wastes and slags and to interpret the chemistry and transport in and around a large uranium ore body at Cigar lake in Canada.

The water composition changes along the flow path through the medium and thus there will be an ongoing change of the composition of the water as well as of the solid phases. The changes of the local solid composition are, in general, slow compared to that of the water because the water carries little dissolved constituents. The presence and composition of the solid phases will, for a long time, determine the composition of the water by its large buffer capacity for pH and Eh and the soluble compounds which may act as complexing agents.

The solubility of individual constituents will be influenced by the master variables pH, Eh and the presence of other constituents carried by the water from locations upstream. The water composition will thus change with time in a location depending on how the composition of solid phases have changed upstream. Over longer times the redox conditions and pH will be determined by the influx of protons and oxygen and by the buffer capacity of the solids. Rocks containing pyrite and ferrous iron for example will be strongly reducing while these compounds are still present. Sharp redox and pH fronts may develop in the rock. At such fronts, solubilities of many constituents may change by several orders of magnitude.

2. MODELS

The description of this kind of problem requires the use of models and programs that simulate coupled reaction, equilibrium/kinetics and transport. Neretnieks (1993) recently summarized the properties and capabilities of the most commonly used programs. These models describe the reaction rates of the different waste forms as influenced by the local chemical composition of the gas and water. In addition these models include the mass balances needed to follow the evolution of composition of solid phases along the flow path of the water through the medium. The changes of the composition of the solids are also accounted for by "book keeping" of how the solids have reacted earlier. The models also account for mineral solubilities as determined by the presence of minerals and the water composition including the formation of various complexes. The models have been and are adapted from what are called geochemical transport models. A short description of some of the simpler equilibrium models and the considerably more complex coupled reaction, equilibrium and transport models is given below.

The solubility and sorption equilibria in inorganic systems can be estimated with the help of *equilibrium programs* such as PHREEQE (Parkhurst et al., 1985), EQ3/6 (Wolery 1983), and other similar programs. They can also be modified to account for organic solutes and to handle adsorption and ion exchange phenomena on the mineral surfaces. Few of the programs can

handle kinetics. These equilibrium programs cannot, however, handle the above described situation where there is a constant change of composition along the flow paths.

Coupled transport and chemical programs have been developed and are being developed which can handle the evolution of the water chemistry along a flow path. The CHEMTRN family of programs (Miller 1983; Noorishad et al., 1987) with the programs CHEMTRAN, CHEMTRANS and THCC can in principle be used to calculate the water composition along a flow path accounting for precipitation and dissolution of minerals, redox reactions and the presence of complexing agents. Some of the programs can handle surface complexation, ion exchange and also kinetics. Some versions of the programs can handle changing temperatures also. In our experience these programs have failed when there are sharp redox and/or dissolution fronts present (Zhu 1988). The program CHEQMATE (Haworth et al., 1988) is based on the equilibrium program PHREEQE. This program has successfully been used to calculate the development of redox fronts, dissolution fronts and the simultaneous dissolution and precipitation of uranium at the fronts (Cross et al., 1991). This program, although robust, is very computer time consuming for cases where the mineral reactions dominate the mass balances in the system. We have also tested some other programs that recently have become available. HYDROGEOCHEM (Yeh and Tripathi 1991) and PhreeqEM (Willemsen, 1992)

Solids composition and structure and water composition change continuously along a flow path. Water is often far away from local equilibrium with the solid matrix. This may be due to the fact that the reaction rates are slow and there is not time to reach the equilibrium.

We have ourselves recently developed and used a program, CHEMFRONTS, which is specifically aimed to be efficient for cases where mineral reactions dominate the mass balances and where sharp reaction fronts occur (Bäverman, 1993). It is based on the quasi steady approximation proposed by Lichtner (1988). The basic ideas go to back to Helgeson's work (Helgeson and Murphy, 1983). The program is very fast.

We have used CHEMFRONTS to simulate the release of potentially toxic heavy metals from the Aitik waste rock heaps (Strömberg et al., 1994). The model considered pyrite weathering, acid consumption by trace calcite dissolution and the formation of gypsum and ferrihydrate. The release of Cu and Zn due to oxidative weathering of chalcopyrite and sphalerite was studied in detail.

3.

CHEMFRONTS

There are many computer programs for calculating geochemical evolution. Most fail to calculate sharp redox fronts, and some programs need very long computing times even with the largest computers. One promising approach for sharp reaction fronts is to use the kinetic dissolution of minerals and the quasi-stationary state approximation (Lichtner, 1988).

Most of programs use a discretization in "boxes," and the accuracy of them depends on the size of the "boxes." These programs do not seem to handle sharp fronts well, for example those that occur in rocks with reducing minerals like pyrite. CHEMFRONTS follows the fronts very accurately because it has no need to discretize the space.

The quasi-stationary state approximation (Lichtner, 1988) describes the evolution of geochemical processes, by including advective, diffusive and dispersive mass transport, in a sequence of stationary states. The mineral reactions are described by kinetic rate laws for both precipitation and dissolution. Thus, the sequence of mineral reaction products is determined directly from the transport equations.

The computer programs PRECIP (Noy, 1990) and MPATH (Lichtner, 1990) were under development and not fully available to us at that time. As it was impractical to calculate the evolution of redox fronts and other simultaneously moving fronts with the programs available, CHEMFRONTS was developed. A short description of the governing equations in CHEMFRONTS is presented below. More details are found in Bäverman (1993).

3.1

MATHEMATICAL MODEL

A mass balance for the system gives

$$\frac{\partial}{\partial t}(\phi Y_j) + \nabla W_j = - \sum_{m=1}^M v_{mj} \frac{\partial X_m}{\partial t} \quad (j = 1, \dots, N) \quad (1)$$

where the first term is the amount of component j that has accumulated in the system, ϕ is the porosity, Y_j is the total aqueous concentration of component j and W_j is the transport of the component j by fluid flow and diffusion. The term Y_j refers to the concentration of component j both as a free component and in any complex. The right-hand side of the equation is the sum of the amounts of component j transferred from the mineral to the aqueous phase by dissolution of minerals. M is the number of minerals, X_m is the concentration of mineral m in the solid phase, and t is the time.

The total concentration of component j, Y_j , is the sum of all aqueous forms of the component j

$$Y_j(\mathbf{r},t) = C_j(\mathbf{r},t) + \sum_i v_{ij} C_{xi}(\mathbf{r},t) \quad (2)$$

where C_j is the free concentration of component j, C_{xi} is the free concentration of complex i, and r is the distance from the column inlet. The free concentration of the complexes is calculated from the assumption that the aqueous species are always in local equilibrium.

As the amount of compounds in the solution is very small compared to that in the mineral phases, the accumulation of the species in the system can usually be ignored. The first term in Equation (1) is neglected without any substantial loss in accuracy,

$$\nabla W_j = - \sum_{m=1}^M v_{mj} \frac{\partial X_m}{\partial t} \quad (j = 1, \dots, N) \quad (3)$$

The flux of mass in the system, W_j , is the sum of the fluxes of the components, J_j , and the complexes, J_i . When there is a large advective flux, the diffusive flux is small and may be neglected.

The mineral precipitation or dissolution rate is given by

$$\frac{\partial X_m}{\partial t}(\mathbf{r},t) = \zeta_m(\mathbf{r},t) I_m(\mathbf{r},t) \quad (4)$$

where ζ_m is a logical factor, which is unity both if the solution is supersaturated and precipitation is possible, and if minerals are present so that dissolution is possible. Otherwise, ζ_m is zero. I_m is expressed as:

$$I_m(\mathbf{r},t) = \alpha_m(\mathbf{r},t) k_m^f (Q_m(\mathbf{r},t) - K_m^{-1}) \quad (5)$$

where α_m is the specific surface of the mineral, k_m^f the mineral reaction rate, and $(Q_m(\mathbf{r},t) - K_m^{-1})$ the driving force of the system. The driving force is the difference between the ion activity product of the water solution, Q_m , and the ion activity product at saturation (the inverse of the equilibrium constant of the formation for the mineral m)

Program CHEMFRONTS has been used for calculating several situations (Bäverman, 1993), one of these sample calculations is the redox front in an uranium mine at Poços de Caldas. Cross et al. (1990) have modelled the movement of the redox front in the mine with the computer program CHEQMATE (Harwoth et al., 1988). Similar input data was used in the verification of CHEMFRONTS. A good agreement was obtained when the results from both programs were compared. Total concentration of aqueous species downstream is shown in Table 3.1. The successful separation of the redox and dissolution fronts is an important issue of CHEMFRONTS. The location of some fronts as a function of time is shown in Figure 3.1.

Table 3.1. Comparison of total concentration of aqueous species downstream from redox front. (Bäverman, 1993)

| Species | Cross et al. mol/l | Chemfronts mol/l |
|-------------------------------|-----------------------|---------------------|
| K | $6 \cdot 10^{-4}$ | $4.9 \cdot 10^{-4}$ |
| SiO ₂ | $3 \cdot 10^{-4}$ | $1.9 \cdot 10^{-4}$ |
| Total carbon | $2 \cdot 10^{-4}$ | $1.6 \cdot 10^{-4}$ |
| SO ₄ ²⁻ | $2 \cdot 10^{-4}$ | $1.7 \cdot 10^{-4}$ |
| Al | 10^{-8} | $3.0 \cdot 10^{-8}$ |
| Fe | no value | $1.2 \cdot 10^{-6}$ |
| U | $1 \cdot 10^{-10}$ | $1 \cdot 10^{-10}$ |

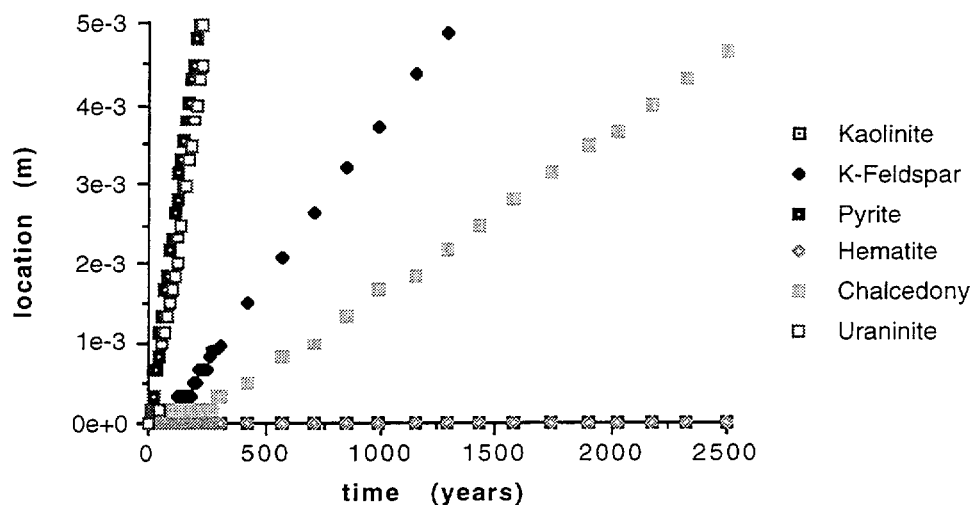


Figure 3.1 The movement of the dissolution fronts (Bäverman, 1993).

4. CONCLUSIONS

Water-rock interaction is a complex problem. Solid phases may dissolve, precipitate, or react with some constituents. Rapid reactions produce sharp reaction fronts propagating through the medium. The description of this kind of problem requires the use of models and programs that simulate coupled reaction, equilibrium/kinetics and transport.

There are many computer programs for calculating geochemical evolution. Most fail to calculate sharp redox fronts. One promising approach for sharp reaction fronts is to use the kinetic dissolution of minerals and the quasi-stationary state approximation (Lichtner, 1988). Based on these concepts CHEMFRONTS was developed. It has been used to calculate chemical evolution in several situations. Calculations made by using this program show a good agreement with observations or with results calculated by other similar programs.

REFERENCES

- Bäverman, C. (1993). Development of "Chemfronts", a coupled transport and geochemical program to handle reaction fronts, Licentiate Thesis, Department of Chemical Engineering., KTH.
- Casas, J., Vargas T., Martínez J., Moreno L. (1993). Modelling of bioleaching from low grade copper sulphide ore, In Biohydrometallurgical Technologies, Vol 1, Bioleaching Processes, Proceedings of International, Biohydrometallurgy Symposium at Jackson Hole, Wyoming., 22-25 August 1993, A.E. Torma, J.E. Wey, and V.I. Lakshmanan Eds. TMA edition.

Cross J.E., Haworth A., Neretnieks I., Sharland S.M., Tweed C.J. (1991). Modelling of Redox Front and Uranium Movement in a Uranium Mine at Poços de Caldas. Radiochimica Acta. 52/53, p 459-464, 1991.

Haworth A., Sharland S.M., Tasker P.W., Tweed C.J. (1988). A Guide to the Coupled Equilibria and Migration Code CHEOMATE. Harwell Laboratory Report, NSS R113.

Helgeson H.C., Murphy W.M. (1983). Calculation of mass transfer along minerals and aqueous solutions as a function of time and surface area in geochemical processes. Computational approach. Math. Geol 15, p 109-130, 1983.

Lichtner P. (1988). The quasi-stationary state approximation to coupled mass transport and fluid-rock interactions in a porous medium. Geochim. Cosmochim. Acta 52, p 143-165.

Lichtner, P. (1990). Redox front geochemistry and weathering: theory with application to the Osamu Utsumi uranium mine, Poços de Caldas, Brazil, Submitted to Chemical Geology, Special issue on the Poços de Caldas, December 3.

Miller C.W. (1983). CHEMTRN User's Manual, March 1983, LBL Report 16152, Report 161523, Lawrence Berkeley Laboratory, Earth Science Division, University of California.

Neretnieks I., Diffusion (1993). Flow and fast reactions in Porous media. NATO ASI Series, VolG32, Ed Petruzzelli D., Helfferich F.G. Springer Verlag Belin Heidelberg.

Noorishad J., Carnahan C.L., Benson L.V. (1987). Development of the Non-Equilibrium Reactive Transport Code CHMTRNS, Sept 1987. LBL Report 22361, Lawrence Berkeley Laboratory, Earth Science Division, University of California.

Noy, D. J. (1990). PRECIP: A program for coupled groundwater flow and precipitation/dissolution reactions, National Environment Research Council British Geological Survey, Technical Report WE/90/38C.

Parkhurst D.L., Thorstenson D.C., Plummer L.N (1985). Report USGS/WRI 80-96, NTIS Tech. Rep. PB81-167801, 1980, Revised 1985, (PHREEQE code).

Strömberg, B., Moreno L., Crawford J. (1994). Modelling of transport and initial weathering processes in a sulphidic mining waste rock heap, In B. Strömberg's Licentiate treatise, Department of Chemical Engineering and Technology, Royal Institute of Technology, 1994

Willemsen, A. (1992). PHREEQM-2D, PHREEQE in a multicomponent mass transport model, coupled to HST2D, Manual and user guide version 0.1, IF Technology bv, Frombergstraat 1, 6814 EA Arnhem, Nederland, 1992.

Wolery, T. (1983). EQ3nr a computer program for geochemical aqueous speciation-solubility calculations: user's guide and documentation. Lawrence Livermore National Laboratory, April 18, 1983.

Yeh G.T., Tripathi V.S. (1991). A model for simulating transport of reactive multispecies components: Model development and demonstration. Water Resources Research 27:3075-3094.

Zhu Ming (1988). Some aspects of modelling of the Migration of Chemical Species in Groundwater Systems. Licentiate Thesis, Dep. Chem. Eng., KTH.

- D -

**FIELD INVESTIGATIONS AND MODELLING
WITHIN OTHER PROGRAMMES**

D.1 Geochemical Investigations at Rokkasho Site for the Second-Phase LLW Disposal

Toshifumi Igarashi
CRIEPI
Abiko, Japan

Yasunori Mahara
CRIEPI
Abiko, Japan

Tadashi Miki
Kansai Electric Power Co., Inc.
Osaka, Japan

Takayuki Shiomi
Kansai Electric Power Co., Inc.
Osaka, Japan

1. INTRODUCTION

The Central Research Institute of the Electric Power Industry (CRIEPI) has conducted geological, geohydrological and geochemical investigations for over ten years at Rokkasho where low-level radioactive wastes (LLW) from nuclear power plants in Japan have been disposed. Wastes solidified with cement and asphalt in 200-liter drums were selected for the first phase of the disposal programs because of homogeneity, well-known inventories of nuclides and radioactivity in the drums. The disposal was started at the end of 1992. However, there are many other types of wastes that remain at each nuclear power plant. Combustible and incombustible solid wastes, which consist of cloth, paper, rubber, insulators, filters and ion exchange resins are required to be disposed of in the near future.

For the first phase of the shallow land disposal, performance assessment of natural barriers was conducted intensively through geological and geohydrological investigations. However, geochemical investigations are regarded to be the most important for the evaluation of the groundwater flow and mixing behavior and for the predictions of nuclide behavior in the underground environment. These investigations lead to more reliable and detailed assessments. We carried out groundwater dating by the $^3\text{H} - ^3\text{He}$ method (Mahara et al., 1991;1993) and analysis of chemical forms of redox-sensitive elements (Igarashi et al.,1992) as geochemical investigations for the second-phase disposal of LLW at Rokkasho. This paper briefly describes the surveyed in situ results and their preliminary evaluation.

2.

STUDY AREA

Rokkasho is located as shown in Figure 2.1. The disposal site is on a hilly terrain 30 to 60 meters above sea level. The Tertiary Taka hoko formation, composed of sedimentary rocks such as sandstone, tuff and sandy tuff, is distributed around the disposal site, and is covered by the Quaternary layer (Shimoda et al., 1991).

The water table is easily located within the Quaternary layer. The groundwater flow analyses indicate that precipitation over the site is the major source of recharging groundwater and that the groundwater flow rate in the Quaternary layer is larger than that in the Tertiary layer due to the great difference in permeability between the two layers.

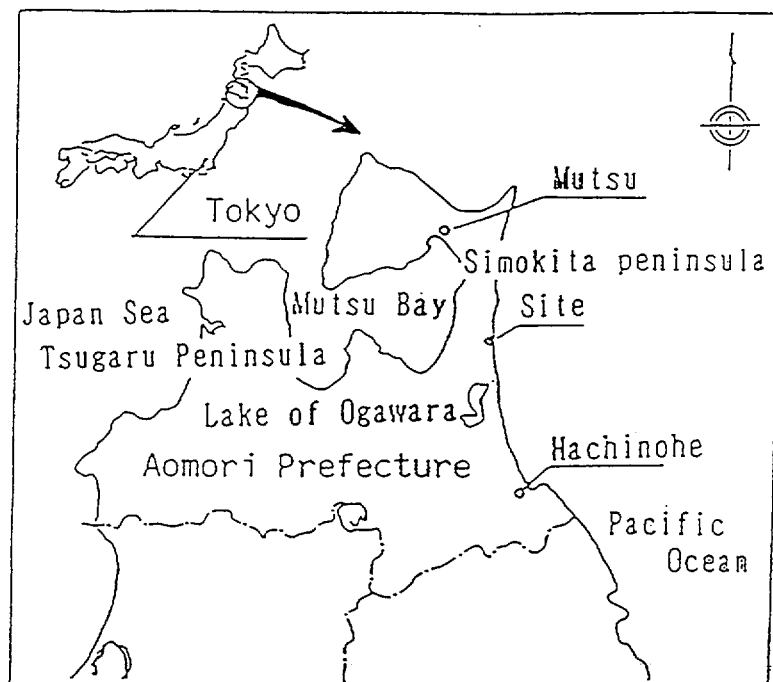


Figure 2.1. Location of the LLW disposal site in Japan. The site is located on the Pacific coast of the Simokita peninsula.

3.

GEOCHEMICAL INVESTIGATIONS OF SECOND-PHASE DISPOSAL

Geochemical investigations were carried out not only to improve reliability in understanding the groundwater flow behavior but also to clarify the geochemical conditions represented by variable such as pH, redox and chemical constituents which dominate the chemical forms of various elements. In particular, we focused on dating groundwater and determining the redox-sensitive elements.

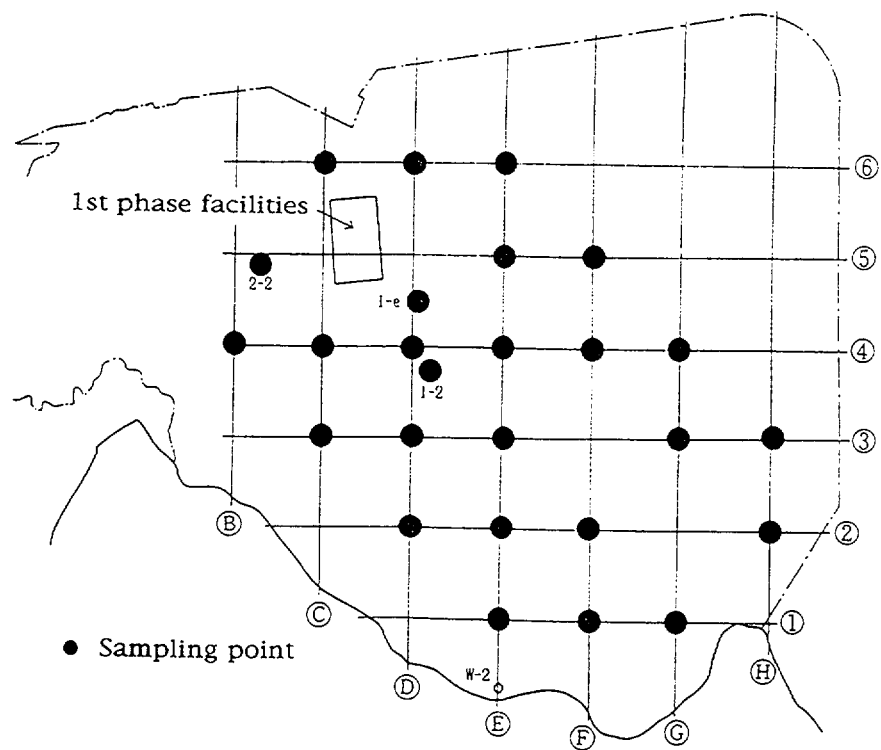


Figure 3.1. Sampling points for groundwater from boreholes.

Prior to the aforementioned geochemical investigations, major cations and anions (Na, K, Ca, Mg, Cl, HCO₃, SO₄) and stable isotopes (²H, ¹⁸O) were analyzed for the groundwater samples collected at the boreholes shown in Figure 3.1. Almost all the boreholes have casing pipes made of polyvinyl chloride or steel with full strainers installed to prevent collapse of a borehole wall. This means that the groundwater within the borehole is probably mixed.

Figure 3.2 illustrates the vertical profile of major ions at borehole 1-2. The sum of the concentrations of Ca and Mg decreased with depth, corresponding to the sedimentary rock type. This suggests that the effect of groundwater mixing phenomena in the borehole is restricted and therefore vertical distributions of chemical components could correspond to the geochemical conditions related to water-rock interactions surrounding the borehole. The chemical composition of major ions in the groundwater samples taken at the depth where the LLW disposal facility is built shows Na-HCO₃, or Na-Cl type depending on the geological conditions of the sampling sites.

The relations between $\delta^2\text{H}$ (D) and $\delta^{18}\text{O}$ of groundwater samples are shown in Figure 3.3. Although there were some exceptions, the measured data were distributed along the local meteoric water line (Waseda et al., 1983) expressed by the following equation.

$$\delta D = \delta^{18}\text{O} + 18$$

3.1

GROUNDWATER DATING BY THE ³H-³HE METHOD

Dating based on the concurrent reaction of the decay of ³H and the production of tritiogenic ³He was applied to the groundwater samples (Mahara et al., 1991, 1993). If the ³H concentration and the tritiogenic ³He concentration in a groundwater sample are measured at the same time, the average residence time T can be calculated according to the radioactive decay formula expressed by the following equation.

$$T = 17.69 \ln(4.01 \text{Ch}/\text{Ct} \cdot 1014 + 1)$$

Ch is tritiogenic ³He concentration (cc STP/g), Ct is ³H concentration (TU).

When we take groundwater samples for dating and measure the ³He concentration, the samples must be prevented from having contact with atmospheric air and from degassing to the environment because the chemical form of ³He is dissolved gas and the amount of dissolved ³He is very small. The detailed sampling procedures were presented by Mahara et al. (1991, 1993). The ³H concentration was measured by a low-background liquid-scintillation counter, and the ³He concentration was measured by a

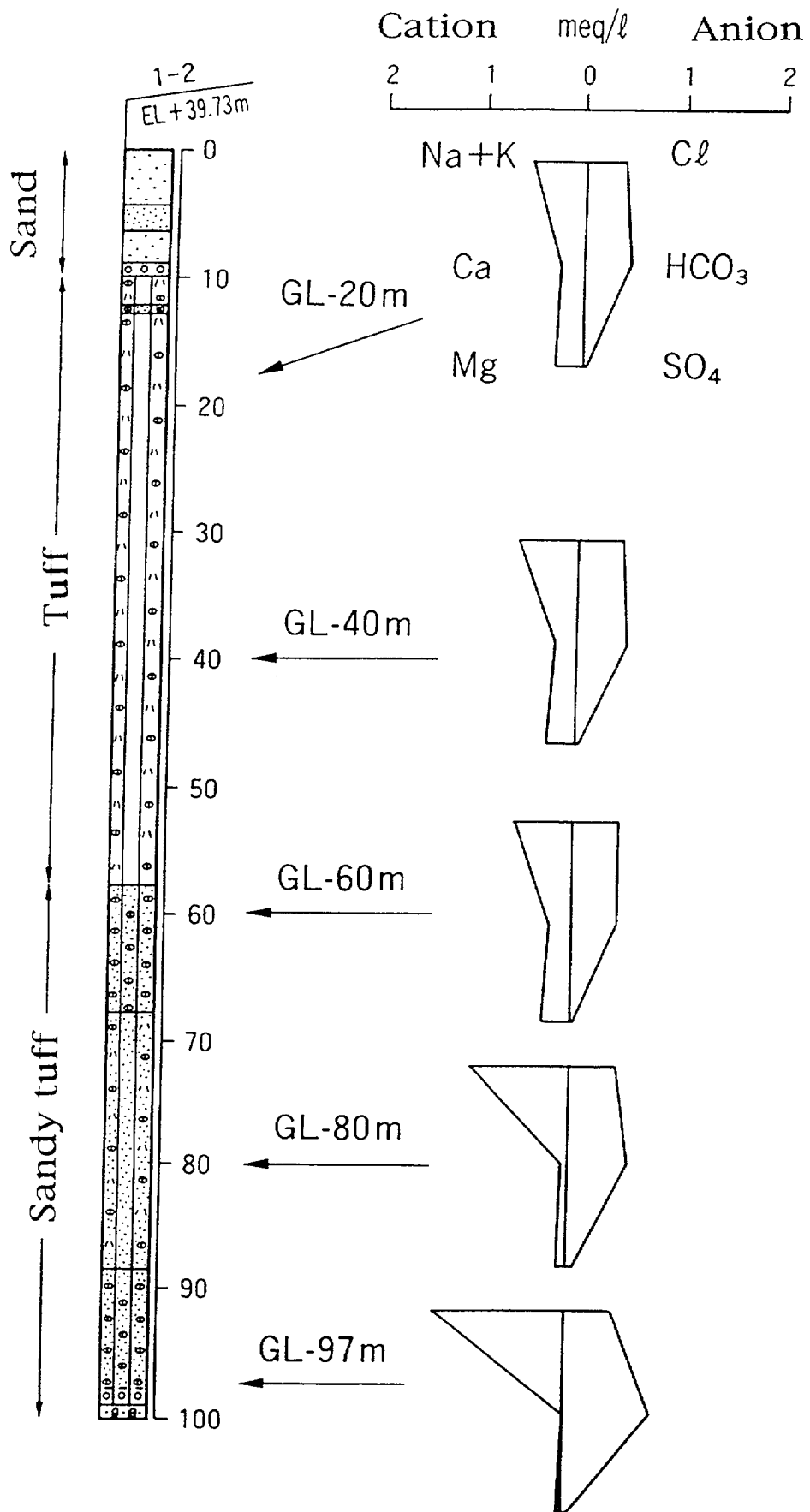


Figure 3.2. Vertical profiles of major ions and strata in borehole 1-2.

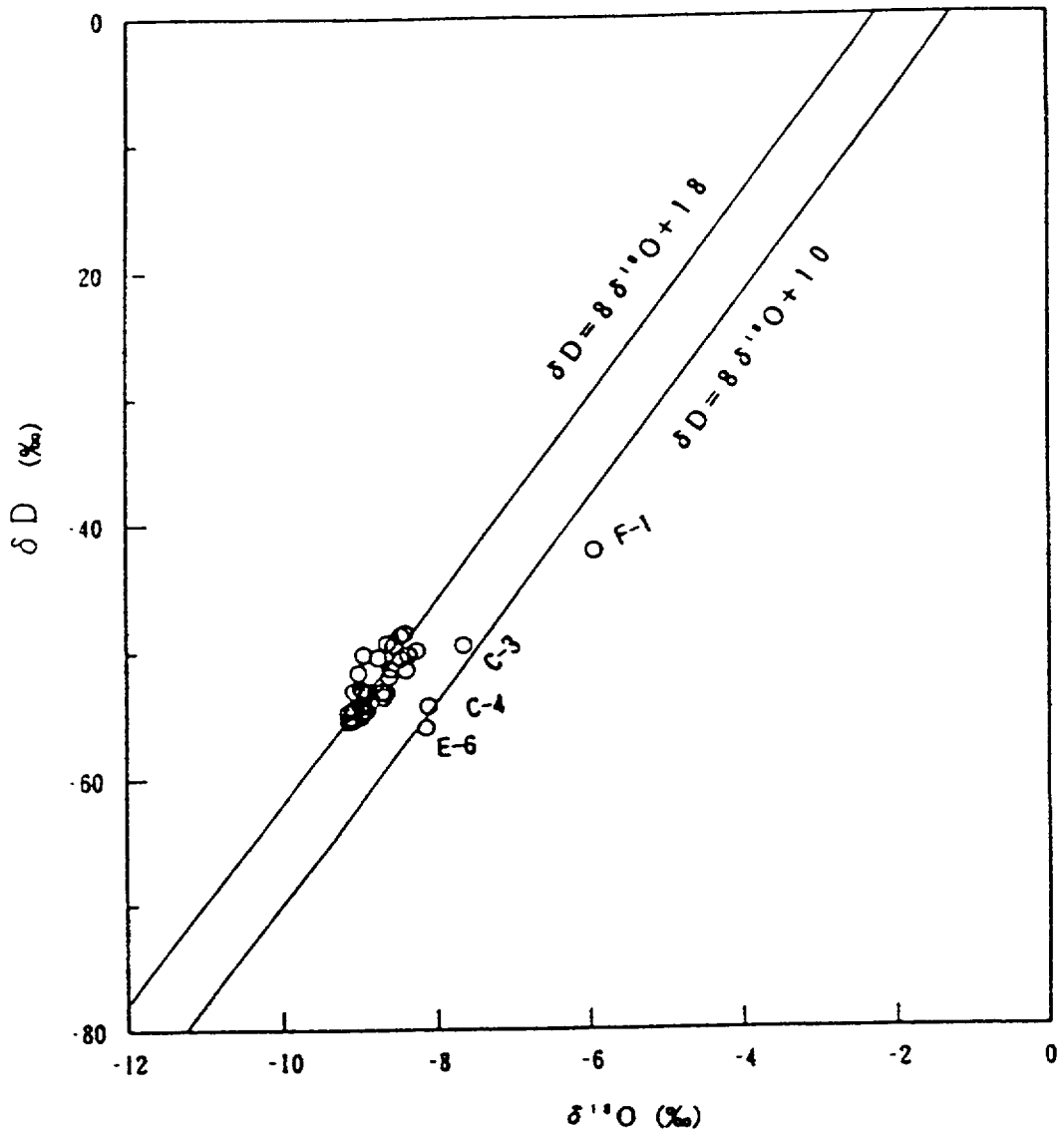


Figure 3.3. Stable isotope composition of groundwater samples, plotted as δD (o/oo) vs. $\delta^{18}O$ (o/oo).

mass spectrometer VG-5400 after extraction and purification of gasses with a conventional technique (Takaoka et al., 1987).

Figure 3.4 shows the groundwater dating results based on the ^3H - ^3He method in relation to the sampling depth. The average residence time increased with decreasing sampling depth down to 20 meters. On the other hand, the average residence time did not depend on the sampling depth when the depth was lower than 20 m. This result probably corresponds to the topographical characteristics of the site. The measured groundwater residence time ranged from 0 to 40 years.

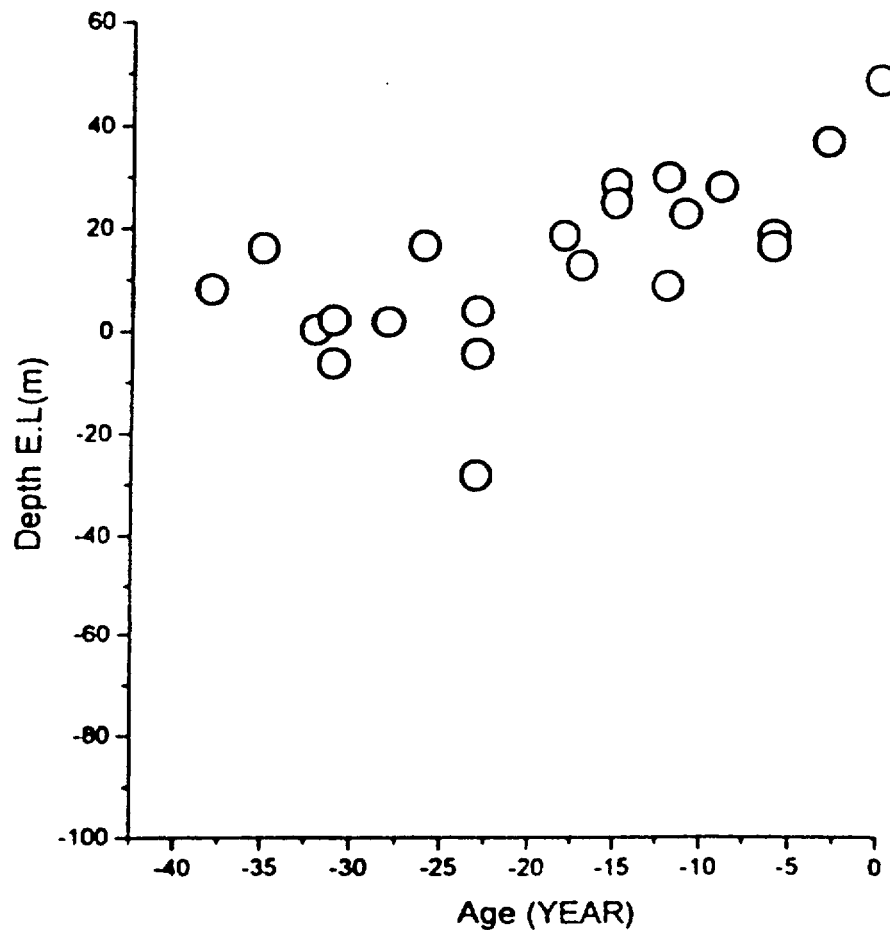


Figure 3.4. Relation between ^3H - ^3He dating results and sampling depths of groundwater samples.

The chemical forms of redox-sensitive elements in groundwater samples were analyzed to determine the redox condition of the site. We selected iron and iodine for the analysis because these redox-sensitive elements have different redox states of soluble forms, Fe^{2+} vs. Fe^{3+} and I^- vs. IO_3^- . The other redox-sensitive elements such as manganese and sulfur do not have ideal soluble forms or species with different oxidation states, e.g. solid phases of Mn^{4+} and gaseous phases of S^{2-} . In addition, one of the familiar geochemical codes, PHREEQE developed by Parkhurst et al. (1980), was applied to the observed data and the predicted chemical forms of the redox-sensitive elements were compared with the measured chemical forms to confirm the applicability of the geochemical code to the LLW disposal site.

The measured and predicted chemical forms of Fe were compared as shown in Figure 3.5. Either Fe^{2+} or Fe^{3+} as a major chemical form of soluble iron was dependent upon the sampling points at the site. It is apparent that the measured $\text{Fe}^{2+}/(\text{Fe}^{2+} + \text{Fe}^{3+})$ agreed with the calculated results. On the other hand, the measured chemical form of iodine was I^- . The result is in agreement with the results calculated by the PHREEQE code. This indicates that PHREEQE is useful for evaluating the chemical forms of elements in the shallow groundwater at this site.

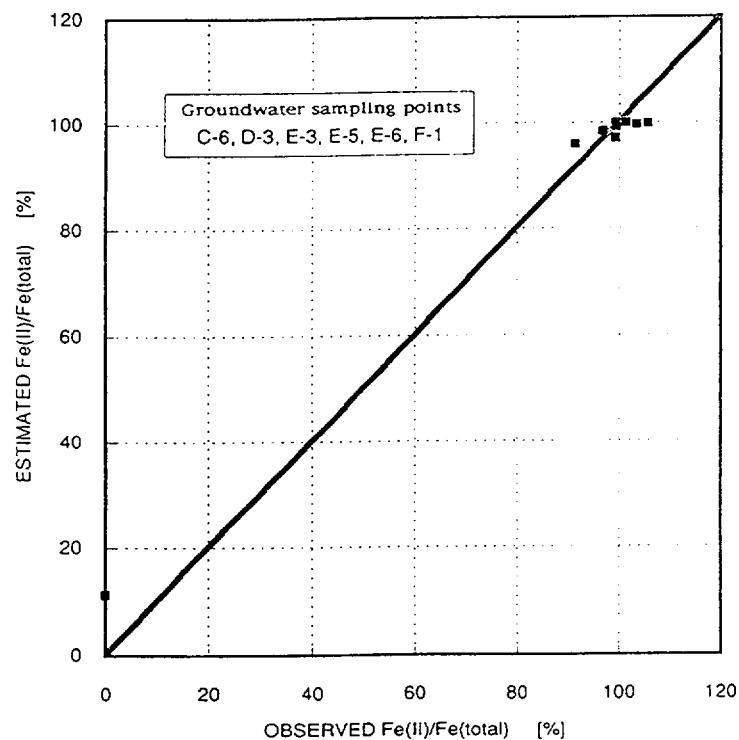


Figure 3.5. Comparison of the observed ratio of $\text{Fe}^{2+}/\text{Fe}(\text{total})$ with the ratio of $\text{Fe}^{2+}/\text{Fe}(\text{total})$ predicted by PHREEQE.

We estimated the chemical forms of several critical nuclides for safety assessment by applying the PHREEQE code to the observed data on chemical properties of groundwater samples taken at the LLW disposal site. The nuclide concentration was determined by considering the inventories of LLW and the background stable isotope concentrations. For example, the calculated chemical forms of cobalt and uranium as a function of pH are shown in Figures 3.6 and 3.7, respectively. The pH values range from 5.5 to 9.5 and the other chemical characteristics were measured at the different sampling points at the site. These Figures illustrate that the major chemical form of cobalt is Co^{2+} and the only sensitive factor affecting the chemical form of Co is pH whereas the chemical form of U depends on not only pH but also a dissolved carbonate concentration.

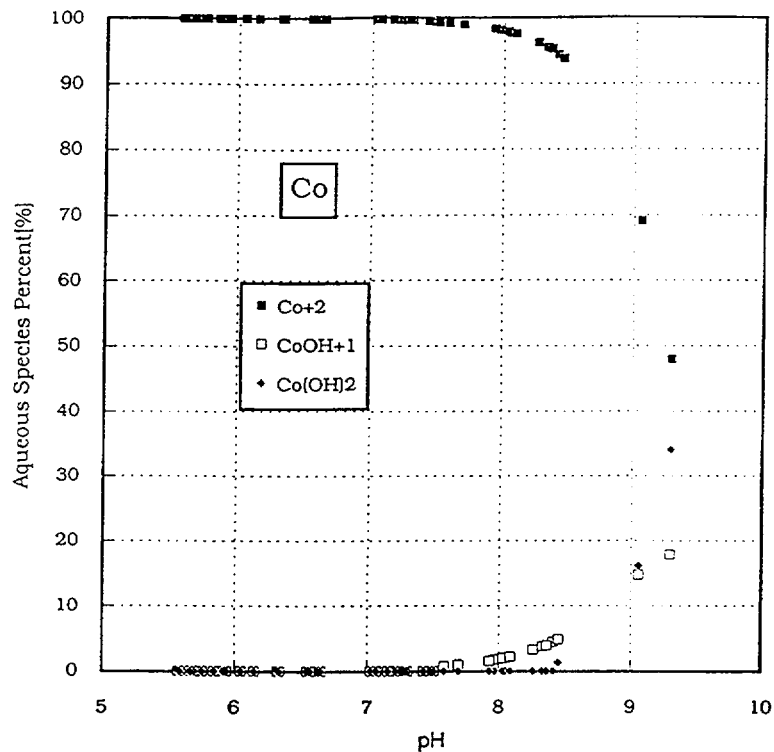


Figure 3.6. The chemical species of cobalt predicted by PHREEQE based on measured chemical properties of groundwater samples.

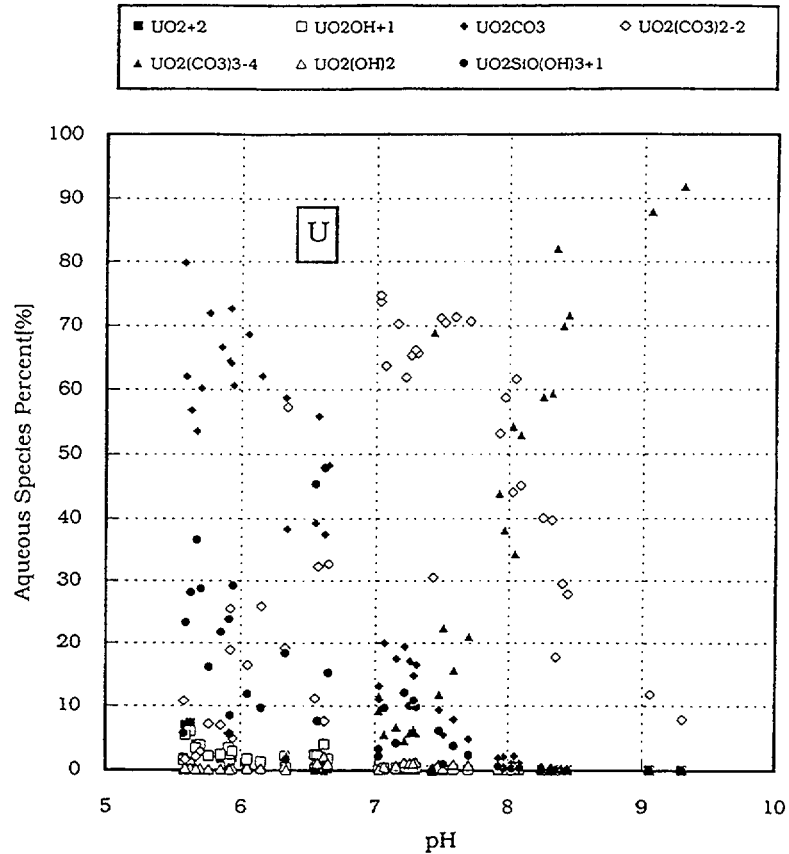


Figure 3.7. The chemical species of Uranium predicted by PHREEQE based on measured chemical properties of groundwater samples.

Once the chemical information including pH, redox and chemical constituents are obtained for the groundwater sample, the distributions of chemical forms of nuclides which may be leached into the subsurface environment can be calculated with an appropriate geochemical code, e.g. PHREEQE, in case of contact with the original groundwater or the pore water in cement. The major chemical forms of several nuclides in the groundwater and in the cement pore water calculated by PHREEQE are listed in Table 3.1. To understand the chemical forms of nuclides is effective for determining adsorption parameters (e.g., K_d) of each nuclide.

Table 3.1. The Major Chemical Species of Nuclides in Natural Groundwater and in Pore Water in Cement Predicted by PHREEQE

| Nuclide | Natural Groundwater | Pore Water in Cement |
|---------|---|--|
| C | $\text{H}_2\text{CO}_3, \text{HCO}_3^-$ | CaCO_3 |
| Co | Co^{2+} | $\text{Co}(\text{OH})_2$ |
| Ni | Ni^{2+} | $\text{Ni}(\text{OH})_2, \text{Ni}(\text{OH})_3^-$ |
| Sr | Sr^{2+} | Sr^{2+} |
| I | I | Γ |
| Tc | TcO_4^- | TcO_4^- |
| Cs | Cs^+ | Cs^+ |
| Pu | $\text{Pu}(\text{CO}_3)_3^{2-}$ | $\text{Pu}(\text{OH})_5^-$ |
| Am | Am^{3+} | $\text{Am}(\text{OH})_2\text{CO}_3^-$ |

4. SUMMARY

Geochemical investigations are important in order to better understand the groundwater flow and mixing behavior and to evaluate the geochemical conditions which control the underground mobility of nuclides. The groundwater dating based on the ^3H - ^3He method and the applicability of the familiar geochemical code PHREEQE to the LLW disposal site by comparing the calculated and measured chemical forms of redox-sensitive elements were described. These geochemical investigations combined with the geological and geohydrological investigations are available for the safety assessment of the second-phase LLW shallow disposal.

REFERENCES

- Mahara Y., Igarashi T., and Tanaka Y. (1991). Survey of groundwater using H-3+He-3 dating method. Proceedings of the Third International Symposium on Advanced Nuclear Energy Research -Global Environment and Nuclear Energy-, Mito, I-14, 85-89.
- Mahara Y. and Igarashi T. (1993). Survey of groundwater flow in a volcanic aquifer by the $3\text{H}+3\text{He}$ dating method. Selected papers on Environmental Hydrogeology from the 29th International Geological Congress, Kyoto, Vol. 4, 173-183.
- Igarashi T. and Mahara Y. (1992). Chemical forms of redox-sensitive elements in groundwater in a sedimentary rock area. Proceedings of the 29th International Geological Congress, Kyoto, Vol.3, II-20-3,O-3, 888.

Parkhurst D.L., Thorstenson D.C. and Plummer L.N. (1980). PHREEQE-A computer program for geochemical calculations. U.S. Geological Survey, Water Resources Investigations 80-96.

Shimoda H. and Iimura H. (1991). Shallow land disposal of low-level radioactive waste by burying in concrete vault: Design and construction of the facility at Tokkasho storage center. Proceedings of the Third International Conference on Nuclear Fuel Reprocessing and Waste Management, Sendai, Vol.1, 439-443.

Takaoka N. and Mizutani Y. (1987). Tritogenic ^3He in groundwater in Takaoka, Earth Planet. Sci. Lett., **85**, 74-78.

Waseda A. and Nakai N. (1983). Isotopic compositions of meteoric and surface waters central and northeast Japan, Geochem. Jour., **17**, 83-91 (in Japanese).

Modelling of Hydrochemistry at TVO Investigation Sites - Case Study: Olkiluoto Site

Petteri Pitkänen
Technical Research Centre of Finland (VTT)
FIN-02044 VTT, Finland

Margit Snellman
Imatran Voima Oy IVO
FIN-01019 IVO, Finland

Hilkka Leino-Forsman and Ulla Vuorinen
Technical Research Centre of Finland (VTT)
FIN-02044 VTT, Finland

ABSTRACT

A preliminary model for probable processes responsible for the evolution of the groundwater at the nuclear waste investigation site Olkiluoto is presented (Pitkänen et al. 1994). The hydrogeological data was collected from boreholes drilled down to 1000-m depth into crystalline bedrock. Based on chemical, isotopic, petrographic and hydrological data as well as ion plots and speciation calculations with PHREEQE, the thermodynamic controls on the water composition and trends constraining these processes are evaluated. In order to determine the reactions which can explain the changes along the flow path during the evolution of the groundwater system and to determine to which extent these reactions take place, mass balance calculations with the NETPATH program were used. Mass transfer calculations with the EQ6 program were used to test the feasibility of the model derived, to predict reaction paths and composition of equilibrium solutions for the redox reactions.

According to this first geochemical model mixing of relict Baltic seawater and deep saline groundwater seems to be the main sources of salinity for the different groundwaters at ambient temperatures. Water-rock interaction seems to play a major role only at shallow depths in the groundwater recharge environment. Deeper in the bedrock water-rock interaction probably has only a minor, but important, role in controlling the pH and redox conditions. Downward intrusion of seawater type brackish and surficial fresh groundwater layers as a result of coastal regression is indicated by ion exchange calculations. The former is replacing saline groundwater at intermediate depths, and, the latter, brackish groundwater at shallow depths. The slightly basic conditions in the bedrock groundwaters seem to result from the buffering of pH by calcite dissolution and precipitation coupled with silicate hydrolysis. The mass-balance calculations indicate anaerobic respiration of organic matter coupled with bacterially catalysed

sulphate and ferric iron reduction leading to pyrite precipitation, to be feasible redox-controlling processes in the fresh and brackish groundwaters. Methane is probably the main reducing agent in the metastable environment at the interface between the brackish and saline groundwaters. The deeper saline groundwater seems to be chemically stable. Similar Br/Cl ratios in the saline groundwater and bedrock as well as heavier ^{18}O and ^2H than in overlaying fresh and brackish groundwaters also indicate hydraulic stagnancy at ambient conditions.

The geochemical model of the evolution of groundwaters at Olkiluoto is based on the isotopic data from groundwater and minerals as well as mineralogical evidence, but it is to be noted that the data available for validating the model has been insufficient. The ongoing detailed site investigation programme (1993-2000) (TVO 1993) is expected to complement the hydrogeological data, and thus enables extension of the preliminary geochemical model to a conceptual hydrogeochemical flow model in the near future.

1. INTRODUCTION

Characterization and interpretation of groundwater chemistry is an important component of radioactive waste disposal. Transport of radionuclides in groundwaters is affected by a number of adsorption and desorption processes and dissolution and precipitation reactions. In order to understand and characterize these processes, a model describing the rock-water reactions controlling the basic hydrochemistry along the flow path in the groundwater system is needed.

The geochemistry of the groundwaters of the investigation sites, Kivetty, Romuvaara, Syyry and Olkiluoto, has been evaluated since 1990 as part of the site investigation programme of Teollisuuden Voima Oy (TVO) for nuclear waste disposal (TVO 1992). The goal of the studies has been to identify probable processes responsible for the evolution of the groundwater in the areas, and to quantify the reactions playing a role in producing the observed water compositions. Based on chemical, isotopic, petrographic and hydrological data, as well as ion plots and speciation calculations with PHREEQE (Parkhurst et al. 1980), the thermodynamic controls on the water composition and trends constraining these processes have been identified (Pitkänen et al. 1992, Pitkänen et al. 1994). The hydrogeological characterization is based on measurements and interpretations from surface and boreholes drilled down to a 1,000 m-depth.

The Olkiluoto site is the first area for which a preliminary model for probable processes responsible for the evolution of the groundwater was constructed (Pitkänen et al. 1994). The mass balance model NETPATH (Plummer et al. 1991) was used in order to determine the reactions which can explain the changes along the flow path during the evolution of the

groundwater system, and to determine to which extent these reactions take place. Mass transfer calculation with the EQ6 (Wolery 1992) program was used to test the thermodynamic feasibility of the model derived, to predict reaction paths and the composition of equilibrium solutions for redox reactions.

This study presents the preliminary evolutionary model for the Olkiluoto area.

2. HYDROGEOLOGICAL SETTING

The Olkiluoto site is an island off the coast of the Gulf of Bothnia (Figure 4.1). The site is situated in that part of the Fennoscandian shield where the modern postglacial land uplift is moderate, about 6 mm per year. The elevation on the island is mainly less than 10 m above the mean sea level.

The investigation site is located in Svecokarelian terrain of Proterozoic age (1900 - 1860 Ma). The bedrock consists of coarse-grained granite migmatized mica gneiss. Ancient fracture controlled hydrothermal activity in several stages has produced complex mineral assemblages in the fractures. The alteration of primary minerals has been penetrative and the most distinct kaolinization of plagioclase may cover tens of centimetres thick interfaces around fractures.

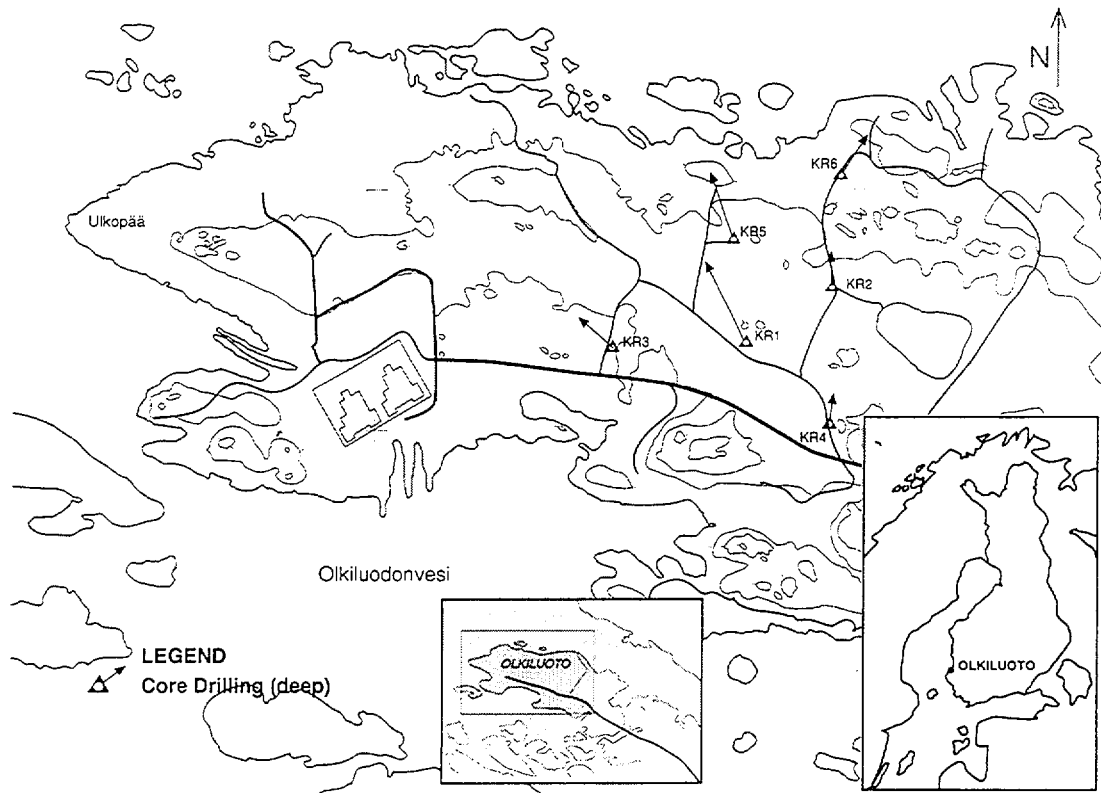


Figure 4.1. Location of the Olkiluoto site.

Calcite, pyrite, kaolinite, illite and chlorite are abundantly occurring fracture minerals in all boreholes from top to bottom. The low temperature calcites according to fractionation of oxygen isotopes have been observed above 600 m and occasionally in fractured zones below that level (Blomqvist et al. 1992, Frape et al. 1992). Rust has been observed only once as a fracture-coating mineral at a depth of 40 m. The results indicate limited and slow intrusion of reactive surface water in the bedrock and is consistent with the low hydraulic gradient in the area. Pyrite has also been observed as coatings on the low temperature calcites (Blomqvist et al. 1992).

3. HYDROGEOCHEMISTRY

The groundwater types encountered at the site are a diluted recharge Ca-Na-(Mg)-HCO₃-SO₄ water, a shallow fresh Na-Cl-(HCO₃) type, a brackish Na-Cl type in intermediate depth resembling modern Baltic seawater (3,250 mg/l in Cl) with increasing salinity, and a deep saline Ca-Na-Cl type that reaches 22,000 mg/l in Cl (Table 4.1 and Figure 4.2.).

Table 4.1. Groundwater Types at Olkiluoto Including Baltic Sea Water.

| Parameter | Recharge water | Shallow fresh water | Upper brackish water | Deeper brackish water | Upper saline water | Intermediate saline water | Deep saline water | Seawater |
|---------------------|----------------|---------------------|----------------------|-----------------------|--------------------|---------------------------|-------------------|----------|
| Na, mg/l | 2.2 | 190 | 570 | 1250 | 2800 | 3900 | 6600 | 1700 |
| Ca, " | 3.6 | 21 | 110 | 350 | 1700 | 3300 | 6200 | 91 |
| Mg, " | 1.9 | 6.4 | 37.4 | 55.3 | 57 | 49.3 | 59.8 | 230 |
| K, " | 1.04 | 2.7 | 6.7 | 10.3 | 13.9 | 19 | 15.6 | 61.4 |
| Fe, " | 0.49 | 1.45 | 0.05 | 0.17 | 0.21 | 0.38 | 0.38 | <0.1 |
| Br, mg/l | <0.05 | 0.7 | 3.4 | 12.8 | 52.4 | 95 | 157 | 11.5 |
| Cl, " | 1.8 | 203 | 910 | 2600 | 7580 | 12000 | 22000 | 3250 |
| SO ₄ , " | 15.1 | 17 | 198 | 170 | 11 | 0.14 | <0.1 | 501 |
| HS, " | | <0.05 | | <0.05 | 3.1 | 0.12 | <0.1 | |
| Alk, meq/l | 0.25 | 3.9 | 4.18 | 0.67 | 0.66 | 0.4 | 0.12 | 1.63 |
| pH | 5.4 | 8.5 | 8.1 | 8.6 | 9 | 8.9 | 8.8 | 7.7 |
| Eh, mV | | | -270 | -250 | -244 | -290 | -140 | |

In general, the salinity and Na, Ca, Cl, and Br concentrations increase with depth, whereas Mg, K, HCO₃ and SO₄ show varying trends. Fe, Al, HS and dissolved silica concentrations are low, max. a few mg/l. Na, Ca, SO₄ and Br follow the seawater dilution line in low and moderate Cl concentrations, up to 1,000 mg/l. With higher Cl concentrations they turn towards the composition of deep saline groundwater. Mg and K are depleted compared to seawater dilution. Alkalinity shows a great increase in fresh groundwater until the concentration decreases steeply in brackish groundwater. The pH increases immediately from 5 - 6 of the recharging water to the level of 8 - 9 in bedrock groundwater. The redox conditions are sulphidic in the bedrock groundwater, even methanic in saline groundwater.

OLKILUOTO

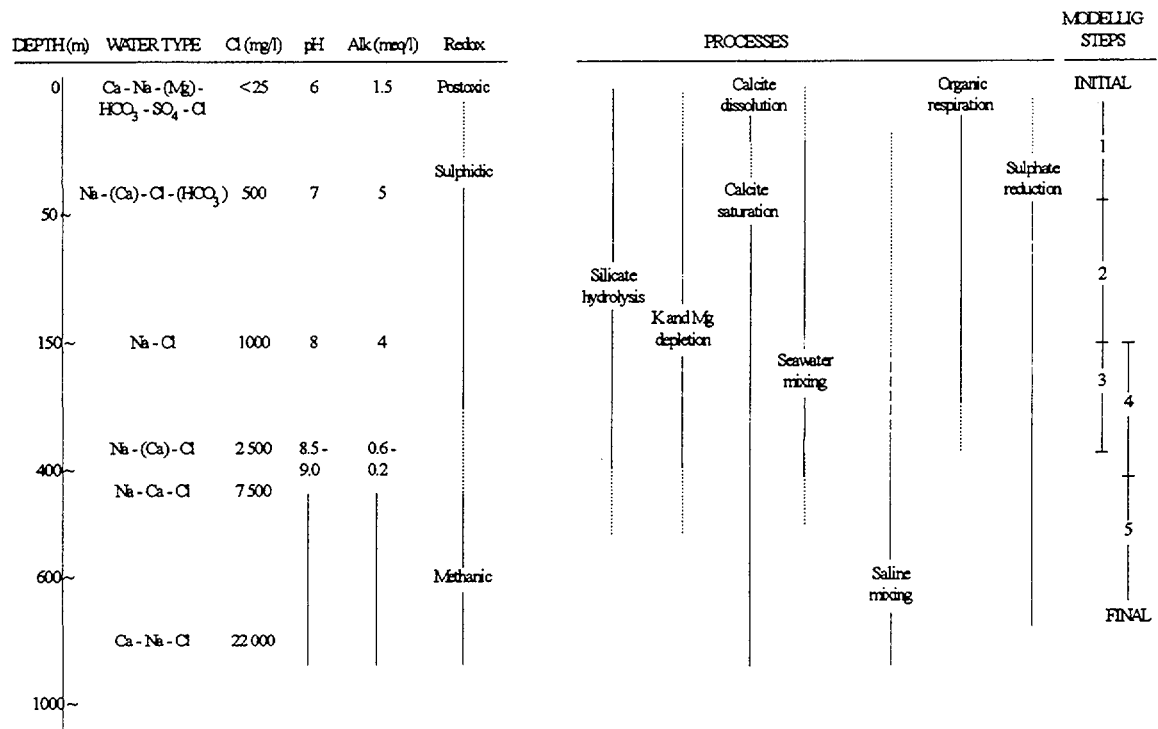


Figure 4.2. Schematic representation of the geochemical evolution of groundwater with depth at Olkiluoto.

4. MASS TRANSFER MODELLING

A set of six analyses was selected for mass balance modelling (NETPATH) (six analyses from left in Table 4.1), representing the most extreme chemical changes from recharge water via fresh groundwater, brackish groundwater and the transition zone between brackish and saline groundwater to intermediate saline groundwater (Figure 4.3). The selected

processes (Figure 4.2) which can explain the changes between the initial and final water of the modelling steps are based on the observations in chemical, isotopic, mineralogical and hydrological data and the results of speciation calculations. As Olkiluoto is a coastal regression area, mixing of different waters is very probable. Modern seawater and the most saline deep groundwater sample (Table 4.1) from the area were used as mixing end-members. Chloride is considered the most sensitive and conservative indicator of compositional changes, in the water chemistry at low temperatures which according to fracture calcite studies (Blomqvist et al. 1992, Frapé et al. 1992) have prevailed at least hundreds of thousands of years, probably longer, since the Precambrian. Bromide was also considered to show conservative behaviour and it with Cl has been used as conservatively mixing parameters in calculations.

Mass transfer calculations with the EQ3/6 was used to look at the resulting thermodynamic state in the mixing of waters at the brackish-saline water interface, and particularly at the iron and sulphide relations in the system.

5. RESULTS AND DISCUSSIONS

The calculated results show that Na and Ca in brackish water and SO₄ in fresh and low saline brackish water are produced mainly (> 80%) by the mixing of fresh recharging groundwater descending into the bedrock containing Baltic-type seawater and saline deep groundwater. The same principal sources were expected for these ions, because Na, Ca, SO₄, and Br compared to Cl show a linear increase of the same kind from fresh to brackish groundwater. Stable isotope compositions (²H, ¹⁸O, ³⁴S/³²S, ⁸⁷Sr/⁸⁶Sr and ¹⁸O(SO₄)) of groundwaters and sea water (Blomqvist et al. 1992, Pitkänen et al 1994) also support the conclusion. However, Na, Ca and SO₄ also take part in chemical interaction. Cation exchange was considered a probable process in the coastal regression area, where seawater has first intruded into an originally Ca-rich saline aquifer. Later seawater has been replaced by recharging Ca-dominated diluted water. The calculated results also indicate these replacement processes (Figure 4.4). Ca is released in the brackish groundwater layer, representing the seawater-type intrusion, and in the shallow fresh groundwater, where brackish aquifer is diluted, Na is released. The depletion of Mg and K is well explained by ion exchange. The exchange of Na and Ca during the last two steps is more considered as being due to balancing of groundwater chemistry of the high-salinity groundwaters than actual ion-exchange.

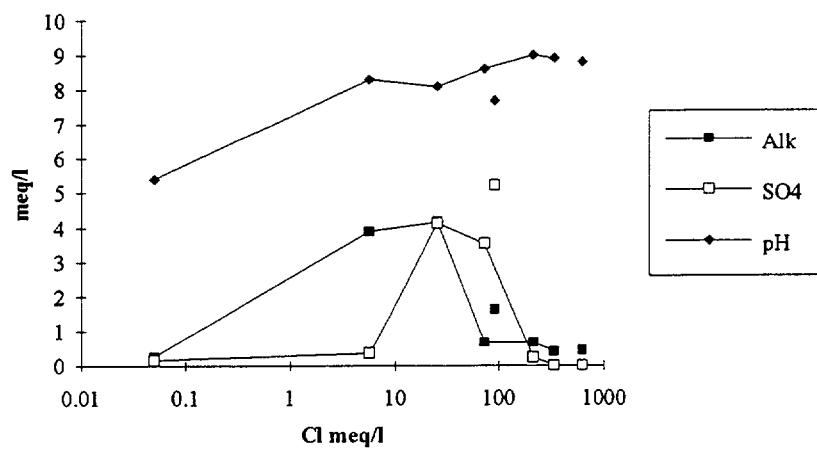
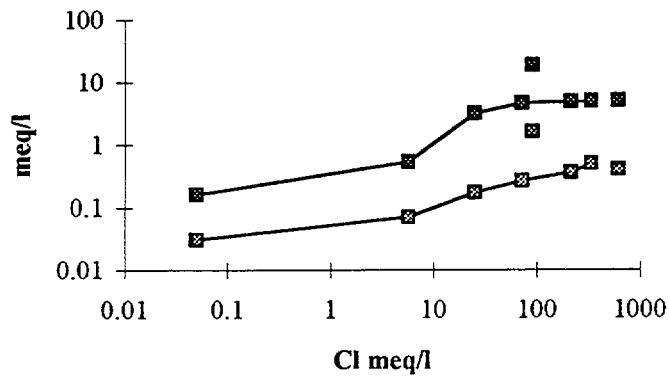
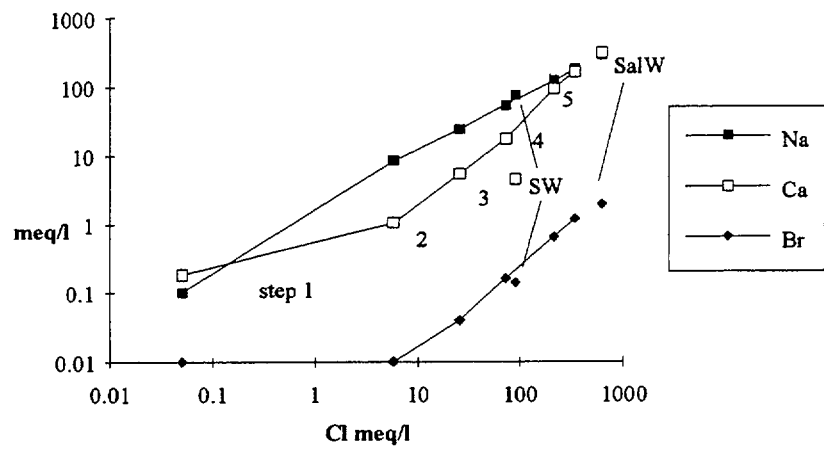


Figure 4.3. Changes in concentration of dissolved chemical constituents (water samples in Table 4.1) along the evolutionary path at Olkiluoto. Numbers in the uppermost figure refer to modelling steps shown in Figure 4.2. Values of sea water (SW) are shown at 100 meq/l and saline water (SalW) far right.

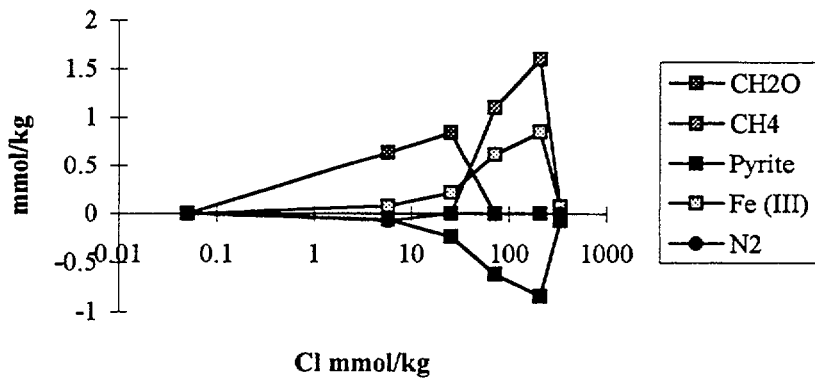
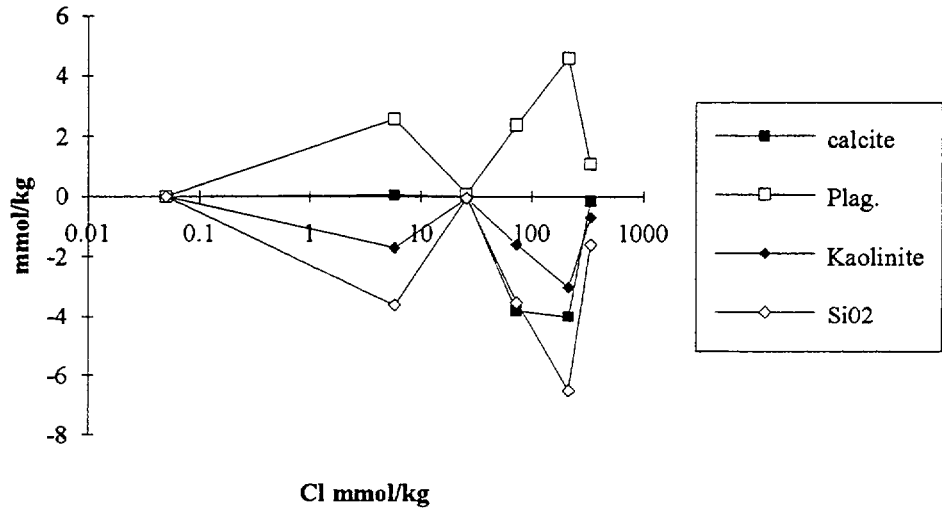
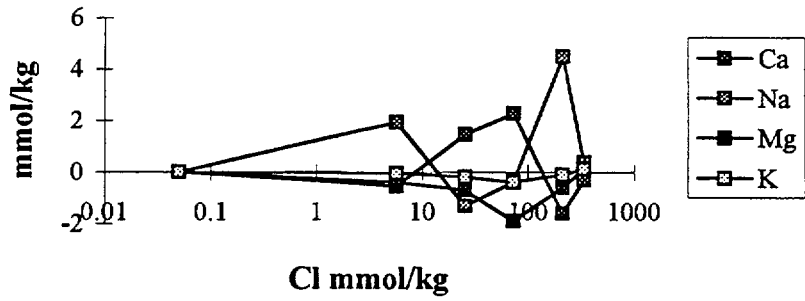
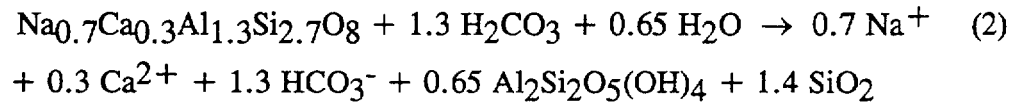
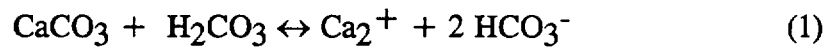


Figure 4.4. Mass transfer of cation exchange (uppermost), hydrolysis (middle) and reactions of redox phases (lowest) of model results. A positive value means dissolution and a negative value, precipitation. The recharge water is far left and the modelled steps are in succession to the right so that the rightmost points represent the mass transfer of the fifth step.

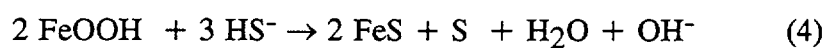
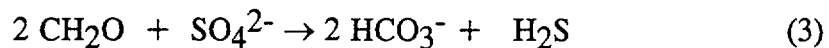
The slightly basic conditions of the bedrock groundwater at all depths seem to result from the buffering of pH by calcite dissolution (reaction 1), which is limited to very shallow depths according to fracture mineralogy, and precipitation (reaction 1 reverse) coupled with silicate hydrolysis being calculated as plagioclase weathering to kaolinite and silica (reaction 2) according to fracture mineralogy. The release and consumption of protons is reasonably conserved in these reactions. The calcite precipitation reaction also consumes a significant part of the dissolved bicarbonate in the brackish groundwater.



However, calcite dissolution does not seem to play a major role in the steep increase in bicarbonate of the fresh groundwater at shallow depths. The high calculated pCO_2 values ($-3.5 < \log \text{pCO}_2 < -2.6$) in fresh and brackish groundwater and available data on the $\delta^{13}\text{C}$ (DIC) content (-17 PDB) of brackish groundwater indicate an organic source for the bicarbonate.

The $\delta^{13}\text{C}$ content of fracture calcites at shallow depths is about $-50/00$ PDB (Blomqvist et al. 1992). The mass-balance calculations (Figure 4-4) emphasize silicate hydrolysis, which is promoted by carbonic acid (aerobic respiration) in the recharge water, to be the net bicarbonate-producing reaction.

The calculations also indicate anaerobic respiration of organic matter (reaction 3), coupled with microbially catalyzed sulphate and ferric iron reduction leading to pyrite precipitation (reactions 4 and 5), to be an important bicarbonate source in fresh and brackish groundwater (Figure 4.4).



These also seem to be plausible redox-controlling processes in Olkiluoto. Pyrite coatings on low- temperature fracture calcites (Blomqvist et al. 1992), lack of ferric precipitates, comparable amounts of measured and

calculated organic carbon in groundwater and sulphidic redox-conditions even at shallow depths in bedrock support the calculated results. Deeper in the methanic region methane has been used as an oxidising agent (reaction 6). In the brackish-saline water interface a metastable state in the redox chemistry, as indicated by the simultaneous occurrence of methane and sulphate, may have been maintained by kinetically constrained iron dissolution according to the reaction path modelling by the EQ6 program. A small amount of iron reducing bacteria, or the strong bonding of ferric iron in silicates, might be the reason for the slow kinetics of iron.

REFERENCES

- Blomqvist R., Nissinen P., Frapé S. (1992). Dating of fracture minerals from Olkiluoto, Eurajoki (in Finnish, with an English abstract), Teollisuuden Voima Oy/Site Investigations, Technical Report 92-27, 117.
- Frapé S., Blyth A.R., Jones M.G., Blomqvist R., Tullborg E.-L., McNutt R.H., McDermott F., Ivanovich M. (1992). A comparison of calcite fracture mineralogy and geochemistry for the Canadian and Fennoscandian Shields. In: Water-Rock Interaction (eds. Kharaka Y.K. & Maest, A.S.), Vol. 1, Proceedings of the 7th International Symposium on Water-Rock interaction - WRI-7, Balkema, Rotterdam, 787-791.
- Parkhurst D.L., Thorstenson D.C., Plummer N. (1980, revised 1990). PHREEQE- A Computer Program for Geochemical Calculations, U.S.Geological Survey, Water-Resources Investigation Report 80-96, 195.
- Pitkänen P., Snellman M., Leino-Forsman H. (1992). Modelling of water-rock interaction at TVO investigation sites - summary report, Nuclear Waste Commission of Finnish Power Companies, Report YJT-92-30, 71.
- Pitkänen P., Snellman M., Leino-Forsman H., Vuorinen, U. (1994) Geochemical modelling of the groundwater at the Olkiluoto site, Nuclear Waste Commission of Finnish Power Companies, Report YJT-94- 10, 75.
- Plummer L.N., Prestemon E.C., Parkhurst, D.L. (1991). An interactive code (NETPATH) for modelling NET geochemical reactions along a flow PATH. U.S.Geological Survey, Water-Resources Investigation Report 91-4078, 101.
- Teollisuuden Voima Oy (1992). Final disposal of spent nuclear fuel in the Finnish bedrock, preliminary site investigations, Nuclear Waste Commission of Finnish Power Companies, Report YJT-92-32E, 324.
- Teollisuuden Voima Oy (1993). Detailed site investigations programme 1993-2000, TVO Site investigation project, Work report PATU-93-01E, 43.

Wolery, T.J (1992). EQ3/6 A softpackage for geochemical modeling of aqueous systems (Version 7), Lawrence Livermore National Laboratory, UCRL-MA-110662 PT1-4.

**THE GEOLOGY AND HYDROGEOLOGY OF
THE SELLAFIELD AREA:
hydrochemical data acquisition and interpretation**

(for submission to Special Issue of Quarterly Journal of Engineering Geology)

A. H. Bath
British Geological Survey
Nottingham, United Kingdom
Present address:
Golder Associates (UK) Ltd
Nottingham, United Kingdom

R. A. McCartney
Geoscience Ltd
Falmouth, United Kingdom

H. G. Richards, R. Metcalfe and M.B. Crawford
British Geological Survey
Nottingham, United Kingdom

ABSTRACT

Hydrochemical investigations form an important part of the Nirex Site Characterisation Programme at Sellafield. They support the development of a conceptual hydrogeological model of the area as it is now, are the main basis for reconstructing the palaeohydrogeological evolution of the area over the recent geological past (which will assist predictions of future evolution) and allow characterisation of the baseline hydrochemical conditions in the potential repository rock volume. The deep hydrochemistry of the area of interest is dominated by its location on the margin of the East Irish Sea Basin. To the west of the potential repository zone, the influence of basinal brines has been a feature of the deep sedimentary rocks and the Borrowdale Volcanic Group (BVG) basement for a considerable period of geological time. The brines currently present are inferred to be the result of partial dissolution of Permo-Triassic halite by ancient (? Tertiary) meteoric recharge. Within the BVG of the potential repository zone itself, stable isotopic data and estimates of recharge temperature (based on noble gas data) indicate a predominance of old meteoric recharge (possibly late Pleistocene). These groundwaters are moderately saline (Cl concentration about $\frac{3}{4}$ that of seawater) and of Na-Cl type. Br/Cl ratios suggest that a significant component of this salinity is derived from a putative saline groundwater within the Lake District basement further to the east. The BVG within the potential repository zone is overlain by a Permo-Triassic sedimentary sequence containing fresh groundwaters of Ca-HCO₃ type, which are separated from the underlying

saline groundwaters by a fairly sharp salinity transition near the base of the sedimentary formations and locally within the topmost part of the BVG.

1. INTRODUCTION

The Nirex Site Characterisation Programme at Sellafield includes the most intensive hydrochemical investigation of deep groundwaters yet undertaken in the U.K. By the end of 1993, deep boreholes had been drilled at 11 locations within the Sellafield area (Chaplow, to be published, special issue of Quarterly Journal of Engineering Geology (QJEG)). Hydrochemical data from 8 of these boreholes have been reported to varying degrees of completeness by Nirex (1993a). In addition, pre-existing and new hydrochemical data have been acquired for the shallow groundwaters and surface waters of the Sellafield District. These data are also summarised by Nirex (1993a). The geology of the Sellafield area is described by Michie (1994, to be published, special issue QJEG).

This paper summarises the acquisition of hydrochemical data and the interpretation of those data for which analysis and processing have been completed to date. This work has involved many different contractors and consultants at various stages whose contributions to this paper are acknowledged:

Sir Alexander Gibb Deep Geology Group (GDGG) - project management and site supervision (except Borehole 1/1A).

Geoscience Ltd - design and implementation of deep borehole hydrochemical data acquisition programme, correction of raw data for drilling fluid contamination and calculation of recharge temperatures from noble gas data (except Borehole 1/1A).

Wimpey Environmental Ltd - collection and chemical analysis of water samples from Nirex deep boreholes (except Boreholes 1/1A and 2).

Robertson Group plc - collection, analysis and preliminary interpretation of hydrochemical samples from Borehole 1/1A.

Entec Hydrotechnica Ltd - regional hydrology and hydrogeology chemistry surveys.

British Geological Survey (Fluid Processes, Hydrogeology and Analytical Geochemistry Groups) - overall hydrochemical interpretation, stable isotope and gas analyses, porewater analyses, shallow groundwater analyses, duplicate analyses of groundwater samples from Borehole 1/1A.

Postgraduate Research Institute of Sedimentology, University of Reading - noble gas analyses and recharge temperature calculations.

AEA Technology, Harwell - collection and analysis of samples from Borehole 2 (for chemical composition, stable O and H isotopes, ^{14}C and ^3H). Analysis of samples from Boreholes 1/1A, 3, 4 and 5 for ^3H .

NERC Scientific Services Radiocarbon Dating Laboratory - ^{14}C sample processing.

University of Toronto (Radiocarbon Dating Laboratory) - ^{14}C analyses by tandem accelerator mass spectrometry (TAMS).

Institute of Geological and Nuclear Sciences (New Zealand) - environmental ^3H and TAMS ^{14}C analyses.

The objectives of the hydrochemistry data acquisition programme are threefold:

(a) To support the development of a conceptual model of the present-day hydrogeology of the Site and its surrounding District;

(b) To investigate how the groundwater system has evolved over time, including evidence of past groundwater flow directions (palaeohydrogeological interpretation);

(c) To characterise the baseline hydrochemical condition within the Borrowdale Volcanic Group (BVG) beneath the Potential Repository Zone (PRZ); an area lying between Sellafield Works and Gosforth (Chaplow, I preparation, special issue QJEG). (In this paper, the volume of BVG within the PRZ currently identified as the potential repository rock volume will be referred to as the PRV).

The development of a conceptual hydrogeological model of the Site is the subject of a companion paper (Black et al., to be published, special issue QJEG). This model depends to a large extent upon hydrochemical information, particularly the distribution of salinity and inferences regarding the origins of salinity. Given that large variations in groundwater salinity (and therefore density) exist beneath the Site, salinity data are essential for the correct interpretation of environmental pressure measurements as driving forces for groundwater movement. In addition, the distribution of non-reactive solutes such as Cl, Br and the stable isotopes of H and O are indicators of hydrochemically distinct groundwater masses and of zones of mixing between such masses. More localised variations in groundwater compositions can also indicate flow heterogeneities, and hence provide evidence of flow zones.

The basic conceptual model integrates the physical hydrogeology and hydrochemical zonation and thus assumes that the driving forces and the boundary conditions for groundwater flow have been sufficiently constant over recent time for this integration to be meaningful. However, given the low permeability of the deeper formations and the known variations in climatic and geological conditions in the last 10^4 - 10^6 years, the possibility exists that parts of the groundwater system are in a transient rather than steady state. This applies particularly to hydrochemical phenomena (mass transfers), which have much longer response times than hydraulic phenomena (pressures). Thus the interpretation of hydrochemical variations inevitably concerns palaeohydrogeology.

In addition to developing a conceptual model of the site as it is now, the site characterisation also contributes to predicting future changes in the hydrogeological conditions. This issue is addressed by considering the evidence for such changes over an equivalent period of past geological time. Hydrogeological conditions may have changed episodically or by gradual evolution, and will in turn have influenced the transient hydrochemical response. The evidence of hydrogeological change comes not only from hydrochemical data but also, potentially, from mineral phases which might record past fluid chemistries. Palaeo-groundwaters of relevant age may be trapped in fluid inclusions in fracture-filling or diagenetic minerals, or the signatures of the passage of such groundwaters may be recorded in the chemical and isotopic compositions of minerals precipitated from them. In the case of Sellafield, it is likely that most or all of this geochemical evidence is related to episodes of fluid movement in the distant geological past, compared to the timescale of more recent climate-related phenomena. However this evidence may show the extent to which some components of the hydrogeological system have been persistent over very long timescales.

The groundwaters presently occupying low permeability formations are expected to be very old; i.e. there has been a considerable average transit time since recharge. Natural isotopic data may be used to put limits on the average transit times of water or isotopic solutes (Fontes, 1994). The validity of a groundwater model based on present hydrodynamics can be examined by comparing it with such transit time estimates. Evidence of long transit time since recharge is not a direct indication of the solute transit time through the natural system from the sampled location back to the biosphere. However, if such comparisons increase confidence in a given conceptual model (e.g. one that defines regimes of greatly differing transit times), confidence in predicted solute return times based on such a conceptual model is also increased.

The characterisation of baseline hydrochemical conditions in the PRV addresses a number of issues. Firstly, detailed characterisation of the variation of groundwater compositions within the PRV will provide concerning the existence of preferential flow paths and concerning the possible heterogeneity of water/rock reactions (e.g. control of fluid

chemistry by different mineral/water reactions in different fracture types). Accurate characterisation of groundwater chemistry is also needed for predictive modelling of the short-term and long-term chemical evolution of the "near-field" of the potential repository (i.e. the waste containers, the repository backfill and the immediately surrounding mechanically and chemically disturbed zone). Similar data are being used to constrain the conditions of laboratory experiments designed to simulate the geochemical processes affecting transport of radionuclides within the "far-field" (i.e. the undisturbed geosphere). Hydrochemical data also have a direct impact on some aspects of engineering design for the repository (e.g. materials selection).

Hydrochemical characterisation of the PRV prior to disturbance also provides a baseline against which to evaluate hydrochemical changes brought about by major invasive operations, such as construction of the shafts of the proposed Rock Characterisation Facility (RCF). These monitoring results will form part of the experimental programme in the RCF programme aimed at testing numerical models of the PRV.

2. HYDROCHEMICAL DATA ACQUISITION

2.1 REGIONAL SURFACE WATER AND GROUNDWATER SURVEY

Hydrochemical data for shallow on-shore groundwaters and surface waters of the Sellafield District have been compiled from existing sources and from new surveys. The existing data principally comprise baseline data held by the National Rivers Authority, the NERC Institute of Freshwater Ecology (IFE) and British Nuclear Fuels plc. Most of the existing shallow boreholes are less than 100 m deep and completed in Sherwood Sandstone Group and/or drift. Some very limited historical data are available for minewaters in the Florence/Beckermet haematite mines within the Carboniferous Limestone near Egremont.

About 100 springs, including some identified from airborne infrared surveys at the coast below high water mark, eight shallow boreholes currently monitored by NRA, and two deeper mineral exploration boreholes have been sampled for hydrochemical analysis. The latter two boreholes are situated 5 km NW and 2.5 km E of Sellafield Works (between Boreholes 4 and 5) and are 358 m and 545 m deep respectively. Two new rainfall chemistry monitoring stations have been established: on the coast at Sellafield Works and 6 km inland in the Calder valley. Average rainfall compositions are given in Table 2.1.

Two areas outside the Sellafield District where hydrochemical data are of relevance are the offshore East Irish Sea Basin (EISB) and the Lake District massif. Limited published information (Stuart and Cowan, 1991) suggests that formation waters in Triassic sandstones of the South Morecambe gas

field in the EISB are highly saline brines, but undersaturated with respect to halite (see below). Within the Lake District, the IFE has undertaken extensive characterisation of surface waters (e.g. Sutcliffe and Carrick, 1983) and a more recent follow-up study has reviewed data for known saline springs and has obtained pore water chemistry profiles from the lake bed sediments of Derwentwater (30 km northeast of Sellafield), which also indicate the presence of saline groundwaters (Hamilton-Taylor et al., 1988). The Derwentwater data are discussed further below.

Table 2.1 Weighted Means and Ranges of Compositions of Rainfall at Two Locations in the Sellafield Area

| Site | Sellafield Works | | | Calder Valley | | |
|----------------------------|-------------------|-------|-------|-------------------|-------|-------|
| Period | 13/10/91-17/12/92 | | | 23/06/91-14/06/92 | | |
| Rainfall (mm) | 1158 | | | 1129 | | |
| | Mean | Min. | Max. | Mean | Min. | Max. |
| Na (mg/l) | 8.9 | 0.94 | 21.1 | 6.2 | 0.17 | 36.5 |
| Ca (mg/l) | 1.2 | 0.08 | 10.8 | 1.5 | 0.5 | 4.3 |
| Mg (mg/l) | 1.1 | 0.18 | 16.8 | 1.0 | 0.06 | 3.89 |
| SO ₄ (mg/l) | 6.2 | 2.07 | 27.5 | 7.0 | 0.81 | |
| 30.2 | | | | | | |
| Cl (mg/l) | 13.5 | 2.58 | 34.8 | 10.1 | 1.39 | |
| 72.3 | | | | | | |
| δ ² H (‰ SMOW) | 39.9 | 75.9 | -13.5 | 42.0 | 95.9 | -13.5 |
| δ ¹⁸ O (‰ SMOW) | 6.14 | 10.38 | -2.39 | 6.39 | 12.48 | +1.13 |

2.2

HYDROCHEMICAL DATA FROM DEEP BOREHOLES

The acquisition of hydrochemical data from deep boreholes which are representative of *in situ* groundwater conditions is a major technical challenge. Taking groundwater samples from boreholes which have been constructed to meet several competing requirements involves inevitable technical difficulties and compromises. These difficulties and the approaches to resolving them are illustrated by experience in similar programmes in other countries (e.g. Smellie and Laaksoharju, 1992; Gascoyne and Kamineni, 1993).

At Sellafield, the deep boreholes (except Borehole 1/1A) were drilled with water containing organic xanthan polymer (to enhance viscosity and reduce

drilling fluid losses to the formation), NaOH (to maintain pH >9 and hence reduce corrosion) and LiCl (approximately 1000 mg/l Li, to allow drilling fluid contamination of groundwater samples to be traced). Samples of drilling fluids were collected analysed throughout the drilling of each borehole. Borehole 1/1A was drilled with NaNO₃ as the drilling fluid tracer. From groundwater samples collected from this borehole, it was inferred that the brines at that locality contained up to 12 mg/l Li and that less saline groundwaters contained lower Li concentrations. The presence of higher Li concentrations in most of the groundwater samples collected from subsequent deep boreholes indicated that they were contaminated with drilling fluids lost from the borehole during drilling.

Samples of groundwaters from the Nirex deep boreholes have been obtained during various types of hydraulic test, described in detail by Sutton (this issue). These tests may be summarised as follows:

(a) Drill stem tests (DSTs; only used for Borehole 1/1A) and swabbing environmental pressure measurements (SEPMs). These tests were similar. A single packer was set in the open hole at the bottom of a test string. Water was normally lifted out of the test string using a wireline swab cup, which reduced the hydraulic pressure below the packer and induced water to flow from the formation into the test string and thence to the surface. In one DST, water was induced to flow from the formation by partially emptying the test string before placing it in the borehole. In all cases, water flowed into the open hole between the packer and the bottom of the borehole at the time the test was performed. Groundwater samples were collected at the surface from the fluid discharged from the test string during swabbing (SEPMs only), downhole within the test string using wireline samplers (see below) and directly from the test string at the surface as it was removed from the borehole (DSTs only).

(b) Environmental pressure measurements (EPMs). These tests were similar to DSTs, except that water was produced from the test string by injecting air into it. Water samples were collected downhole in a sample chamber adjacent to the packer assembly.

(c) Discrete extraction tests (DETs). These tests were similar to DSTs, except that the section of the formation of interest was isolated using a straddle packer on the bottom of the test string and fluid was lifted from the test string using nitrogen gas injection. Water samples were collected from DETs at the same locations as in DSTs, SEPMs and EPMs, but the surface discharge samples were collected during gas injection from a gas-liquid separator connected to the test string.

(d) Post-drilling DETs (PDDETs). These were similar to DETs, except that a downhole pump was used to produce water from the test string. Water samples have been collected downhole in wireline samplers and at surface from the test string as it was removed from the borehole.

EPMs, DSTs and SEPMS were performed during the drilling of the boreholes. DET were performed either after a section of the borehole has been drilled (prior to it being cased) or upon completion of the borehole. PDDETs were usually performed some months after completion of drilling and associated DETs.

Test intervals for EPMS, SEPMS and DSTs were up to 75 m and those for DETs and PDDETs were generally less than 10 m. Fluid was normally produced from the test interval for one hour for EPMS, and for 12-36 hours for all other tests. Although dependent on the permeability of the test interval, larger volumes of fluid were normally produced during the DETs, as a result of the longer duration of these tests and the larger hydraulic drawdown imposed on the test section. Generally, the larger the volumes of fluid produced during a test, the lower the levels of drilling fluid contamination observed in the groundwater samples. In Tables 2.2 and 2.3, values are given for the minimum extent of contamination (as a percentage of the sample) for each test. This is represented as the minimum Li concentration observed in the groundwater samples from the test, divided by the prescribed Li concentration in the drilling fluid (i.e. 1000 mg/l). In several cases the percentage contamination has been <1% (i.e. the minimum Li concentration has been <10 mg/l). Groundwater samples were only analysed if they were less than 80% contaminated with drilling fluids. Thus, the distribution of hydrochemical data from tests on the Nirex deep boreholes is biased by (a) the availability of flowing features to test and (b) the level of contamination observed in the groundwater samples collected during the tests.

To estimate the in situ groundwater compositions, groundwater sample analyses have been corrected for the effect of contamination by drilling fluids but have not been corrected for the effects of any other source of contamination. The drilling fluid contamination correction technique involves applying linear regression to the analyses of Li and the constituent of interest, for both the groundwater samples collected during the test and the drilling fluids which may have contacted the test interval during drilling. The statistical uncertainty associated with these regressions was also calculated.

The regression method assumes that Li and the constituents of interest are inert with respect to interactions between the drilling fluid, groundwater and formation, and that the groundwater contains an insignificant concentration of Li relative to the drilling fluid. It is believed that Li behaves conservatively under the conditions of its use, given that the estimated ³H content of deeper groundwaters is calculated to be close to zero (see below) using the regression method, and it has been shown above that the in situ Li content of the groundwaters is low relative to that of the drilling fluids.

Table 2.2 Representative Estimates of Deep Groundwater Compositions from the Borrowdale Volcanic Group Beneath the Sellafield Area

| Nirex deep borehole no. | 2 | | 3 | | 4 | |
|-------------------------|----------|------|-----------|------|----------|------|
| Test no. | DET9 | | DET7 | | DET1 | |
| Depth (mbOD) | 646-656 | | 1654-1665 | | 730-737 | |
| % Contamination† | 4.35 | | 2.3 | | 0.287 | |
| | Estimate | 2σ | Estimate | 2σ | Estimate | 2σ |
| Na | 7500 | 300 | 65100 | 3400 | 8070 | 610 |
| K | 95.8 | 4.2 | 539 | 21 | 134 | 6 |
| Ca | 484 | 14 | 2910 | 110 | 867 | 45 |
| Mg | 62 | 1.7 | 489 | 15 | 105 | 5 |
| Sr | 11.6 | 0.5 | 51.6 | 2.5 | 20.9 | 2.0 |
| Si | 2.26 | 0.36 | 1.74 | 0.78 | 2.25 | 0.53 |
| Cl | 12600 | 360 | 104000 | 4800 | 13600 | 600 |
| SO ₄ | 962 | 25 | 3340 | 400 | 1110 | 30 |
| Br | 22.1 | 0.9 | 108 | 3 | 24 | 0.8 |
| F | 2.66 | 0.11 | 0.79 | 0.1 | 2.68 | 0.67 |
| Total alkalinity* | 197 | 42 | 20.4 | 20.3 | 69.5 | 13.8 |
| Total inorganic C# | 38.7 | 5.9 | 30.5 | 33.2 | 66.0 | 11.2 |
| Calculated TDS¶ | 21900 | n/a | 177000 | n/a | 24000 | n/a |
| Measured pH‡ | 6.52 | 0.14 | 7.31 | 0.04 | 7.73 | 0.16 |
| Elect. conductivity§ | 36.6 | 2.3 | 203 | 10 | 35.3 | 1.7 |

σ = standard deviation.

Concentrations in mg/l.

† = 100 × (minimum Li concentration observed in groundwater samples from test) / (1000 mg/l), as %.

¶ Calculated TDS (total dissolved solids) = sum of concentrations of Na, K, Ca, Mg, Cl, SO₄ and Total alkalinity (as HCO₃).

* Total alkalinity expressed as mg/l HCO₃⁻ equivalent.

Total inorganic C expressed as mg/l HCO₃ equivalent.

§ Electrical conductivity in mS/cm @20_C (Borehole 2) or @25°C (other boreholes).

n/a = not applicable.

‡ See text for discussion of interpretation of pH measurements and uncertainties.

Table 2.3. Estimates of Deep Groundwater Chloride and Bromide Concentrations from Nirex Deep Boreholes

| HOLE | TEST NO. | DEPTH (mbrt*) | FORMATION | % CONTAM.‡ | CHLORIDE (mg/l) | | BROMIDE (mg/l) | |
|-------|------------|---------------|---------------|--------------|-----------------|-------|----------------|-------|
| | | | | | Estimate | 2σ | Estimate | 2σ |
| 1/1A | DST1 | 462-497 | Calder Sst. | n.c. | 3250# | n.c. | 4# | n.c. |
| | DST3 | 921-945 | St Bees Sst. | n.c. | 56100# | n.c. | 38# | n.c. |
| | DST8 | 1104-1115 | St Bees Sst. | n.c. | 56800# | n.c. | 58# | n.c. |
| 2 | DET1 | 200-223 | St Bees Sst. | 0.34 | 12.0 | 6.7 | 0.101 | 0.008 |
| | DET2 | 317-323 | St Bees Sst. | 0.50 | 25.2 | 7.2 | 0.059 | 0.006 |
| | DET3 | 360-364 | St Bees Sst. | 1.88 | 10.0 | 13.4 | 0.103 | 0.015 |
| | DET10 | 543-555 | BVG | 3.0 | 13000 | 700 | 23.6 | 1.0 |
| | PDDDET4 | 547-558 | BVG | 4.04 | 14600 | 680 | 23.4 | 0.7 |
| | DET9 | 711-721 | BVG | 4.35 | 12600 | 360 | 22.1 | 0.9 |
| | PDDDET3 | 711-721.5 | BVG | 5.69 | 15700 | 730 | 23.2 | 0.7 |
| | PDDDET7 | 913-969 | BVG | 2.52 | 15800 | 730 | 24.8 | 0.8 |
| | DET8 | 1011-1026 | BVG | 3.4 | 15700 | 800 | 25.9 | 1.1 |
| | PDDDET2 | 1011-1026 | BVG | 3.68 | 16700 | 780 | 27.5 | 0.9 |
| | PDDDET6/6B | 1191-1221.5 | BVG | 4.11 | 15200 | 700 | 24.0 | 0.8 |
| | PDDDET5 | 1423.5-1473.5 | BVG | 3.74 | 15100 | 700 | 24.1 | 0.8 |
| | DET7 | 1587-1602 | BVG | 0.50 | 17400 | 900 | 30.3 | 1.3 |
| | PDDDET1 | 1586-1601.5 | BVG | 0.35 | 17200 | 800 | 30.1 | 1.0 |
| 3 | SEPM5 | 487-640 | St Bees Sst. | 44 | 16400 | 760 | 19.1 | 1.2 |
| | DET4 | 691.5-700 | St Bees Sst. | 1.3 | 64200 | 3100 | 65.4 | 1.8 |
| | DET3 | 776-782 | St Bees Sst. | 0.7 | 65800 | 4900 | 69.1 | 1.9 |
| | DET2 | 931-941 | St Bees Sst. | 9 | 85800 | 5200 | 82.4 | 2.3 |
| | EPM13 | 1040-1094 | St Bees Sst. | 19.8 | 100500 | 4900 | 91.0 | 2.6 |
| | EPM14 | 1089.5-1143 | St Bees Sst. | 16.9 | 100300 | 4900 | 91.7 | 2.6 |
| | DET1 | 1107.5-1117.5 | St Bees Sst. | 1.3 | 108000 | 10100 | 96.6 | 2.7 |
| | EPM15 | 1141-1191.5 | St Bees Shale | 47.8 | 102200 | 5700 | 91.7 | 2.9 |
| | EPM16 | 1141-1242 | St Bees Shale | 63.4 | 70500 | 4800 | 65.9 | 2.4 |
| | DET8 | 1538-1555.5 | CL | 3.1 | 77700 | 3600 | 78.0 | 2.2 |
| | DET7 | 1671-1682 | BVG | 2.3 | 104000 | 4800 | 108 | 3 |
| | 4 | SEPM1 | 160-209 | St Bees Sst. | 36 | 223 | 226 | 0.18 |
| SEPM2 | | 208-261 | St Bees Sst. | 7.3 | 95 | 215 | 0.12 | 0.12 |
| SEPM3 | | 260-306 | St Bees Sst. | 5.6 | 290 | 438 | 0.09 | 0.14 |
| SEPM4 | | 295-361 | St Bees Sst. | 11.6 | 79 | 728 | 0.37 | n.c. |
| EPM6 | | 413-464 | Brockram/BVG | 72.8 | 1140 | 1380 | 1.6 | 0.14 |
| DET3B | | 415-427 | BVG (top) | 0.5 | 1140 | 149 | 1.92 | 0.22 |
| DET2 | | 580.5-587 | BVG | 1.08 | 12300 | 570 | 22 | 0.7 |
| DET1 | | 804-811 | BVG | 0.29 | 13600 | 633 | 24 | 0.8 |
| 5 | SEPM3 | 202.5-312.5 | St Bees Sst. | 13.5 | <20 | n.c. | <0.08 | n.c. |
| | SEPM5 | 366.5-415.3 | St Bees Sst. | 9.5 | 249 | 49 | 0.329 | 0.098 |
| | DET1 | 882-889 | BVG | 42.4 | 13400 | 620 | 22 | 0.6 |
| 7A | EPM1 | 49-105 | St Bees Sst. | 48.8 | 160 | 490 | 0.22 | 0.02 |
| | EPM10 | 513-563 | Brockram/CL | 77.7 | 22050 | 3450 | 29.1 | 1.0 |
| | EPM13 | 666-711 | BVG | 70.8 | 35800 | 2600 | 40.9 | 1.4 |

Table 2.3. (continued)

| | | | | | | | | |
|-------|-------|------------|---------------|-------------|--------|-------|-------|-------|
| 10A | DET3 | 469.5-476 | St Bees Sst. | 1.34 | 98.6 | 20 | 0.20 | 0.013 |
| | DET2 | 558-612.5 | St Bees Sst. | 1.22 | 291 | 20 | 0.422 | 0.013 |
| | DET1 | 662.5-682 | St Bees Sst. | 0.93 | 1900 | 88 | 3.01 | 0.10 |
| | EPM14 | 675-729 | St Bees Sst. | 71.5 | 1870 | 1310 | 3.2 | 0.12 |
| | DET4 | 744-759 | St Bees Shale | 0.62 | 20300 | 950 | 27.9 | 0.9 |
| | DET9 | 855-864 | Brockram | 8.18 | 29400 | 1400 | 36.4 | 1.2 |
| | EPM18 | 868-916 | Brockram | 52.4 | 33070 | 2700 | 42.7 | 1.5 |
| | DET8 | 915-919 | Brockram | 5.91 | 30100 | 1400 | 38 | 1.2 |
| | DET7 | 925-931 | Brockram/CL | 7.58 | 31200 | 1450 | 39.5 | 1.3 |
| | EPM19 | 916-971 | Brockram/CL | 56.9 | 31300 | 2100 | 38 | 1.3 |
| | DET6 | 933.5-941 | CL | 0.74 | 31700 | 2300 | 38.8 | 1.2 |
| | DET5 | 963-969 | CL | 0.68 | 37300 | 1700 | 43 | 1.7 |
| | EPM20 | 971-1013.5 | CL/BVG | 75.5 | 15980† | 2250 | 8.8 | 0.4 |
| | EPM22 | 1056-1105 | BVG | 68 | n.d. | - | 45.3 | 1.5 |
| | EPM23 | 1103-1154 | BVG | 20.7 | n.d. | - | 52.9 | 1.7 |
| | EPM24 | 1153-1207 | BVG | 69.5 | n.d. | - | 11.7 | 0.5 |
| | EPM25 | 1207-1256 | BVG | 74.8 | n.d. | - | 30.1 | 1.2 |
| | 12A | DET3 | 120-127 | Calder Sst. | 5.37 | 350.8 | n.c. | 0.081 |
| DET2 | | 128-137.5 | Calder Sst. | 4.89 | 346.6 | n.c. | 0.081 | 0.013 |
| EPM18 | | 900-952 | CL | 75.5 | 23100 | 2700 | 28.5 | 0.9 |

*mbrt = measured depth in m below rotary table. Rotary table elevations in m above OD were: 25.50 (BH1/1A), 65.20 (BH2), 15.66 (BH3), 73.60 (BH4), 85.63 (BH5), 53.06 (BH7A), 40.48 (BH10A), 44.60 (BH12A). Boreholes are not perfectly vertical (especially BH1/1A) and so conversion to true vertical depth in m below OD requires well survey data.

‡Percentage contamination computed as $100 \times (\text{minimum Li concentration observed in groundwater samples from test}) / (1000 \text{ mg/l})$.

#These values have not been corrected for drilling fluid contamination and may therefore underestimate the concentrations in groundwater.

†Suspect value

Sst. = Sandstone

CL = Carboniferous Limestone

BVG = Borrowdale Volcanic Group

σ = standard deviation

n.c. = not calculated

n.d. = no data available

Although it cannot be demonstrated that the other constituents behave conservatively, it can be stated that this assumption becomes less important (with respect to interactions between drilling fluid, groundwater and the formation) at lower degrees of drilling fluid contamination.

Regression techniques cannot and have not been applied to pH and Eh, which are affected non-linearly by contamination. The reported uncertainties in pH (Table 2.2) are the precisions of the measured values, and do not reflect uncertainties in the *in situ* pH, which are unquantified at present (see below). The regression correction method would also be invalid for total alkalinity, if this does not predominantly consist of carbonate species. Linear regression techniques can be applied to C isotope data as long as they take account of the relative masses of inorganic C in the drilling fluid and in the contaminated groundwater samples. Where the concentration of a constituent in the drilling fluid is substantially

greater than that calculated for the groundwater, the statistical uncertainty associated with the calculated value tends to be greater (e.g. Al, C isotopes and Cl in fresh groundwaters).

It is emphasised that the regression techniques only attempt to correct for the effects of drilling fluid contamination. No correction has been made for contamination from other sources (e.g. testing equipment) which have been identified by comparing the compositions of samples collected from different locations within the testing/sampling equipment. Total alkalinity, TIC and pH have been affected by degassing during depressurisation of the groundwater samples. pH and redox sensitive measurements and species concentrations (e.g. Eh, HS, Fe^{II}/Fe^{III}, Mn) have probably been affected by interaction with the mild steel components of the testing equipment. Al and Fe analyses probably include a proportion due to dissolution of colloidal material when the samples were acidified. For these various reasons, results for Eh, HS, Fe, Mn and Al are not given in Table 2.2.

Some of these problems are being addressed in the specification for Borehole 9A, which is currently (September 1994) being drilled. The aim of this borehole is to improve the quality of some key parameters, particularly those which are most sensitive to drilling fluid contamination (e.g. pH, C isotopes, Cl in fresh groundwaters). The drilling fluid tracer is KI in place of LiCl and, where practicable, the drilling fluid is fresh water without other additives. In addition, the circulating pressure of the drilling fluid is less than in previous Nirex deep boreholes. These improvements will not eliminate the need for a contamination correction but will reduce the magnitude of this correction by reducing the salinity and organic C content of the drilling fluid and by limiting its invasion into the formation.

Additional detail of vertical salinity variations within boreholes has been obtained from geophysical logs (formation resistivity) and by analysing pore waters trapped in preserved drillcore. Pore waters were extracted from the more porous sedimentary rock samples (i.e. from the Sherwood Sandstone Group) by centrifugal displacement with inert heavy liquid. For less porous samples, including all BVG drillcore, the residual solutes have been leached from dried crushed drillcore with deionised water. The Cl concentration of original pore solution has been calculated from the composition of the leachate solution and the measured water content of the preserved saturated drillcore. This approach is considered to be reliable for Cl, a non-reactive solute, but is less reliable for other solutes which might be subject to water-rock reactions during the leaching procedure. Correction of Cl data for drilling fluid contamination is achieved using the observed Li concentration in the pore water or residual solute leachate, and an appropriate drilling fluid composition.

3.

RESULTS

3.1

DISTRICT-SCALE HYDROCHEMICAL REGIMES

The data reported in Nirex (1993a) have led to the recognition of three hydrochemically distinct groundwater regimes, which also have distinct physical hydrogeological attributes. These regimes are discussed at greater length by Black et al. (to be published, special issue QJEG) and are as follows:

- (a) Coastal Plain (CP) regime
- (b) Irish Sea Basin (ISB) regime
- (c) Hills and Basement (H&B) regime

The hydrochemical distinction is primarily in terms of gross salinity, which may be expressed in terms of Cl concentration. A second distinction is on the basis of Br/Cl ratios, which are discussed further below. The CP regime is characterised by relatively fresh groundwaters (Cl < 1000 mg/l), the ISB regime by saline groundwaters and brines (Cl > 20000 mg/l, which is approximately the salinity of seawater) and the H&B regime mainly by brackish to saline groundwaters (Cl between 1000 and 20000 mg/l), although fresh groundwaters are expected to be present at shallow depths within the H&B regime within the outcrop of the BVG. This scheme is illustrated in Figure 3.1, which shows tentative interpolated Cl contours for 1000 mg/l and 20000 mg/l. It must be emphasised that these contours are not synonymous with the boundaries between the different regimes. These "boundaries" are characterised as follows:

- (a) The lateral transition between the ISB and H&B regimes is assumed to be gradational, reflecting an extensive mixing zone which (on the basis of data published in Nirex (1993a) is not yet well characterised. The 20000 mg/l contour shown within this transition zone in Figure 3.1 is quite speculative.
- (b) The vertical transition between the CP and ISB regimes (i.e. between Cl concentrations of about 1000 mg/l and about 20000 mg/l) occurs within the Sherwood Sandstone Group (SSG) in Borehole 3 (Figure 3.2).
- (c) The vertical transition between the CP and H&B regimes is generally defined by the base of the Triassic Sherwood Sandstone Group (SSG). However, although the transition (from about 1000 to 5000 mg/l Cl) occurs near the base of the SSG in Borehole 2 (Figure 3.2), it is within the BVG in Borehole 4.

Table 3.1 Chloride and Bromide Data for Water Samples from Derwentwater

| Sample | Sample Description | Sample Code | Cl | Br | Cl* | Br* | Br/Cl | Br/Cl* |
|--------|--------------------|--------------------|------|------|------|------|---------|---------|
| 5962 | Mini-corer | DM 0-4cm 13 | 14.1 | - | 14.3 | 0.07 | | 0.00472 |
| 5963 | Mini-corer | DM 4-14cm 9 | 40.3 | 0.18 | 39.9 | 0.17 | 0.00442 | 0.00424 |
| 5964 | Mini-corer | DM 14-35cm 7 | - | 0.61 | - | 0.59 | | |
| 5965 | Mini-corer | DM 35-60cm 2 | 298 | 1.81 | 298 | 1.33 | 0.00605 | 0.00447 |
| 5966 | Mini-corer | DM 60-81cm 14 | 373 | 1.87 | 380 | 1.59 | 0.00503 | 0.00418 |
| 5967 | Mackereth corer | DC 1 0-27cm 15 | 274 | 1.13 | 270 | 1.20 | 0.00412 | 0.00444 |
| 5968 | Mackereth corer | DC 2 27-54cm 31 | 396 | 1.69 | 417 | 1.66 | 0.00426 | 0.00398 |
| 5969 | Mackereth corer | DC 3 54-81cm 21 | 511 | 2.13 | 545 | 2.16 | 0.00416 | 0.00396 |
| 5970 | Mackereth corer | DC 4 81-108cm 29 | 774 | 3.34 | 768 | 3.03 | 0.00432 | 0.00395 |
| 5971 | Mackereth corer | DC 5 108-135cm 32 | 911 | 3.72 | 930 | 3.75 | 0.00408 | 0.00403 |
| 5972 | Mackereth corer | DC 6 135-162cm 26 | 667 | 2.85 | 677 | - | 0.00427 | |
| 5973 | Mackereth corer | DC 7 162-189cm 20 | 1379 | 5.58 | 1283 | 5.20 | 0.00404 | 0.00405 |
| 5974 | Mackereth corer | DC 8 189-216cm 6 | 1567 | - | 1569 | 6.34 | | 0.00404 |
| 5975 | Mackereth corer | DC 9 216-243cm 36 | 1773 | 7.19 | 1796 | 7.14 | 0.00406 | 0.00398 |
| 5976 | Mackereth corer | DC 10 243-270cm 23 | 1981 | 8.16 | 1955 | 8.31 | 0.00412 | 0.00425 |
| 5977 | Mackereth corer | DC 11 270-297cm 33 | 2205 | 8.82 | 2148 | 8.41 | 0.00400 | 0.00391 |
| 5978 | Mackereth corer | DC 12 297-324cm 35 | 2370 | 9.40 | 2403 | 9.46 | 0.00397 | 0.00394 |
| 5979 | Mackereth corer | DC 13 324-351cm 25 | 2622 | 10.4 | 2751 | 10.7 | 0.00398 | 0.00390 |
| 5980 | Mackereth corer | DC 14 351-378cm 30 | 2898 | 12.3 | 2865 | 11.3 | 0.00425 | 0.00395 |
| 5981 | Mackereth corer | DC 15 378-405cm 24 | 2990 | 12.4 | 2979 | 11.6 | 0.00414 | 0.00389 |
| 5982 | Mackereth corer | DC 16 405-432cm 34 | 3310 | 12.5 | 3426 | 13.5 | 0.00377 | 0.00395 |
| 5983 | Mackereth corer | DC 17 432-459cm 22 | 3538 | 13.7 | 3481 | 13.5 | 0.00388 | 0.00389 |
| 5984 | Mackereth corer | DC 18 459-486cm 28 | 3410 | 13.1 | 3665 | 14.1 | 0.00385 | 0.00385 |
| 5985 | Mackereth corer | DC 19 486-513cm 5 | 3772 | 14.4 | 4363 | 16.8 | 0.00381 | 0.00385 |
| 5986 | Mackereth corer | DC 20 513-540cm 37 | 4750 | 19.4 | 4716 | 18.0 | 0.00409 | 0.00381 |
| 5987 | Mackereth corer | DC 21 540-567cm 27 | 4492 | 17.4 | 4375 | 16.7 | 0.00388 | 0.00381 |
| 5988 | Lake water | 1 | 12.2 | 0.05 | - | - | 0.00402 | |
| 5989 | Lake water | 2 | 10.9 | 0.05 | 10.7 | 0.04 | 0.00431 | 0.00374 |

The samples were obtained by Hamilton-Taylor *et al.* (1988)

* Duplicate analysis

= no data

Sample codes include depths of core samples below lake bed

D-208

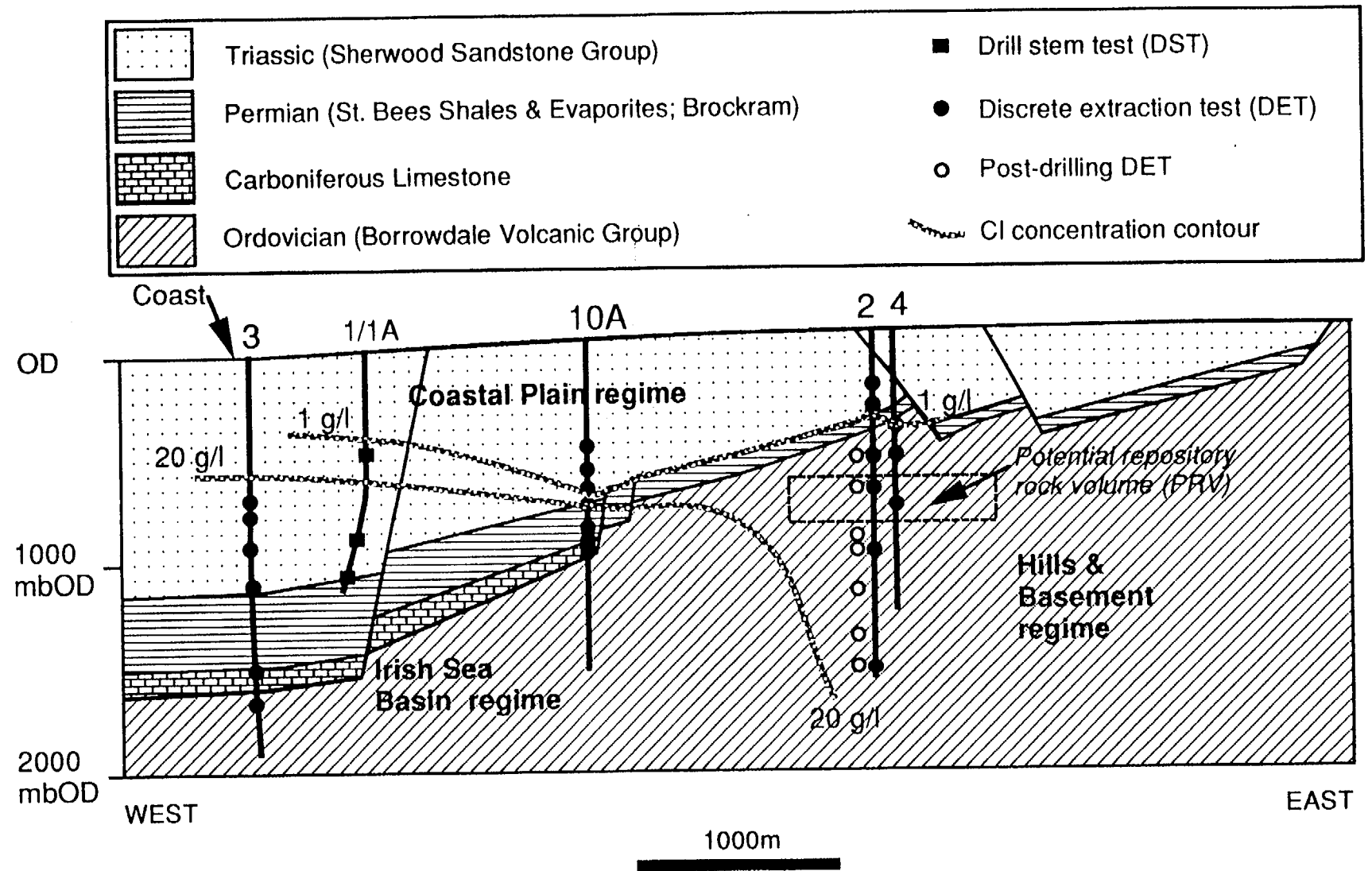


Figure 3.1. Simplified West-to-East section showing principal lithological units, major faults, borehole trajectories, locations of DSTs, DETs and PDDETs, and the three hydrogeological regimes. Tentative interpolated salinity contours at 1 and 20 g/l Cl are also shown. These contours also take account of Cl data from EPMs and SEPMs (Table 3.3).

Sellafield Borehole 2

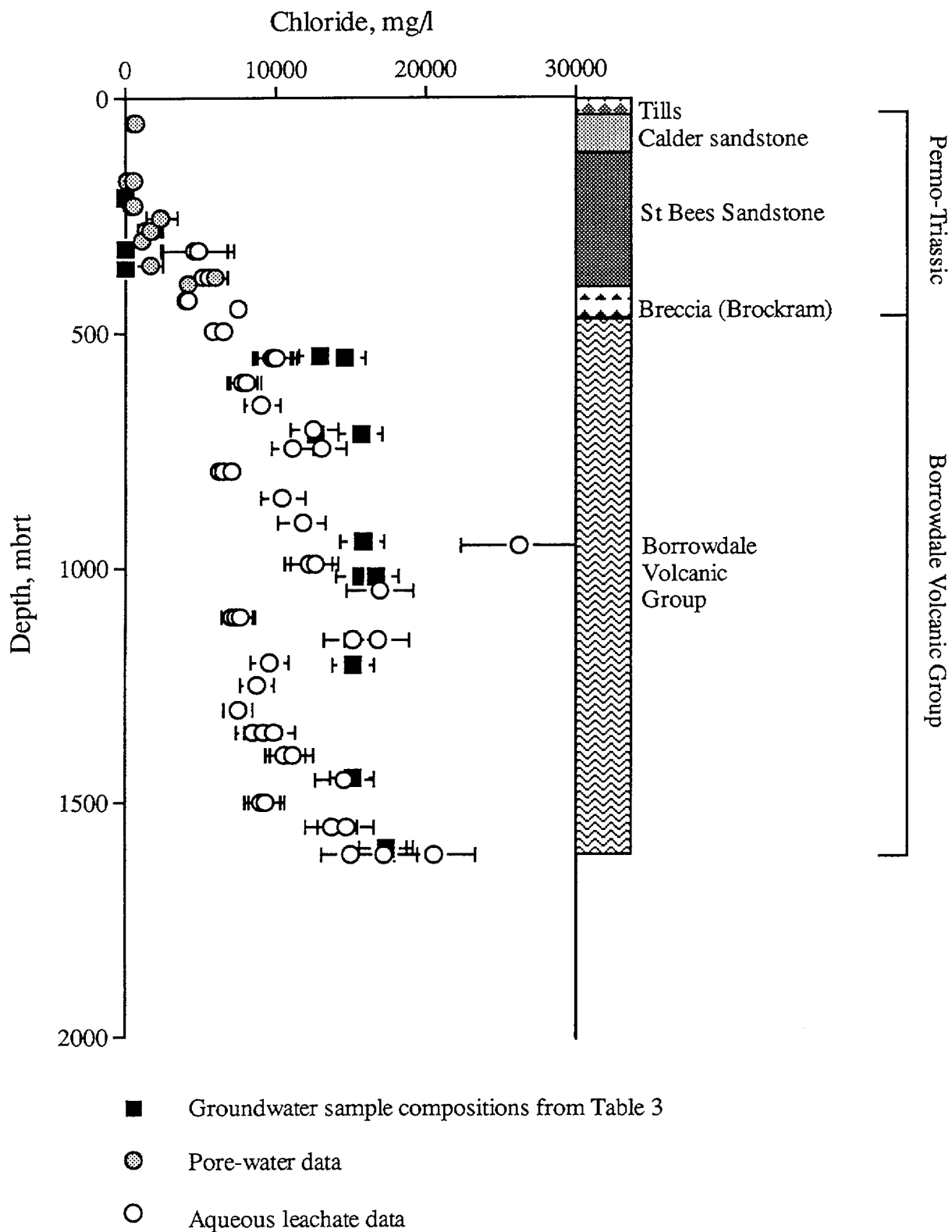


Figure 3.2a. Profiles of estimates of Cl concentrations in groundwaters from Nirex Borehole 2, obtained by groundwater sampling, core pore fluid displacement and crushed core leaching. Error bars are 2σ .

Sellafield Borehole 3

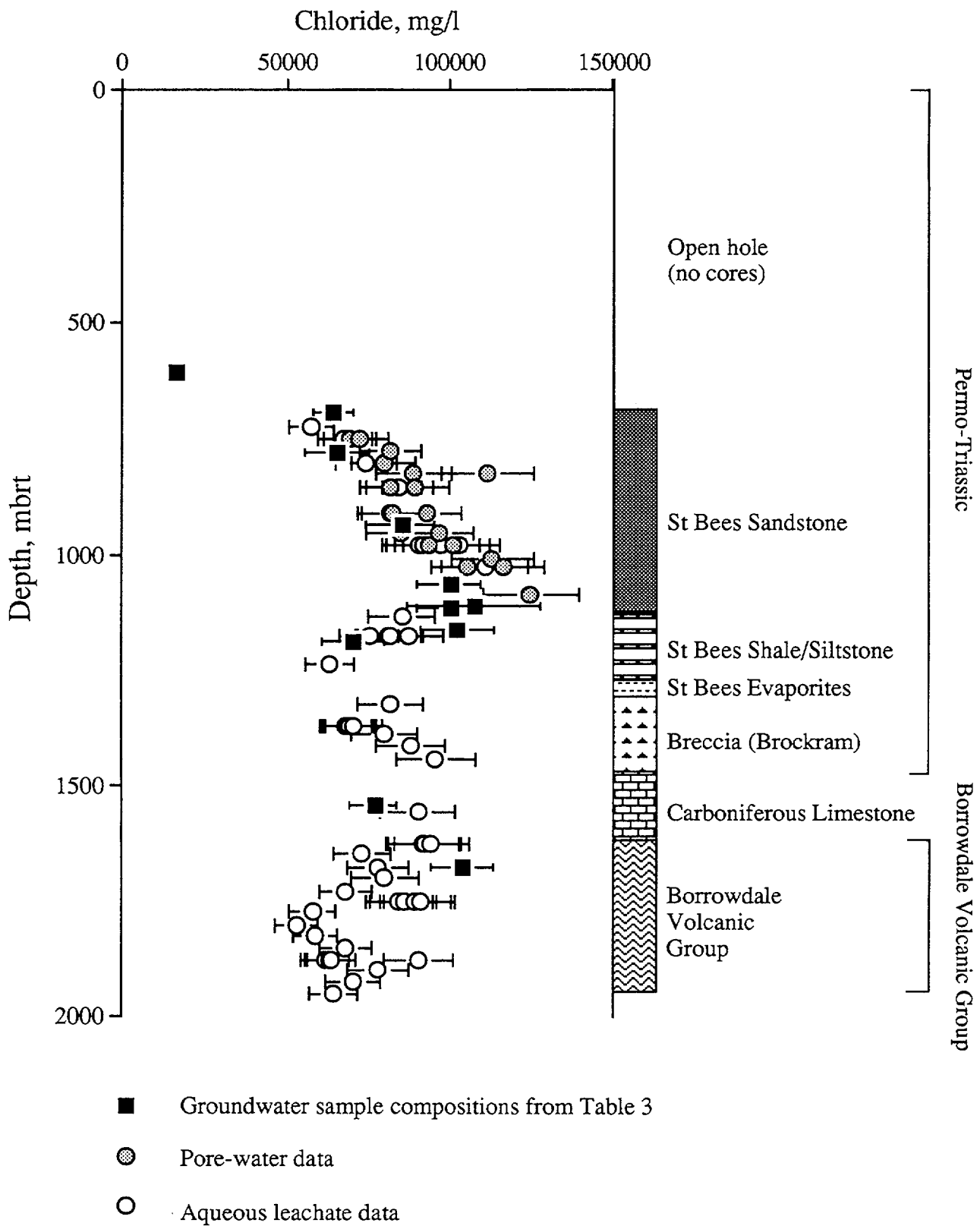


Figure 3.2b. Profiles of estimates of Cl concentrations in groundwaters from Nirex Borehole 3, obtained by groundwater sampling, core pore fluid displacement and crushed core leaching. Error bars are 2σ .

The fresh groundwaters of the topmost 100 m of the CP regime have been sampled in shallow boreholes and springs. They are predominantly of Ca-HCO₃⁻ type. There is a general increase of electrical conductivity towards the coast within the Site area. This mainly reflects increasing Ca, alkalinity and SO₄, attributable to progressive dissolution of calcite, dolomite and anhydrite, as the shallow groundwaters flow down-gradient towards the coast. Calculated calcite saturation indices correspondingly increase towards the coast.

Detailed interpretation of the shallow groundwater chemistry must also take account of anthropogenic inputs, mainly fertiliser use leading to elevated nitrate. A significant number of samples contain Cl concentrations exceeding 50 mg/l, which is twice the estimated value for recharge, based on rainfall chemical monitoring data (Table 2.1) and allowance for concentration by evapotranspiration. Most instances of excess Cl can be accounted for by anthropogenic inputs, but the possibility of minor contribution from deeper saline groundwater is also possible and is being assessed in further investigations.

The brines of the ISB regime are of Na-Cl type (see Borehole 3 data in Table 2.2) and reach Cl concentrations of over 100,000 mg/l (91,000 ppm). Salinities for formation waters from the off-shore South Morecambe gas field (about 60 km south of Sellafield) are said to be "about 200,000 ppm total chlorides" (Stuart and Cowan, 1991). Taken together with the reported reservoir temperature (32°C) and fluid resistivity (0.036 Wm at 32°C), this evidently means 200,000 ppm NaCl equivalent (i.e. about 120,000 ppm Cl). This is well below halite saturation, which would be at about 160,000 ppm Cl, according to calculations using EQ3/6 and the "Harvie-Møller-Weare" database supplied with the EQ3/6 package (Wolery, 1992; Wolery and Daveler, 1992).

The most obvious source of the salinity in the ISB brines is the Triassic Mercia Mudstone Group, which subcrops beneath the Quaternary about 2 km offshore from Sellafield, and contains halite deposits hundreds of metres thick in the centre of the EISB (Jackson et al., 1987; Jackson and Mulholland, 1993). Another possible source are offshore halite deposits within the equivalents of the Upper Permian St. Bees Evaporites, which reach thicknesses of 200 m, some 35 km southwest of Sellafield (Jackson et al., 1987). The low Br/Cl ratios of the brines (around 0.001 by mass, compared to the seawater value of 0.0034) are consistent with the salinity being primarily derived from halite dissolution. The origin of the water itself is predominantly non-marine, as indicated by the stable O and H isotope data discussed below.

The saline groundwaters within BVG rocks of the H&B regime are also of Na-Cl type (see Borehole 2 sample in Table 2.2), with significantly higher Ca/Na ratios than the ISB regime brines, and, more diagnostically, higher Br/Cl ratios (around 0.0017). Br and Cl are both non-reactive solutes in most groundwater systems, and so Br/Cl ratios are potentially useful for

distinguishing different groundwater salinity sources. All the deep borehole Br and Cl data reported by Nirex (1993a) are reproduced in Table 2.3 and form the basis of Figure 3.3. Figure 3.3 also shows the results of recent additional Br and Cl analyses (by the British Geological Survey) of preserved samples of pore waters extracted from lake bed sediment cores from Derwentwater, originally obtained by Hamilton-Taylor et al. (1988). The reason for including these data (given as numerical values in Table 3.1) is that the Derwentwater pore waters have been postulated by Hamilton-Taylor et al. (*op. cit.*) to indicate a regional deep saline groundwater, first suggested by Sutcliffe and Carrick (1983). Stable O and H isotope data led Hamilton-Taylor et al. (*op. cit.*) to conclude that the salinity is of non-marine origin. The new Br/Cl data, especially from the more saline of the Derwentwater samples, suggest that such deep groundwaters might have Br/Cl ratios around 0.0040, exceeding those found at depth in the Nirex deep boreholes.

It may be postulated that the saline groundwaters in the BVG of the PRV are mixtures of three components:

- (a) Saline groundwater from the Lake District basement (with a Br/Cl ratio of about 0.004);
- (b) Brine from the EISB (with a Br/Cl ratio of about 0.001; based on Borehole 3 data);
- (c) Fresh water with effectively zero Br and Cl.

The Br/Cl ratios in the PRV groundwaters are about 0.0017 (e.g. DET9 in Borehole 2). If it is assumed that the Cl concentration of component (b) is about 100,000 mg/l, then mass balance calculations show that about 10% (by volume) of the DET9 groundwater could be made up component (b) (i.e. EISB brine). The proportions of components (a) and (c) making up the remaining 90% depends on the Cl concentration assumed for component (a). The deepest, most saline Derwentwater lake sediment porewaters contain about 4500 mg/l Cl. Hamilton-Taylor et al. (1988) cite historical analyses of saline springs near Derwentwater that give Cl concentrations of around 14000 mg/l. Higher salinities are likely to be present at depth at these sites. Taking a range of values between 5000 and 20000 mg/l Cl for component (a) would imply between 63% and 16% (respectively) of component (a) in the DET9 groundwater.

These calculations are quite tenuous because the existence of a regional saline groundwater beneath the Lake District is not well established, and even if it does exist, its Br/Cl signature is so far based only on the Derwentwater porewaters. However, such calculations are important, because they have implications for past groundwater flow directions in the BVG of the PRV. Therefore, the postulated Lake District basement source of salinity requires more regional confirmation (as far as is possible) and more detailed characterisation.

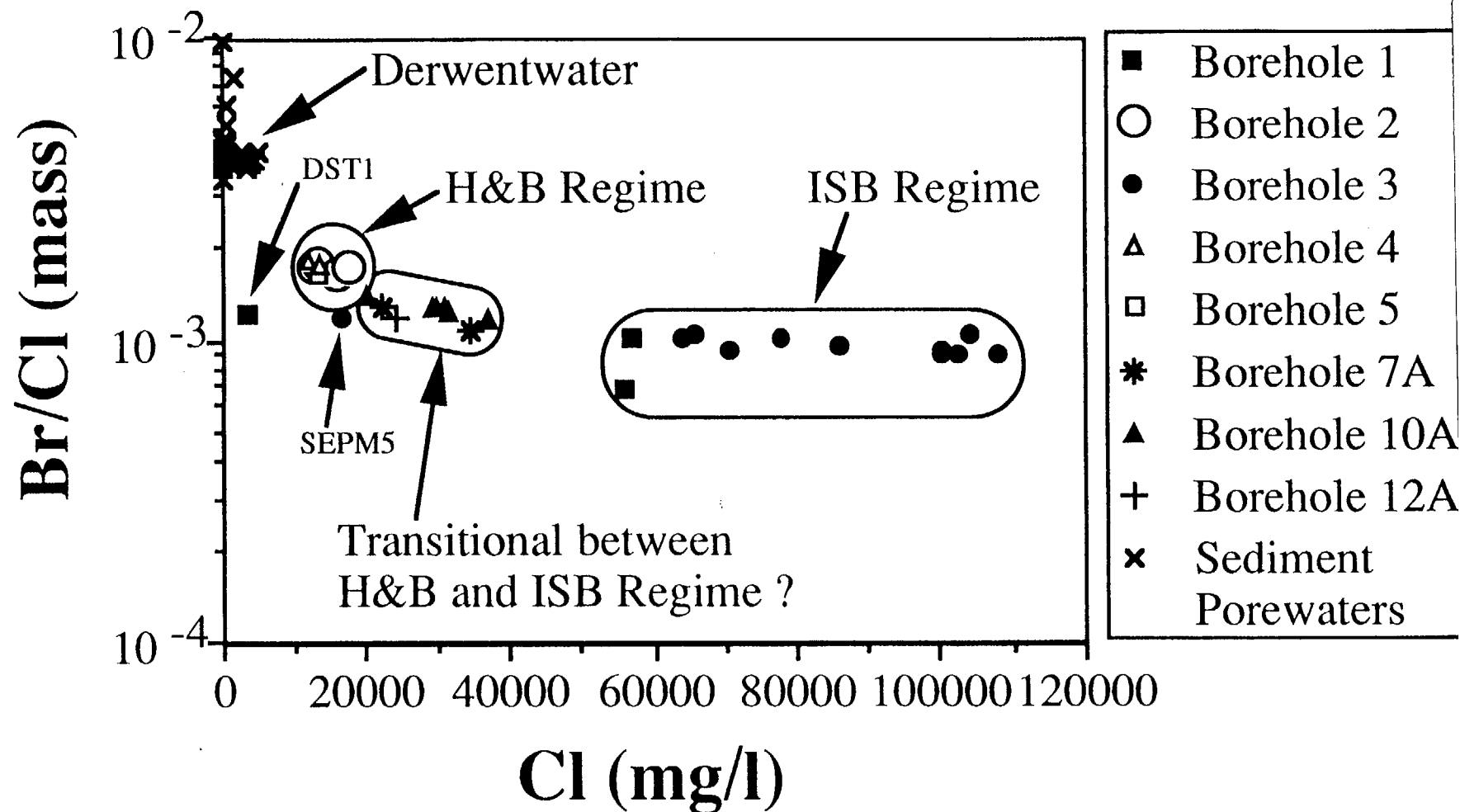


Figure 3.3. Plot of Br/Cl mass ratio versus Cl for saline (>10000 mg/L Cl) groundwater from NIREX deep boreholes (estimated groundwater compositions) and Derwentwater sediment pore waters. Uncertainties in Br/Cl for saline groundwater are typically < 10%, but for fresh CP regime groundwater sampled in NIREX deep boreholes (not shown), uncertainties are often very large (>100%) because of Cl contamination by drilling fluid.

Boreholes 7A, 10A and 12A form a line of boreholes running more or less at right angles to the section shown in Figure 3.1, with Borehole 7A about 1800 m north-northwest of Borehole 10A and Borehole 12A about 900 m southeast of Borehole 10A (see Chaplow, this issue). As shown in Figure 3.3, the Br/Cl ratios for saline waters from Boreholes 7A, 10A and 12A are intermediate between those of the Borehole 3 brines and the saline groundwaters in the PRZ (Boreholes 2,4 and 5). This suggests that there is a zone of mixing between the H&B saline groundwaters and ISB brines in the area of Boreholes 7A, 10A and 12A.

3.2

O AND H STABLE ISOTOPE DATA

The stable isotope ratios $^{18}\text{O}/^{16}\text{O}$ and $^2\text{H}/^1\text{H}$ in a groundwater are indicators of the origins of the water itself. All of the groundwaters sampled at Sellafield to date are depleted in ^{18}O and ^2H with respect to seawater (Table 3.2). The O and H isotopes are closely correlated, falling along or close to the Global Meteoric Water Line ($\delta^2\text{H}=8 \delta^{18}\text{O}+10$). A plot of $\delta^{18}\text{O}$ versus Cl (Figure 3.4) shows that three groups of groundwaters may be identified, corresponding to the three hydrochemical regimes described above:

(a) Fresh waters of the CP regime with isotopic compositions close to modern recharge (as indicated by average local rainfall; Table 2.1).

(b) Brackish to saline groundwaters of the H&B regime (Boreholes 2, 4 and 5 within the BVG) with isotopic compositions significantly lighter (by up to 1.5 o/oo $\delta^{18}\text{O}$ and 9 o/oo $\delta^2\text{H}$) than the CP groundwaters. By analogy with other studies of old groundwater systems in NW Europe (e.g. Bath et al., 1979; Bath, 1984; Andrews, 1993), this suggests that these groundwaters were recharged under substantially colder climatic conditions than at present, possibly late Pleistocene or earlier (i.e. $>10^4$ years ago).

(c) Saline groundwaters and brines of the ISB regime (Boreholes 1/1A and 3). The brines have probably migrated from nearer the centre of the EISB (currently beneath the Irish Sea) and their ultimate origins as meteoric recharge could conceivably date from basin uplift in Tertiary times. The correlation between $\delta^{18}\text{O}$ and salinity (Figure 3.4) is typical of basinal formation waters (e.g. Downing and Gray, 1986).

The least saline (shallowest) sampled groundwater from Borehole 3 (SEPM5) has a calculated $\delta^{18}\text{O}$ similar to that of groundwaters of similar salinity in Boreholes 2, 4 and 5, superficially suggesting a H&B regime signature. However, the uncertainty in the $\delta^{18}\text{O}$ of SEPM5 from Borehole 3 could allow that this groundwater (like that sampled by DST1 in Borehole 1/1A) represents a mixture between waters of the CP and ISB regimes (Figure 3.4). This is supported by the Br/Cl ratio (0.00116 ± 0.00015), which is indistinguishable from those of the other

Table 3.2. Estimates of Stable O and H Isotope Compositions and Calculated Recharge Temperatures for Groundwaters from NIREX Deep Boreholes

| BOREHOLE | TEST NO. | $\delta^{18}\text{O}$ (‰ SMOW) | | $\delta^2\text{H}$ (‰ SMOW) | | Noble gas recharge temp. (°C) | | |
|----------|----------|--------------------------------|------------|-----------------------------|------------|-------------------------------|----------|-------|
| | | Estimate† | 2 σ | Estimate† | 2 σ | Estimate | σ | Range |
| 1/1A | DST1 | 6.4# | n.c. | 44# | n.c. | no data | | |
| | DST3 | 6.1# | n.c. | 44# | n.c. | no data | | |
| | DST8 | 6.3# | n.c. | 45# | n.c. | no data | | |
| | DET1 | 6.1 | 0.4 | 36.4 | 4 | 10.9 | 1.2 | (2.5) |
| | DET2 | 6.0 | 0.6 | 34.4 | 5 | 18.6 | 3.7 | (9.8) |
| | DET3 | 6.1 | 0.2 | 36.2 | 4 | 9.9 | 0.2 | (0.0) |
| | DET10 | 7.6 | 0.6 | 41.7 | 6.8 | 6.7 | 1.3 | (0.6) |
| | DET9 | 7.5 | 0.6 | 41.2 | 4.4 | 7.1 | 1.2 | (2.2) |
| | DET8 | 7.5 | 0.2 | 43.6 | 7 | 6.8 | 2.4 | (0.6) |
| | DET7 | 7.7 | 0.2 | 45.9 | 4 | 5.2 | 2.6 | (-) |
| | SEPM5 | 7.0 | 0.5 | 46.9 | 5 | 8.1* | 2.7 | |
| | DET4 | 6.3 | 0.4 | 44.2 | 7.9 | 10.8* | 0.4 | |
| | DET3 | 6.3 | 0.5 | 43.4 | 5.5 | 13.5* | 2.1 | |
| | DET2 | 5.5 | 1.1 | 37.7 | 5.1 | no data | | |
| | DET1 | 5.1 | 0.4 | 32 | 5.5 | 20.8* | 1.4 | |
| | DET8 | 5.8 | 0.4 | 41.7 | 5 | 16.3* | 1.5 | |
| | DET7 | 5.9 | 0.4 | 32.1 | 5 | no data | | |
| | SEPM1 | 6.5 | 0.4 | 39 | 5 | no data | | |
| | SEPM2 | 6.2 | 0.6 | 39.6 | 6.7 | 12.3* | 1.2 | |
| SEPM3 | 6.3 | 0.4 | 40.8 | 5 | 13.8* | 1.6 | | |
| SEPM4 | 6.7 | 0.4 | 40 | 5.6 | 12.7* | 1.3 | | |
| DET3B | 6.5 | 0.4 | 44.7 | 5 | 11.8* | 0.6 | | |
| DET2 | 7.6 | 0.4 | 49.7 | 5 | no data | | | |
| DET1 | 7.6 | 0.4 | 50.5 | 5 | 10.9* | 2.6 | | |
| SEPM3 | 6.3 | 0.4 | 41.2 | 5 | 8.5* | 0.3 | | |
| SEPM5 | 6.0 | 0.4 | 39.5 | 5 | 9.3* | 0.2 | | |
| DET1 | 7.1 | 0.4 | 48.5 | 5.7 | 4.2* | 1.9 | | |

and H isotope data are reported using the δ notation, relative to Standard Mean Ocean Water (SMOW):

$$\delta^{18}\text{O} = \left(\frac{[^{18}\text{O}/^{16}\text{O}]_{\text{sample}}}{[^{18}\text{O}/^{16}\text{O}]_{\text{SMOW}}} - 1 \right) \times 1000$$

Each $\delta^{18}\text{O}$ and $\delta^2\text{H}$ estimate is calculated by regression of data from a number of samples from each test (with the exception of Borehole 1/1A). Hence $\delta^2\text{H}$ estimates are quoted to more than the usual precision.

These estimates have not been corrected for drilling fluid contamination

= standard deviation

“ranges” in brackets are spreads of recharge temperature values for replicate sub-samples for Borehole 2

* = preliminary recharge temperature estimate using non-verified data and without ^{40}Ar correction

c. = not calculated

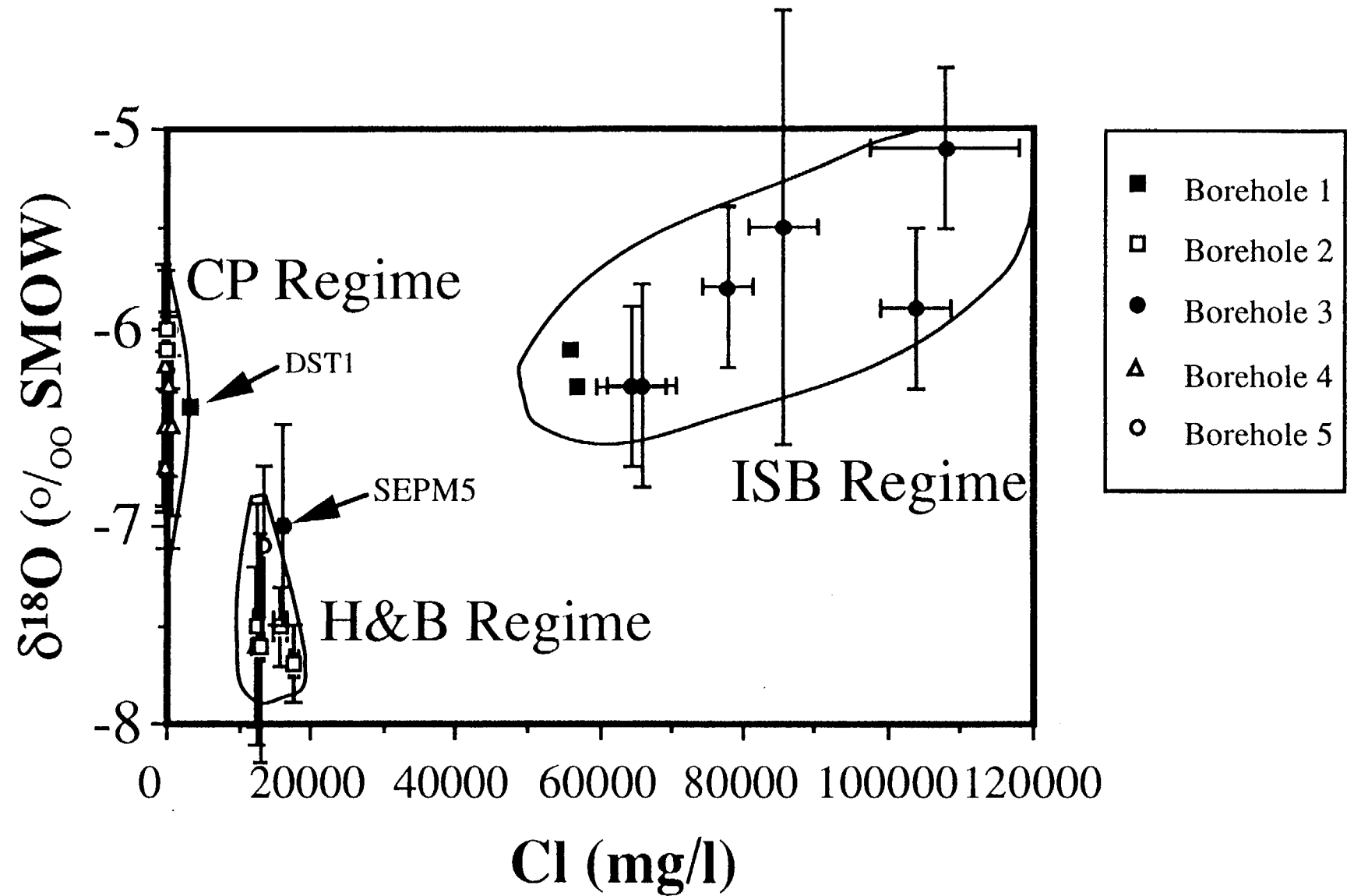


Figure 3.4. Plot $\delta^{18}\text{O}$ versus Cl for Nirex Deep borehole waters (estimated groundwater composition). Error bars reflect uncertainties in the estimated groundwater compositions, as given in Tables 3.3 and 4.2.

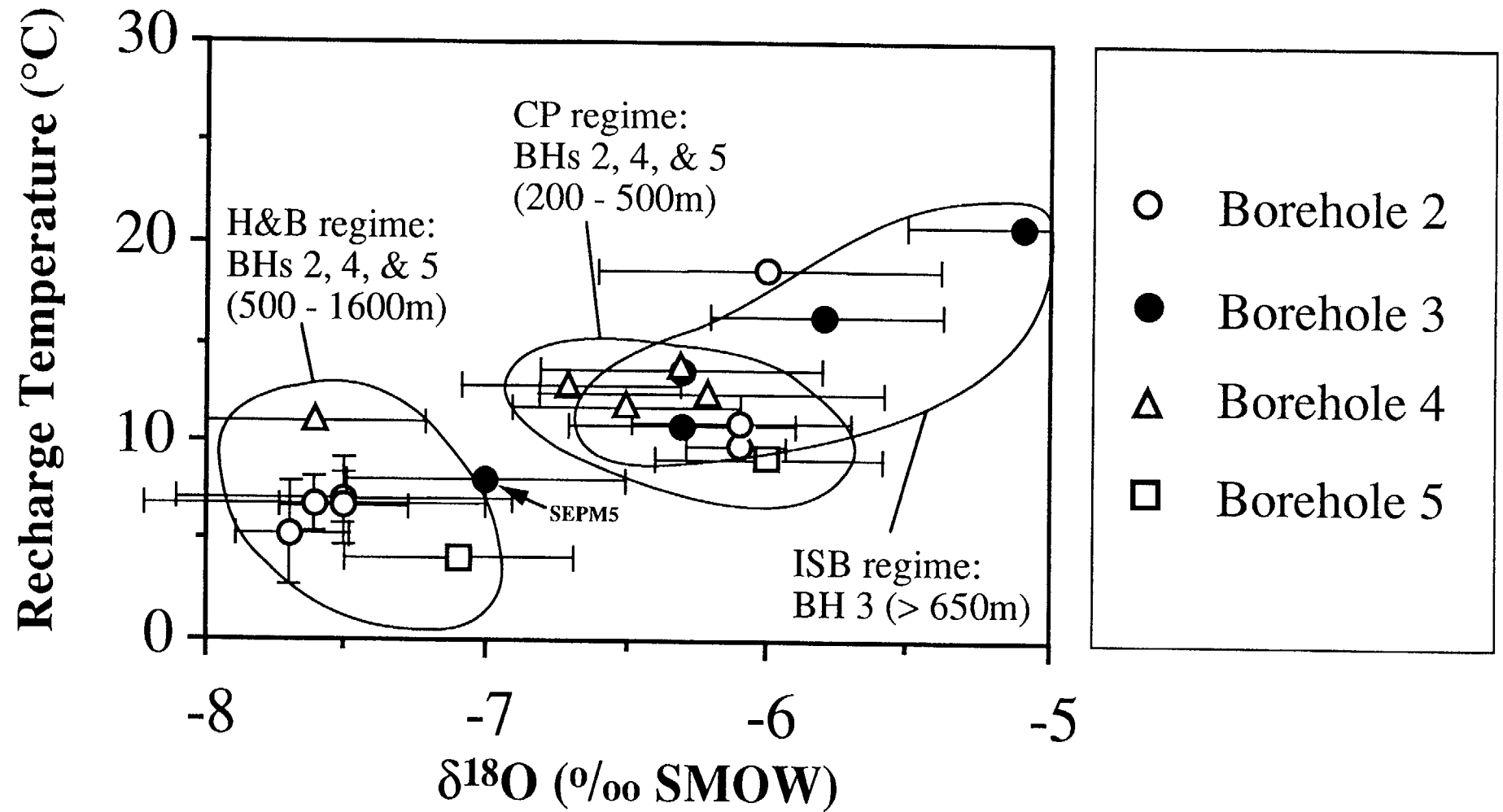


Figure 3.5. Plot of recharge temperatures (calculated from noble gas data) against estimated oxygen isotope compositions, for groundwaters from Boreholes 2, 3, 4 and 5. Calculated recharge temperatures for Boreholes 3, 4 and 5 are preliminary and uncertainties are not plotted (see text for discussion).

This is supported by the Br/Cl ratio (0.00116 ± 0.00015), which is indistinguishable from those of the other groundwaters from Borehole 3 (i.e. ISB regime) but distinct from that of the H&B regime (Figure 3.3). An alternative view is that the $\delta^{18}\text{O}$ of SEPM5 really is lower than that of typical CP regime groundwaters, and that the waters towards the bottom of the CP regime (deep in the SSG) are sufficiently old to have been recharged under colder conditions, as inferred for the deep, saline H&B regime waters. The salinity of the SEPM5 groundwater is sufficiently low that, even if it does represent a mixture between ISB regime brine and more dilute CP regime groundwater, the $\delta^{18}\text{O}$ would be dominated by the latter component.

The preliminary recharge temperature calculated from noble gas data from SEPM5 from Borehole 3 (see below) is midway between those typical of the H&B and CP regimes (Figure 3.5), and so not particularly diagnostic. Future stable isotopic data from Boreholes 10A, 7A and 12A should assist in resolving some of these uncertainties.

3.3 RECHARGE TEMPERATURES CALCULATED FROM NOBLE GAS DATA

Atmospheric noble gases (Ne, Ar, Kr, Xe) dissolve in groundwater at the time of recharge according to their solubilities and their partial pressures in the atmosphere. The solubilities are temperature-dependent, and therefore measured concentrations of these gases in groundwaters are indicative of temperatures at last contact with atmosphere, i.e. in the ground at recharge (Andrews 1991; Stute *et al.*, 1992). Helium occurs similarly but concentrations in deep groundwaters are usually dominated by a radiogenic component. Helium is therefore unsuitable for recharge temperature studies.

Groundwater samples for noble gas analysis have been collected in downhole pressure vessels and preserved so that compositional fractionation due to outgassing is minimised. The recharge temperatures are calculated from the noble gas concentration data by a process which corrects for drilling fluid contamination, 'excess air' entrainment and minimises the overall variance of temperatures calculated for individual gases from the mean value. Noble gas solubility data (Bunsen coefficients) are taken from Benson and Krause (1976). The reported uncertainties in the recharge temperatures are derived from the average of estimates from individual gases. Additional uncertainty arises from the variation with altitude of noble gas partial pressures in the atmosphere. An altitude of 350 m for the recharge surface has been assumed for these calculations; changing this by ± 250 m causes a change of $< \pm 2$ °C in the temperature. The Ar content may be enhanced by small but significant amounts of radiogenic ^{40}Ar , particularly in deeper, older groundwaters; this can be monitored through measurement of the $^{40}\text{Ar}/^{36}\text{Ar}$ ratio. The normal air

value for this ratio is 295.5; sensitivity analysis shows that if this is enhanced by 20% then the recharge temperature calculated from Ar data is raised by about 3 °C relative to the uncorrected value.

Fully processed recharge temperatures derived by this method are presently available only for groundwaters in DETs from Borehole 2; $^{40}\text{Ar}/^{36}\text{Ar}$ data from Boreholes 3, 4 and 5 are not yet available, so provisional estimates for recharge temperatures shown in Figure 3.5 have not been corrected for radiogenic ^{40}Ar . The calculated results (with caveats) are given in Table 3.2. The temperature for DET2 in Borehole 2 is anomalously high; this sample also has a high $^{40}\text{Ar}/^{36}\text{Ar}$ ratio of 334 compared with the other DETs which have no more than 307. The cause of this apparently erroneous value is unclear and could, for example, be due to sample outgassing.

Since stable O and H isotopic compositions of meteoric waters are also indicative of climatic conditions at recharge (Bath, 1984), a correlation between the two independent data sets is expected. The correlation between $\delta^{18}\text{O}$ and mean monthly surface temperature is typically 0.19 to 0.43 ‰/°C, with inferred palaeoclimatic shifts of 5-6 °C (Andrews, 1993). The data for Sellafield are shown in Figure 3.5 and, although the data from Boreholes 3, 4 and 5 are preliminary, and more data are required to confirm the trend, the observed correlation increases confidence in the palaeoclimatic interpretation of stable isotope variations.

Recharge temperature ranges obtained in other isotopic and noble gas studies of groundwaters in the U.K. are about 6-10 °C and 2-5 °C for recent and old groundwaters, respectively (Bath et al., 1979; Edmunds et al., 1987). The recharge temperatures for the H&B saline groundwaters are generally somewhat higher than the 2-5 °C range in the old, isotopically light groundwaters encountered in these other studies. This may reflect the extent of mixing in the H&B regime.

Noble gas recharge temperature estimates for the ISB regime groundwaters of Borehole 3 show a similar correlation with stable isotope composition, indicating recharge temperatures up to 20 °C (Figure 3.5). In this case, the groundwaters are interpreted as mixtures between CP regime groundwaters and an isotopically-heavy EISB brine end-member of uncertain but obviously very old origin. The noble gas data have a less certain interpretation than in the H&B and CP regimes, particularly since 'salting out' (leading to high apparent recharge temperatures) is suspected to reduce noble gas solubilities when brines mix with more dilute meteoric groundwaters (Sonntag and Suckow, 1992; Suckow and Sonntag, 1993), or when recharge takes place through near-surface halite deposits (Zaikowski et al., 1987). The former process may also have affected the noble gas contents of the saline groundwaters in the H&B regime; loss of noble gases could account for the unexpectedly high apparent recharge temperatures.

RADIOISOTOPIC CONSTRAINTS ON GROUNDWATER RESIDENCE TIMES

Groundwater residence times can in principle be constrained by measurements of the concentrations of radioactive solutes which originate in the atmosphere at the time of recharge. Tritium (^3H) is a good example of this, but has limited use in the context of the Sellafield investigations because it has a short half-life (12.43 years) and has only been present in the atmosphere in substantial concentrations since the early 1950's and therefore cannot assist in constraining any but the most rapid recharge phenomena. When the tritium levels in the drilling fluid are well characterised (generally in the range 20-40 Tritium Units), tritium effectively acts as a secondary tracer for the drilling fluid. To date, no tritium concentrations have been observed in deep groundwater samples that cannot be accounted for in terms of drilling fluid contamination.

Potentially the most useful isotope for groundwater 'dating' is ^{14}C which has a half-life of 5730 years. However, C is a reactive element in groundwater/rock systems and dilution or exchange of dissolved ^{14}C with 'dead' (^{14}C -free) carbonate from the rock must be considered. Quantitative interpretation of ^{14}C data depends on the derivation of a valid model which successfully simulates the evolution of both the hydrochemistry and the $^{13}\text{C}/^{12}\text{C}$ system (Plummer et al., 1991; Plummer and Prestemon, 1991). A groundwater which is 'dead' to ^{14}C , i.e. within the detection limit of about 0.5 pmc or better, would indicate a mean residence time at least in the order of 10^4 years. The timescale over which detectable (0.5% pmc) ^{14}C can be interpreted is about 30000 years; i.e. late Pleistocene (Pearson et al., 1991). It must be emphasised that any estimates of groundwater residence times are mean values for highly mixed systems. The longer the mean residence time, the greater the likely dispersion of residence times. Also, the mean residence time for groundwater currently in or near the PRV refers to the mean transit time since recharge, and is not directly comparable with the return time from the PRV to the biosphere.

Interpretation of ^{14}C data from the Nirex deep boreholes is further complicated by the interactions with the alkaline, polymer-based drilling fluid. The alkaline drilling fluid tends to absorb atmospheric CO_2 containing modern ^{14}C , and there is also the possibility of microbial degradation of the polymer to add further modern ^{14}C to the inorganic C content of the mixed groundwater/drilling fluid samples. If samples with good clean-up (very little drilling fluid contamination) are obtained, then ^{14}C data may have some interpretable significance. The interpretation is assisted by reference to the stable $^{13}\text{C}/^{12}\text{C}$ isotopic data, which trace the effects of water/rock interactions and also organic C contributions on the C isotopes. The best quality samples for C isotopes from Borehole 2 were

obtained from PDDT1, in which the minimum Li concentration attained was 4 mg/l, which is probably of the same order as the natural Li content of the groundwater. The ^{14}C values recorded in this test were 11.92 ± 0.18 , 11.15 ± 0.17 and 10.57 ± 0.16 pmc (mean 11.2 pmc). Because of uncertainties in the natural Li content of the groundwater and the extent to which degradation of drilling fluid polymer has contributed modern C to the samples, it cannot be demonstrated whether or not the measured ^{14}C values are due mainly to drilling fluid contamination.

4. DISCUSSION

4.1 IMPLICATIONS FOR CONCEPTUAL MODEL

The District-scale conceptual hydrogeological model presented by Nirex (1993a,b) and discussed by Black et al. (to be published, special issue QJEG) is largely based on the hydrochemical regimes described above. As well as distinguishing different groundwater bodies, the hydrochemical data allow qualitative inferences to be made concerning groundwater movement. The presence of highly saline groundwaters at depth in the ISB regime indicates near-stagnant conditions. Consideration of the geological history of the basin fluids (see below) suggests that the basin margin regime might have been influenced by episodic fluctuations of the brine-freshwater mixing zone. This gradational west-to-east lateral mixing zone is the diffusive boundary between ISB and H&B regimes. The scale of mixing is broadly consistent with the modelled steady-state advective distribution of salinity from two sources (i.e. basin and basement) within the low permeability BVG (Nirex, 1993a).

The other important aspect of the conceptual model is the boundaries of the freshwater CP regime with the more saline H&B and ISB regimes. Within the PRZ, the salinity transition (between the CP and H&B regimes) occurs near the base of the St Bees Sandstone in Borehole 2 (Figure 3.2a), but within the BVG in Borehole 4 (see Cl data for DET3B in Table 2.3). The sharpness of the transition generally indicates low cross-flow relative to lateral fluxes in the CP regime. The changing stratigraphic location of the salinity transition within the PRZ suggests the possibility of structural as well as lithology-permeability factors. Further data for this area will enable these features to be modelled realistically.

The possibility of dual salinity sources (i.e. from the east as well as the west) within the system has implications for the conceptual model because it might constrain fluxes through and between regimes. Br/Cl ratios distinguish these sources and thus provide independent mixing estimates to be compared with modelled values based on physical hydrogeology.

The hydrochemical and isotopic data record the past evolution of the groundwater system. The timescales over which the present hydrochemistry has evolved can only be loosely defined because there is a continuous process of water-rock interaction. The basinal brine component is clearly of great age; i.e. the bulk of this water has almost certainly occupied the basin formations for a very long period of time and has acquired its salinity from indigenous halite. Basin inversion in the Tertiary may have caused the last major flushing of the basin, although fluctuations in sea level in the Quaternary and the late Devensian glaciation may have caused more recent disturbances to these basin brines. The distinctive stable isotopic composition of the brines (Figure 3.4) supports this and resembles similarly very old basin brines in other Mesozoic basins in England (Downing and Gray, 1986).

A further record of the basinal groundwater history is retained in fluid inclusions trapped in fracture-filling minerals. Additional information of fluid history is inferred from petrographic studies of diagenesis and fracture mineral alteration. Details of these studies are beyond the scope of this paper. Preliminary findings are presented in Nirex (1993c) and also summarised in Nirex (1993d). A number of diagenetic processes or 'events' have affected the Permo-Triassic sedimentary formations whilst fracture mineralisation appears variably in both sediments and BVG basement. Relative ages of these alteration events have been inferred from their geological and petrographic relationships. K-Ar dating of fracture illites has also been applied. This indicates that multiple fracturing and illite mineralization took place over a period from 214 Ma (late Triassic) up to and possibly beyond 60 Ma (early Tertiary), which is the youngest illite K-Ar date obtained so far. However, the bulk of the alteration (principally episodic carbonate mineralization/diagenesis) is attributed to late Triassic events accompanying basin subsidence and compaction. Fluid inclusions occurring in these (?late Triassic) fracture minerals are highly saline (similar to present-day ISB brines). This similarity suggests that the brines have been present in the sedimentary and basement sequence for a considerable period of geological time.

The perturbations due to the late-Cimmerian orogeny (late Jurassic and early Cretaceous) and Tertiary basin inversion are less evident in the petrographic record. There is a small amount of evidence (from fluid inclusions in calcite) of post-Triassic diagenesis by warm (90-100 °C) fresh water, in the St Bees Sandstone within the PRZ. The association of this calcite with late illite is tentatively interpreted as indicating a correlation with Tertiary basin inversion. At this stage in the investigations, there is no evidence of fracture mineralisation attributable to any Quaternary episode(s) of fluid movement.

The overall palaeohydrogeological model for the Site is one of domination by basin-derived brines, their eastward penetration depending on basin tectonics which (compared to the major tectonic events in the late Jurassic / early Cretaceous and in the Tertiary) are now relatively stable. Westwards movement of fresh groundwater from meteoric recharge, possibly mixed with moderately saline water from the deep basement, would have been determined by topography and other recharge factors (e.g. glacial conditions) and by the transient position of the brine intrusion. The preliminary stable isotope and noble gas data for groundwaters from the deep boreholes in the PRZ are consistent with the meteoric recharge component of the saline H&B groundwater having been in place for at least a timescale in the order of 10^4 years, i.e. possibly reflecting movement at or before the last glacial period.

4.3 BASELINE HYDROCHEMICAL CONDITIONS IN THE POTENTIAL REPOSITORY ROCK VOLUME (PRV)

The precise depth of the PRV will not be defined until detailed investigations have been carried out in the proposed Rock Characterisation Facility (RCF). The RCF as currently planned will be primarily designed to investigate the Borrowdale Volcanic Group (BVG) at 650 m below Ordnance Datum (bOD), with the deepest shaft reaching 835m bOD. This depth range corresponds to that currently envisaged for the repository vaults (Mogg, 1994). The salinity of the groundwaters extracted in DET's and PDDET's from these depths is fairly constant at about 13000-16000 mg/l Cl (Table 2.2). This salinity is around $3/4$ that of seawater. Leaching of crushed core samples from the same depth interval indicates similar salinities, with a slight increase in salinity with depth (Figure 3.2a). With the possible exception of pH, alkalinity and total inorganic C (discussed below), the calculated groundwater composition for test DET9 from Borehole 2 (Table 2.1) is typical of the groundwaters of the PRV. The composition calculated from DET1 in Borehole 4 (Table 2.1) is generally similar.

Besides salinity, the most important baseline inorganic hydrochemical properties of the PRV groundwaters include pH, redox state and carbonate species concentrations. These parameters are all important in controlling the migration in the geosphere of some of the radiologically most significant radionuclides that would be consigned to a repository, including uranium and its decay products (Nirex, 1993b). Organic species and colloids may also be important, but the interference of drilling fluids used in investigations to date is such as to preclude their characterisation. Borehole 9A (drilled without polymer additives) may provide a better opportunity for such investigations, albeit some distance up the hydraulic gradient from the PRV.

The estimation of in situ pH and carbonate species concentrations is a difficult task, due partly to the problems of outgassing of CO₂ during sample retrieval (especially where this involved gas lifting), partly to contamination by the alkaline drilling fluid, and probably partly to effects of corrosion of mild steel downhole testing equipment. Outgassing could also substantially affect the estimation of in situ total inorganic C concentration, and affect the alkalinity measurements. Measurements of pH have been made in a flow cell directly connected to the transfer line used to extract water from a wireline downhole sampler, provided that the downhole samples are more or less free of drilling fluid contamination. These measurements have been variable, ranging between 6.25 and 7.85 in the case of the DETs from the BVG in Borehole 2. In principle, all these values could be regarded as maxima, given the possibility of outgassing.

Saturation indices (SIs) have been calculated for groundwater compositions inferred from DET's in Borehole 2, using the computer code EQ3 (version 7) and supporting database (version com.R10) (Wolery, 1992). If it is assumed that the pH measurements from downhole samples with good clean-up are representative and that the total alkalinity measurements represent in situ HCO₃⁻ concentrations, the groundwaters in the PRV (DET9) are undersaturated with respect to both calcite and dolomite (at downhole temperatures). Deeper groundwater samples (DET8 and DET7) show apparent oversaturation with respect to both calcite and dolomite, which could be attributed to CO₂ outgassing. Calcite is ubiquitous in the PRV as both a matrix mineral and as a filling in some generations of fractures, while dolomite (and also ankerite) are widespread as minor fracture filling minerals. Therefore the calculated undersaturations are unexpected and suggest that representative pH values may be rather higher than the lowest measured values from DET9 (and DET10), which may reflect corrosion-related artefacts.

The PRV groundwaters are at saturation with respect to quartz (SI = -0.06 for DET9) and slightly undersaturated with respect to chalcedony (SI = -0.36). This is expected, given the ubiquitous presence of quartz as a major mineral in the BVG. Calculation of SIs for aluminosilicate minerals requires reliable measurements of Al and Si concentrations. Reported Al concentrations indicate very large oversaturations for most aluminosilicate minerals present in the rock, including illite (thermodynamically represented by muscovite), kaolinite, K-feldspar and albite. This suggests that the reported values are not representative of in situ Al concentrations. This may be because the groundwater samples were filtered only to 0.45 µm prior to acidification and Al analysis, so that colloidal Al may have been included in the analyses. The uncertainties in the estimated in situ Al concentrations are large (sometimes exceeding the estimated value itself), because the concentrations in drilling fluids are typically two orders of magnitude higher than in the least contaminated groundwater samples and are also highly variable.

With these data limitations, the stabilities of aluminosilicates are best discussed at this stage with reference to activity ratios. Figure 4.1 illustrates how the calculated activity ratios of H^+ , K^+ and Na^+ compare with the theoretical activity ratios expected for various equilibria involving K-feldspar, albite, muscovite and kaolinite (calculated using SUPCRT92; Johnson *et al.*, 1991). In Figure 4.1, the compositions of groundwaters sampled in DET8 (about 950 mbOD) and DET7 (about 1530 mbOD) are plotted twice: once with the reported pH and alkalinity data (and therefore implying calcite oversaturation) and once with a correction for assumed CO_2 loss. The correction has been achieved by using the code EQ6 (Wolery and Daveler, 1992) to simulate the titration of CO_2 into the groundwater composition as analysed, until calcite saturation is achieved (following Pearson *et al.*, 1978). The effect on DET8 is most marked, shifting the calculated activity ratios out of the K-feldspar stability field.

No such correction can be applied to DET9 and DET10, because these compositions are apparently undersaturated with respect to calcite. The general interpretation of Figure 4.1 is that the groundwaters in the BVG within the PRZ (i.e. in the PRV and deeper) could be in equilibrium with muscovite (illite). This would accord with the observation that illite is an abundant fracture-filling mineral in the BVG.

There are considerable practical difficulties in estimating *in situ* redox conditions for the PRV. Moreover, it is well known that most groundwater systems are characterised by redox disequilibrium (e.g. Lindberg and Runnells, 1984) and so the characterisation of redox conditions does not rely solely upon accurate measurement of a single parameter such as electrode Eh. Reported values of electrode Eh from Borehole 2 DETs in the BVG have been 90 mV, but these measurements have probably been influenced by corrosion processes in the downhole test strings, etc., and by degassing artefacts of gas-lifting. Data for redox-sensitive couples have been obtained from the groundwater samples, including Fe^{III}/Fe^{II} , nitrate/nitrite and sulphate/sulphide. Uncertainties in estimates of *in situ* Fe^{III}/Fe^{II} , nitrate, nitrite and sulphide concentrations are generally considered to be too large for reliable estimates to be obtained. No unequivocal hydrochemical evidence of strongly reducing *in situ* conditions has yet been obtained, but there are known to be traces of sulphide minerals in some fractures in the PRV, and so such conditions probably exist locally. As with pH, it is anticipated that progress will be made with measurements of Eh and redox-sensitive species concentrations under less contaminated conditions to be achieved in future deep boreholes, monitoring completions, and ultimately in the RCF.

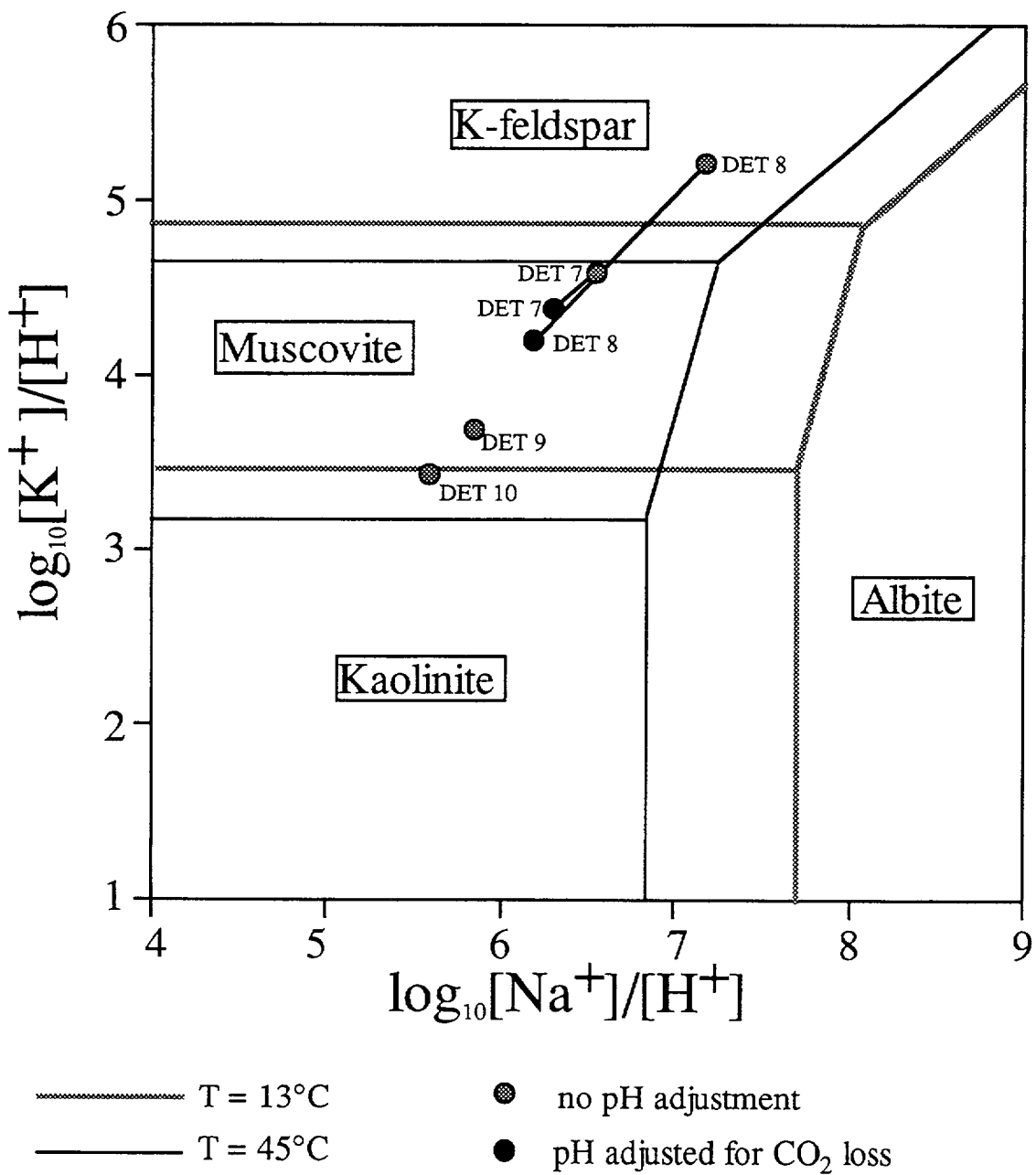


Figure 4.1. Log activity plots of K^+/H^+ versus Na^+/H^+ for estimated groundwater compositions for DETs from Borehole 2 within the BVG. Mineral stability field boundaries calculated (using SUPCRT92; Johnson et al., 1991) at 1 Bar pressure and assuming Si concentration is controlled by quartz solubility.

Hydrochemical data acquisition in the Sellafield investigations is at an early stage, with many data yet to be reported and further refinements to be achieved in obtaining samples and measuring baseline parameters. The present data set has contributed substantially to the construction of a conceptual model of the hydrogeological system, on which numerical modelling of the physical hydrodynamics can be based. Hydrochemical aspects of the conceptual model (particularly salinity sources and mixing zones) will provide specific tests of the adequacy of numerical modelling.

The palaeohydrogeology of the area is dominated by its location on the margin of the East Irish Sea Basin. The influence of basinal brines has been a feature of the deep sediments and the Borrowdale Volcanic Group basement in the west of the area for considerable geological time. Evidence of the movement of the fresher meteoric recharge component is not yet clear. Within the area of the Potential Repository Zone, stable isotopic and noble gas temperature data for groundwaters in the Borrowdale Volcanic Group basement indicate a predominance of old recharge, possibly late Pleistocene. Contamination by drilling fluid has variably affected ^{14}C data, and this problem is being addressed by field testing the feasibility of drilling without polymer additive. The Br/Cl ratios in the BVG groundwaters of the PRZ suggest that the salinity of these groundwaters is derived at in substantial part from a different source than the basinal brines. This source may be within the Lake District basement to the east.

The baseline hydrochemical conditions within the potential repository rock volume have been shown to be moderately saline (Cl concentration about $3/4$ that of seawater), but the pH and redox conditions have not yet been defined with sufficient accuracy, because of the inherent difficulties in making valid measurements in deep, multi-objective boreholes. The ongoing site investigation (including a combination of further measurements and geochemical modelling) will aim to evaluate these baseline parameters, along with characterisation of natural organics and colloids.

ACKNOWLEDGEMENTS

We wish to thank various individuals who have contributed significantly towards the interpretation presented in this paper. J. Ross, P. Flitcroft and M. Turner performed the drilling fluid contamination correction calculations. M.R. Cave and S. Reeder provided the interpreted pore fluid data presented in Figure 3.2. D. Polya and J.N. Andrews performed the recharge temperature calculations. J. Heathcote and N. Rukin provided a preliminary interpretation of the shallow groundwater hydrochemistry. A.E. Milodowski advised on the diagenetic evolution of the East Irish Sea

Basin. D. Savage contributed substantially to the early stages of interpretation. The work reported was funded by Nirex, with the exception of the reanalyses of samples from Derwentwater, which formed part of a project jointly funded by Nirex and the Commission of the European Union. HGR, RM and MBC publish by permission of the Director, British Geological Survey (NERC).

REFERENCES

Andrews J. N. (1991). Noble gases and radioelements in groundwaters. In Downing, R.A. and Wilkinson, W.B. (eds.) Applied Groundwater Hydrology, Oxford University Press, 243-265.

Andrews J. N. (1993). Isotopic composition of groundwaters and palaeoclimate at aquifer recharge. In Isotope Techniques in the Study of Past and Current Environmental Changes in the Hydrosphere and the Atmosphere. Proc. Intl. Symp., Vienna. International Atomic Energy Agency, Vienna, 271-292.

Bath A. H. (1984). Stable isotopic evidence for palaeo-recharge conditions of groundwater. In Palaeoclimates and Palaeowaters: A Collection of Environmental Isotope Studies. International Atomic Energy Agency, Vienna, 169-186.

Bath A. H., Edmunds W. M. and Andrews J. N. (1979). Palaeoclimatic trends deduced from the hydrochemistry of a Triassic sandstone aquifer, United Kingdom. In Isotope Hydrology 1978, Vol. II, International Atomic Energy Agency, Vienna, 545-568.

Benson B. B. and Krause D. (1976). Empirical laws for dilute aqueous solutions of non-polar gases. J. Chem. Phys., 64, 639-709.

Black, J. H. et al., to be published, Special Issue of Quarterly Journal of Engineering Geology.

Chaplow R. The geology and hydrogeology of Sellafield - An overview. to be published, Special Issue of Quarterly Journal of Engineering Geology.

Downing R.A. and Gray, D.A. (1986). Geothermal Energy - The potential in the United Kingdom. Rept. Brit. Geol. Surv., HMSO, London.

Edmunds W. M., Cook J. M., Darling W. G., Kinniburgh D. G., Miles D. L., Bath A. H., Morgan-Jones M. and Andrews, J. N. (1987). Baseline geochemical conditions in the Chalk aquifer, Berkshire, U.K.: a basis for groundwater quality management. Applied Geochemistry, 2, 251-274.

Fontes J.-Ch. (1994). Isotope palaeohydrology and the prediction of long-term repository behaviour. Terra Nova, 6, 20-36.

Gascoyne M. and Kamineni D.C. (1993). The hydrogeochemistry of fractured plutonic rocks in the Canadian Shield. In Proceedings of the International Association of Hydrogeologists Symposium, Oslo, 440-449.

Hamilton-Taylor J., Edmunds W.M., Darling W.G. and Sutcliffe D.W. (1988). A diffusive ion flux of non-marine origin in Cumbrian lake sediments: implications for element budgets in catchments. Geochimica et Cosmochimica Acta, 52, 223-227.

Jackson D.I., Mulholland P., Jones S.M. and Warrington G. (1987). The geological framework of the East Irish Sea Basin. In Brooks, J. and Glennie, K. (eds.) Petroleum Geology of North West Europe, London, Graham and Trotman, 191-203.

Jackson D.I. and Mulholland P. (1993). Tectonic and stratigraphic aspects of the East Irish Sea Basin and adjacent areas: contrasts in their post-Carboniferous structural styles. In Parker, J.L. (ed.) Petroleum Geology of Northwest Europe: Proceedings of the 4th Conference. London, Geological Society, 791-808.

Johnson J.W., Oelkers E.H. and Helgeson H.C. (1991). SUPCRT92: a software package for calculating the standard molal thermodynamic properties of minerals, gases, aqueous species, and reactions from 1 to 5000 bars and 0° to 1000°. University of California, Berkeley.

Lindberg R.D. and Runnels D.D. (1984). Groundwater redox potentials: an analysis of equilibrium state applied to Eh measurements and geochemical modelling. Science, 225, 925-927.

Michie U. McL. (1994). The geology and hydrogeology of Sellafield. Nucl. Energy, 33, 25-39.

Michie, U.McL. The geology and hydrogeology of the Sellafield area: The geological framework and relationship to hydrogeology. to be published, Special Issue of Quarterly Journal of Engineering Geology

Mogg C.S. (1994). Repository design concepts. Nucl. Energy, 33, 44-49.

Nirex (1993a). The geology and hydrogeology of the Sellafield area: Interim Assessment December 1993. Volume 3: The Hydrogeology. U.K. Nirex Ltd. Report No. 524(3).

Nirex (1993b). Nirex deep waste repository project: Scientific update 1993. U.K. Nirex Ltd. Report. No. 525.

Nirex (1993c). The geological structure of the Sellafield area: December 1993 update. U.K. Nirex Ltd. Report No. 520.

Nirex (1993d). The geology and hydrogeology of the Sellafield area: Interim Assessment December 1993. Volume 1: The Geology. U.K. Nirex Ltd. Report No. 524(1).

Pearson F.J., Fisher D.W. and Plummer L.N. (1978). Correction of groundwater chemistry and carbon isotopic composition for effects of CO₂ outgassing. Geochimica et Cosmochimica Acta, 42, 1799-1807.

Pearson F.J., Balderer W., Loosli H.H., Lehmann B.E., Matter A., Peteres T. Schmassmann H. and Gautschi A. (1991). Applied isotope hydrogeology: A case study in Northern Switzerland. Studies in Environmental Science, No. 43. Elsevier, 439pp.

Plummer L.N. and Prestemon E.C. (1991). Geochemical modeling and radiocarbon dating of groundwater: Recent software developments and field examples. Radiocarbon, 33, 232.

Plummer L.N., Prestemon E.C. and Parkhurst D.L. (1991). An interactive code (NETPATH) for modeling net geochemical reactions along a flow path. U.S. Geological Survey Water Resources Investigations Report No.91-4078.

Smellie J.A.T. and Laaksoharju M. (1992). The Äspö Hard Rock Laboratory: Final evaluation of the hydrogeochemical pre-investigations in relation to existing geologic and hydraulic conditions. Svensk Kärnbranslehantering AB (SKB) Technical Report No. 92-31.

Sonntag C. and Suckow A. (1993). Isotope and noble gas investigation of palaeowaters in the sediments above salt dome Gorleben : In Palaeohydrogeological Methods and their Applications : Proc. NEA Workshop, Paris 1992. Nuclear Energy Agency of OECD, Paris, 251-265.

Stuart I.A. and Cowan G. (1991). The south Morecambe Field, Blocks 110/2a, 110/3a, 110/8a, UK East Irish Sea. in Abbotts, I.L. (ed.) United Kingdom Oil and Gas Fields. 25 Years Commemorative Volume. Geological Society Memoir No. 14. 527-541.

Stute M., Schlosser P., Clark J. F. and Broecker W. S. (1992). Palaeotemperatures in the southwestern United States derived from noble gases in ground water. Science, 256, 1000-1003.

Suckow A. and Sonntag C. 1993. The influence of salt on the noble gas geothermometer. In Isotope Techniques in the Study of Past and Current Environmental Changes in the Hydrosphere and the Atmosphere. Proc. Intl. Symp., Vienna. International Atomic Energy Agency, Vienna, 307-318.

Sutcliffe D.W. and Carrick T.R. (1983). Chemical composition of waterbodies in the English Lake District: relationships between chloride and other major ions related to solid geology, and a tentative budget for Windermere. Freshwater Biology, 13, 323-353.

Sutton J.S. to be published, Special Issue of Quarterly Journal of Engineering Geology.

Wolery T.J. (1992). EO3NR, a computer program for geochemical aqueous speciation-solubility calculations: Theoretical manual, user's guide and related documentation (Version 7.0). University of California Lawrence Livermore National Laboratory Report. UCRL-MA-110662 Part III.

Wolery T.J. and Daveler S.A. (1992). EO6, a computer program for reaction path modeling of aqueous geochemical systems: Theoretical manual, user's guide and related documentation (Version 7.0). University of California Lawrence Livermore National Laboratory Report. UCRL-MA-110662 Part IV.

Zaikowski A., Kosanke J. and Hubbard N. (1987). Noble gas composition of deep brines from the Palo Duro Basin, Texas. Geochimica et Cosmochimica Acta 51, 73-94.

LIST OF PARTICIPANTS

Jean-François Aranyossy

ANDRA
B.P. 38
F-92266 FONTENAY AUX ROSES, Cx
Frankrike
Tel: + 33-1-4117 82 82
Fax: +33-1-4117 84 08

Steven Banwart

KTH
OOK
100 44 STOCKHOLM
Sweden
Tel: + 46-8 790 60 00
Fax. +46-8-21-26-26

Adrian Bath

Golder Associates (UK) Ltd
Landmere Lane
Edwalton, Nottingham NG12 4DG
England
Tel: +44 115 945 6544
Fax: +44 115 945 6540

Catherine Beaucaire

CEA, DCC/DSD
B.P. 6
92265 FONTENAY-AUX-ROSES, Cx
Frankrike
Tel: +33-1-46 54 89 11
Fax: +33-1-46 54 88 32

Carol Bruton

LLNL, Earth Sciences Div
P.O. Box 808, Mail Stop L-219
Livermore, CA 94550
USA
Tel: +1-510-423-1936
Fax: +1-510-422-0208

Joël Chupeau

ANDRA
B.P. 38
F-92266 FONTENAY AUX ROSES, Cx
Frankrike
Tel: +33-1-4117 81 07
Fax: +33-1-4117 84 08

Kristina Gillin

SKB
Box 5864
102 40 STOCKHOLM
Sweden
Tel: +46 8 665 28 45
Fax: +46 8 661 57 19

Erik Gustafsson

Geosigma
Box 894
751 08 UPPSALA
Sweden
Tel: +46-18 65 08 14
Fax: +46-18 12 13 02

Toshifumi Igarashi

CRIEPI/SKB Äspölaboratoriet
Pl 300
572 95 FIGEHOLM
Sweden
Tel: +46-491 820 00
Fax: +46-491 820 05

Nick Jefferies

AEA
Harwell Laboratory
Didcot, Oxon UK OX11 0RA
Storbritannien
Tel: +44-235-821 11
Fax: +44-235-43 49 42

Fred Karlsson

SKB
Box 5864
102 40 STOCKHOLM
Sweden
Tel: +46 8 665 28 30
Fax: +46 8 661 57 19

Katina Klingberg

SKB/Äspölaboratoriet
Pl 300
572 95 FIGEHOLM
Sweden
Tel: +46 491 820 00
Fax: +46 491 820 05

Marcus Laaksoharju

GeoPoint AB
Malmvägen 75 C, lgh 961
191 62 SOLLENTUNA
Sweden
Tel: +46+8 92 77 14
Fax: +46+8 92 77 14

Ove Landström

Studsvik AB
611 82 NYKÖPING
Tel: +46-155 22 10 00
Fax:

Didier Louvat

CEA-DCC-DESD
Centre d'Etudes Nucl de Cadarache
Batiment 307
F-13108 Saint Paul lez Durance Cx
Frankrike
Tel: +33-42 25 25 19
Fax: +33-42 25 62 72

Hiroya Matsui

PNC/SKB Äspölaboratoriet
PI 300
572 95 FIGEHOLM
Sweden
Tel: +46 491 820 00
Fax: +46 491 820 05

Martin Mazurek

RWIG, Inst of Mineralogy and Petrology
Baltzer Strasse 1
CH-3012 BERN
Schweiz
Tel: +41-31631 4769 (31631 8781)
Fax: +41-31631 4843

Thierry Merceron

ANDRA
B.P. 38
F-92266 FONTENAY AUX ROSES, Cx
Frankrike
Tel: +33-1-4117 81 08
Fax: +33-1-4117 84 08

Luis Moreno

KTH
Inst f kemisk aparatteknik
100 44 STOCKHOLM
Sweden
Tel: +46 8 790 64 12
Fax: +46 8 10 52 28

Ann-Chatrin Nilsson

KTH
OOK
100 44 STOCKHOLM
Sweden
Tel: +46 8 790 60 00

Karsten Pedersen

Göteborgs universitet
Lundberglaboratoriet: mikrobiologi
Medicinaregatan 9 C
413 90 GÖTEBORG
Sweden
Tel: +46 31 773 25 78
Fax: +46 31 773 25 99

Zell Peterman

US Geological Survey
MS 963, Box 25046 DFC
Denver, CO 80225
USA
Tel: +1-303-236-7883
Fax: +1-303-236-4930

Petteri Pitkänen

VTT
P.O. Box 1941
SF-02044 VTT
Finland
Tel: +358-0 456 4854
Fax: +358 0 46 79 27

Ingvar Rhén

VBB VIAK AB
Box 2203
403 14 GÖTEBORG
Sweden
Tel: +46-31 62 75 00
Fax: +46 31 62 77 22

Paula Ruotsalainen

Fintact
Hopeatie 1B
SF-00440 HELSINGFORS
Finland
Tel: +358-0 503 21 74
Fax: +358-0 503 21 75

Christina Skårman

GeoPoint AB
Malmvägen 75 C, lgh 961
191 62 SOLLENTUNA
Sweden
Tel: +46+8 92 81 57
Fax: +46+8 92 77 14

John Smellie

Conterra AB
Box 493
751 06 UPPSALA
Sweden
Tel: +46-18 12 32 41
Fax: +46-18 12 32 62

Margit Snellman

IVO
Box 112
01601 VANTAA
Finland
Tel: +358-0 5081
Fax: +358 0 563 22 25

Eva-Lena Tullborg

Terralogica AB
Box 140
440 06 GRÅBO
Sweden
Tel: +46-302 420 66
Fax: +46 302 420 26

Brian Viani

LLNL, Earth Sciences Div
P.O. Box 808, Mail Stop L-219
Livermore, CA 94550
USA
Tel: +1-510 423 2001
Fax: +1 510 422 0208

Bill Wallin

GEOKEMA
Rönnvägen 9
181 46 LIDINGÖ
Sweden
Tel: +46 8 767 86 75
Fax: +46 8 767 86 75

Thomas Wallroth

CTH
Geologiska inst
412 96 GÖTEBORG
Sweden
Tel: +46-31 772 10 00
Fax: +46-31 772 20 70

Peter Wikberg

SKB
Box 5864
102 40 STOCKHOLM
Sweden
Tel: +46 8 665 28 63
Fax: +46 8 661 57 19

Liisa Wikström

Åbo Akademi
Geol inst
SF-200500 ÅBO
Finland
Tel: +358-21 65 41 58
Fax: +358-21 65 48 18

List of International Cooperation Reports

ICR 93-01

Flowmeter measurement in
borehole KAS 16
P Rouhiainen
June 1993
Supported by TVO, Finland

ICR 93-02

Development of ROCK-CAD model
for Äspö Hard Rock Laboratory site
Pauli Saksa, Juha Lindh,
Eero Heikkinen
Fintact KY, Helsinki, Finland
December 1993
Supported by TVO, Finland

ICR 93-03

Scoping calculations for the Matrix
Diffusion Experiment
Lars Birgersson¹, Hans Widén¹,
Thomas Ågren¹, Ivars Neretnieks²,
Luis Moreno²
1 Kemakta Konsult AB, Stockholm,
Sweden
2 Royal Institute of Technology,
Stockholm, Sweden
November 1993
Supported by SKB, Sweden

ICR 93-04

Scoping calculations for the Multiple
Well Tracer Experiment - efficient design
for identifying transport processes
Rune Nordqvist, Erik Gustafsson,
Peter Andersson
Geosigma AB, Uppsala, Sweden
December 1993
Supported by SKB, Sweden

ICR 94-01

Scoping calculations for the Multiple
Well Tracer Experiment using a variable
aperture model
Luis Moreno, Ivars Neretnieks
Department of Chemical Engineering
and Technology, Royal Institute of
Technology, Stockholm, Sweden
January 1994
Supported by SKB, Sweden

ICR 94-02

**Äspö Hard Rock Laboratory. Test plan for
ZEDEX - Zone of Excavation Disturbance
EXperiment. Release 1.0**

February 1994

Supported by ANDRA, NIREX, SKB

ICR 94-03

**The Multiple Well Tracer Experiment -
Scoping calculations**

Urban Svensson

Computer-Aided Fluid Engineering

March 1994

Supported by SKB, Sweden

ICR 94-04

**Design constraints and process discrimination
for the Detailed Scale Tracer Experiments at Äspö -
Multiple Well Tracer Experiment and Matrix Diffusion
Experiment**

Jan-Olof Selroos¹, Anders Winberg²,
Vladimir Cvetkovic²

1 Water Resources Eng., KTH

2 Conterra AB

April 1994

Supported by SKB, Sweden

ICR 94-05

Analysis of LPT2 using the Channel Network model

Björn Gylling, Luis Morenó,

Ivars Neretnieks¹, Lars Birgersson²

1 Department of Chemical Engineering
and Technology, Royal Institute
of Technology, Stockholm, Sweden

2 Kemakta Konsult AB, Stockholm, Sweden

April 1994

Supported by SKB, Sweden

ICR 94-06

SKB/DOE Hard Rock Laboratory Studies

**Task 3. Geochemical investigations using stable and
radiogenic isotopic methods**

Bill Wallin¹, Zell Peterman²

1 Geokema AB, Liding, Sweden

2 U.S. Geological Survey, Denver, Colorado, USA

January 1994

Supported by SKB and U.S.DOE

ICR 94-07

Analyses of LPT2 in the Äspö HRL with continuous anisotropic heterogeneous model

Akira Kobayashi¹, Ryo Yamashita², Masakazu Chijimatsu², Hiroyuki Nishiyama³, Yuzo Ohnishi³

1 Iwate University, Iwate, Japan

2 Hazama Corporation, Ibaraki, Japan

3 Kyoto University, Kyoto, Japan

September 1994

Supported by PNC, Japan

ICR 94-08

Application of three-dimensional smeared fracture model to the groundwater flow and the solute migration of LPT-2 experiment

T Igarashi, Y Tanaka, M Kawanishi

Abiko Research Laboratory, Central Research Institute of Electric Power Industry, Abiko, Japan

October 1994

Supported by CRIEPI, Japan

ICR 94-09

Discrete-fracture modelling of the Äspö LPT-2, large-scale pumping and tracer test

Masahiro Uchida¹, Thomas Doe², William Dershowitz², Andrew Thomas², Peter Wallmann², Atsushi Sawada¹

1 Power Reactor and Nuclear Fuel Development Co., Tokai, Japan

2 Golder Associates Inc., Seattle, WA, USA

March 1994

Supported by PNC, Japan

ICR 94-10

Äspö Hard Rock Laboratory

International workshop on the use of tunnel boring machines for deep repositories

Äspö, June 13-14 1994

Göran Bäckblom (ed.)

Swedish Nuclear Fuel and Waste Management Co.

October 1994

Supported by SKB, Sweden

ICR 94-11

Data analysis and modelling of the LPT2 Pumping and Tracer Transport Test at Äspö. Tracer experiment

Aimo Hautajärvi

VTT Energy

November 1994

Supported by TVO, Finland

ICR 94-12

Modelling the LPT2 Pumping and Tracer Test at Äspö.

Pumping test

Veikko Taivassalo, Lasse Koskinen,
Mikko Laitinen, Jari Löfman, Ferenc Mészáros

VTT Energy

November 1994

Supported by TVO, Finland

ISSN 1104-3210
ISRN SKB-ICR--94/13--SE
CM Gruppen AB, Bromma 1994